UNIVERSITEIT
GENT

Faculteit Bio-ingenieurswetenschappen

Academiejaar 2012 – 2013

Plant-water relations of the mangrove species *Rhizophora stylosa*: a unique story

Michiel Hubeau

Promotor: Prof. dr. ir. Kathy Steppe

Tutor: dr. ir. Maurits Vandegehuchte

Masterproef voorgedragen tot het behalen van de graad van
Master in de bio-ingenieurswetenschappen: milieutechnologie

UNIVERSITEIT
GENT

Faculteit Bio-ingenieurswetenschappen

Academiejaar 2012 – 2013

Plant-water relations of the mangrove species *Rhizophora stylosa*: a unique story

Michiel Hubeau

Promotor: Prof. dr. ir. Kathy Steppe

Tutor: dr. ir. Maurits Vandegehuchte

Masterproef voorgedragen tot het behalen van de graad van
Master in de bio-ingenieurswetenschappen: milieutechnologie

The promoter	The author
Prof. dr. ir. Kathy Steppe	Michiel Hubeau

Gent, juni 2013

Acknowledgements

Vooraf zou ik graag de mensen bedanken die er mee voor hebben gezorgd dat ik deze thesis kon schrijven.

Allereerst wil ik mijn promotor, Prof. dr. ir. Kathy Steppe, bedanken. Voor ik aan mijn masterjaren begon, had ik nooit gedacht dat mijn thesis een ecofysiologisch onderwerp zou hebben. Het was namelijk vooral tijdens de lessen ecologie van Prof. Steppe dat mijn interesse voor dit vakgebied werd aangewakkerd. Het onuitputtelijke enthousiasme tijdens deze lessen en de gesprekken omtrent mijn thesiskeuze overtuigden me snel dat ik met veel plezier een jaar aan deze thesis wilde werken. Het onderwerp heeft me gedurende de hele totstandkoming geboeid. De unieke plek waar het veldonderzoek doorging, de Australische mangroves, was echt spectaculair en ook het uitdagende en vernieuwende karakter van het onderwerp is me blijven fascineren tijdens de uitwerking van deze thesis.

Tijdens ons verblijf in Australië heb ik met groeiend respect kennis gemaakt met de werkijver van Maurits, onze tutor. Wanneer Mieke, Niels, Stefanie en ikzelf uitgeput uit de mangroves terugkwamen en even neer ploften in de zetel, was Maurits al lang terug in het labo om te sleutelen aan zijn sensoren of om andere problemen op te lossen. Op die manier zette hij ook ons aan om meer te doen dan wat we zelf mogelijk achtten. Als er zich ergens een probleem voordeed, dan had Maurits een oplossing. Meermaals betekende dat met zwaar materiaal op stap gaan en zo werd ons karakter nog wat aangesterkt. Maar we zijn er telkens wel in geslaagd om wat op voorhand misschien een onmogelijk idee leek toch tot een goed einde te brengen. Al die keren dat we als echte "onderzoekertjes" met allerlei (zware) "koffertjes" door de rivier de mangroves introkken, of een zware *vibracore* het strand over trokken zullen zeker nog zeer lang een mooie herinnering blijven. Hierbij hoort natuurlijk ook het aangename gezelschap van mijn medestudenten Mieke, Niels en Stefanie. Ook tijdens de verwerking in België kon ik altijd terecht bij Maurits en mijn dank nogmaals voor de snelle antwoorden en het uiterst nuttige naleeswerk.

In Australia, we could always rely on a lot of people who were ready to help us. Adrien, Matt, Nina, Masha and the very kind and helpful personnel of Moreton Bay Research Station (MBRS). I really had an amazing time in Australia thanks to the hospitality of the Australians and thanks to the people of the MBRS we could feel like home on the island and it was amazing how helpful they were. The people from the University of Queensland (UQ) made the experiment possible: the supporting research groups made it possible to equip the trees with many sensors. Much of the resources we needed were at our disposal: our gratitude goes to Professor David Lockington. Adrien was of great help during the experiment and I enjoyed all the talks about science and other subjects. It was really a pity he was struck by disease during the experiment. I want to express a lot of gratitude to Matt. He was the perfect guide and showed us so many beautiful places in Moreton Bay. The research we did with him was hard work, but his appreciation made us do it with a lot of fun. Dragging the heavy vibracore, running in the deep sand with many kilograms of soil samples and struggling with the boat to make sure we could return to the station were the perfect workout. I am grateful he gave us the opportunity to see so much of the Australian nature and sea wildlife, like the fantastic day when we were so close to the wonderful whales and that we saw huge turtles and dolphins. And thanks for the lovely kangaroo burgers you prepared on the barbeque. In short, I really enjoyed the country, the people, the nature and the work.

Tot slot wil ik heel graag mijn vrienden en familie bedanken. Zij stonden tijdens het uitwerken, analyseren en schrijven toch het dichtst bij mij en moesten ermee kunnen omgaan wanneer ik weer even een kleine paniekaanval kreeg over hoeveel er nog te doen was. Mijn kotgenoten dank ik om zo geduldig naar mijn ongetwijfeld zeer verwarrende ideeën te luisteren. Mijn klasgenoten en vrienden van de universiteit, die in het zelfde schuitje zaten, waren zeer aangenaam gezelschap om waar nodig het hart eens te luchten over het vele werk dat in een thesis kruipt of om gewoon eens stoom af te blazen. Ook de ontspanning in de scouts en tijdens het sporten met vrienden van het thuisfront deden goed om voor afwisseling te zorgen na het werken achter de computer. Uiteraard is ook mijn gezin belangrijk geweest tijdens dit jaar en stonden ze paraat met raad en daad. Bedankt aan mijn ouders die me in elke stap naar het laatste jaar bio-ingenieur ongelooflijk gesteund hebben. Marianne, mijn zus, bedank ik enorm hard voor het intensief nalezen van de thesis. Ik heb veel bijgeleerd uit de opmerkingen en alle voortreffelijke tips over het wetenschappelijk Engels. Als laatste wil ik mijn vriendin, Janne, bedanken, om mij een heel jaar bij te staan en steeds opnieuw te motiveren als dat nodig was, voor alle aanmoedigingen en om het mij te vergeven telkens ik weer een lange avond aan mijn thesis moest werken.

Ik dank iedereen voor het lezen van mijn thesis en hopelijk fascineren de mangroves jullie ook.

Table of contents

Acknowledgements i

List of Figures v

List of Tables vi

Abbreviations vii

Summary ix

Samenvatting xi

Introduction 1

  General introduction 1

  Justification 1

  Objectives 2

Chapter 1: Literature review 3

  1.1 Water in trees: a complex story 3

    1.1.1 The function of water in trees 3

    1.1.2 The Höfler diagram and water potential 3

    1.1.3 Water movement in trees 6

    1.1.4 Stomatal control on water loss from transpiration 7

    1.1.5 The numbers tell the tale 8

  1.2 Stem growth patterns 8

    1.2.1 Diurnal growth patterns 8

    1.2.2 Sap flow and its influence on water depletion and replenishment 10

    1.2.3 Microclimatic factors are the main drivers for plant water household 11

  1.3 Mangroves 12

    1.3.1 Introduction 12

    1.3.2 Classification 13

    1.3.3 Distribution 13

    1.3.4 Root system 14

    1.3.5 Mangroves have to face many challenges 15

    1.3.6 Anatomical adaptations make mangroves less vulnerable to cavitation 16

    1.3.7 Mangrove response to climate change 17

Chapter 2: Materials and Methods 19

  2.1 Study area 19

  2.2 Meteorological data 20

  2.3 Tree sensors 22

        - 2.3.1 Dendrometer: band dendrometer 23
        - 2.3.2 Sap flow sensor: heat ratio method (HRM) 25
        - 2.3.3 Water potential: Stem psychrometer 27
        - 2.3.4 Stomatal resistance: Porometer 29
        - 2.3.5 Water potential: Pressure bomb 30
    - 2.4 Soil salinity 31
- Chapter 3: Results 33
    - 3.1 Meteorological data 33
    - 3.2 Stem radius changes 34
    - 3.3 Sap flow 36
    - 3.4 Water potential 38
    - 3.5 Stomatal behavior 40
    - 3.6 Rain and salinity 41
    - 3.7 Growth pattern characterization 44
    - 3.8 Physiological effects on the growth pattern 48
- Chapter 4: Discussion 51
    - 4.1 The diurnal physiological patterns of *R. stylosa* 51
    - 4.2 The influence of meteorological variables on *R. stylosa* 51
    - 4.3 Branch and leaf water potential 52
    - 4.4 Stomatal behavior 53
    - 4.5 Rain and salinity 53
    - 4.6 The extraordinary growth pattern of *R. stylosa* 56
        - 4.6.1 Is *R. stylosa* a CAM-plant? 56
        - 4.6.2 Periods of growth and shrinkage 56
        - 4.6.3 An osmotic regulated growth pattern 57
        - 4.6.4 Benefits of osmotic regulation 60
- Chapter 5: Conclusion 61
- Chapter 6: Future research 63
- References 65

List of Figures

Figure 1.1 The Höfler diagram (Porporato et al. 2001). 4

Figure 1.2 Range of water potential in which different cell processes and effects occur (Hsiao and Acevedo 1974, Porporato et al. 2001). 5

Figure 1.3 Typical course of Ψ_s, Ψ_r and Ψ_l affecting the plant and the effect of drought (Boyer 1968, Slatyer 1969). 6

Figure 1.4 Schematic drawing of water movement in plants (Leuning et al. 2004). 7

Figure 1.5 A typical circadian course of stem radius (Deslauriers et al. 2007a). 9

Figure 1.6 Sap flow in the stem and the crown (Goldstein et al. 1998). 10

Figure 1.7 The relation between transpiration and stem sap flow (Schulze et al. 1985). 11

Figure 1.8 The amount of mangrove species in the world (Polidoro et al. 2010). 14

Figure 1.9 Areas where different *Rhizophora* species, including *R. stylosa*, can be found in the Indo West Pacific (Duke et al. 2002). 14

Figure 1.10 *Avicennia marina* (a) with a lot of pneumatophores and *Rhizophora stylosa* (b) with stilt roots. 15

Figure 1.11 Zonation for *Avicennia marina* and *Rhizophora mucronata*. (Robert et al. 2009) 17

Figure 2.1 Overview of the study site location. 19

Figure 2.2 Photo of the research site with the three *Rhizophora stylosa* trees. 20

Figure 2.3 A picture of the meteorological Hobo station. 22

Figure 2.4 A fully equipped tree. 23

Figure 2.5 A band dendrometer attached to a *R. stylosa*. 24

Figure 2.6 A typical daily growth pattern of *R. stylosa* (on DOY 266). On this graph, the stem radius values used are highlighted with arrows and a corresponding letter. 25

Figure 2.7 Picture of an installed HRM sensor. 27

Figure 2.8 An example of a good and bad Peltier cooling curve. 28

Figure 2.9 An insulated stem psychrometer and an uninsulated head. 28

Figure 2.10 A porometer. 30

Figure 2.11 A pressure bomb 31

Figure 3.1 Daily averages and continuous measurements (interval of 15 minutes) of the environmental variables. 33

Figure 3.2 Overview of the stem radius increment patterns 35

Figure 3.3 Typical circadian growth patterns for *R. stylosa*. 36

Figure 3.4 Course of the sap flux density. 36

Figure 3.5 Correlation coefficients for the different meteorological variables with sap flux density. 37

Figure 3.6 Regression between sap flux density and VPD and temperature 37

Figure 3.7 Course of the water potential in the branches 38
Figure 3.8 Correlation coefficients for the different meteorological variables with Ψ_b. 39
Figure 3.9 Regression curves which relate Ψ_b with VPD and RH. 39
Figure 3.10 Comparison of two methods to measure water potential. 40
Figure 3.11 Stomatal resistance curve. 41
Figure 3.12 Stem growth patterns during the period in which rainfall occurred. 42
Figure 3.13 The course of sap flux density and its response to rainfall. 42
Figure 3.14 The curve of the water potential of *R. stylosa* in the time frame in which rain fell. 43
Figure 3.15 The soil potential calculated from the actual conductivity. 44
Figure 3.16 Growth and shrinkage during the defined time intervals. 45
Figure 3.17 The relationship between the small time interval and the large time interval 46
Figure 3.18 Comparison between the growth over an entire day and growth during the daytime..... 47
Figure 3.19 Average growth per hour and cumulative growth. 48
Figure 3.20 Correlation analysis of different growth periods with water potential and sap flow........ 49
Figure 4.1 Water exchanges between the xylem vessels and the stem storgage tissue, based on Herzog et al. (1995). 59
Figure 4.2 The phases described in Figure 4.1 on the stem growth pattern. 60

List of Tables

Table 1.1 Classification of mangrove tree species (Lugo and Snedaker 1974, Tomlinson 1995, Medina 1999)... 13
Table 2.1 Details of the position of the roots and tree sensors.. 20
Table 2.2 Definition of different parameters used for the growth pattern characterization. 24
Table 2.3 Wood properties calculated from wood cores. 27
Table 3.1 For each variable the average value from the period depicted in this table is used. In these periods the correlation with the corresponding growth period is highest. 48

Abbreviations

$\Delta R+$	days with positive growth
$\Delta R-$	days with negative growth
κ	actual conductivity
Ω	osmotic potential
Ω_o	osmotic potential of the soil
Ω_p	protoplast osmotic potential
Π_p	protoplast turgor pressure
Ψ	water potential
Ψ_b	water potential in the branches
Ψ_e	water potential in the epidermal cell
Ψ_g	water potential in the guard cell
Ψ_l	water potential in the leaves
Ψ_p	protoplast total potential
Ψ_r	water potential in the roots
Ψ_s	water potential in the soil
Ψ_{st}	water potential in the stem storage cells
Ψ_x	water potential in the xylem vessels
ρ_b	basic density of wood
ρ_s	density of water

ABA	abscisic acid
B	wound correction factor
c	companion cell
CAM	crasulacean acid metabolism
c_s	specific heat capacity of sap
c_w	specific heat capacity of the wood matrix
DOY	day of year
e	epidermal cell
$error_{rs,avg}$	error on the weighted average stomatal resistance
g	guard cell
Gr1H	growth between 0 and 12 h
GrD	growth between 0 and 24 h
GrP	growth between 6 and 12 h
HRM	heat ratio method
J_w	water flux
k	thermal diffusivity
k_r	reference thermal diffusivity
m_c	water content of sapwood
MDS	maximum daily shrinkage
P	statistical p-value
Rad	radiation
RH	relative humidity
$r_{s,avg}$	weighted average stomatal resistance
$r_{s,l}$	average stomatal resistance for 3 consecutive measurements

RWC	relative water content
sc	substomatal cavity
SD	standard deviation
SD_i	standard deviation on the average stomatal resistance
Sh2H	shrinkage between 12 and 24 h
ShP	shrinkage between 12 and 20 h
SRI	stem radius increment
T	transpiration
T_a	air temperature
T_{dew}	dewpoint temperature
Temp	temperature
v_1	downstream increase in temperature
v_2	upstream increase in temperature
V_h	heat pulse velocity
VPD	vapor pressure deficit
V_s	sap flux density
x	distance between temperature probe and heater

Summary

Mangrove trees have been intriguing scientists for a long time. The tree species have adapted their structures in such a way that they are capable of surviving the intertidal zone of tropical and subtropical coasts. While these salty conditions would pose insurmountable water stress to many other species, mangroves thrive under these conditions. The three main tactics that have been encountered in mangroves are (i) exclusion of salts at the roots, (ii) secretion of excess salts through salt glands in the leaves and (iii) accumulation of salts in leaf structures where they do not pose a risk of damaging the tree.

In this master dissertation, the experiment monitored three mangrove trees of the species *Rhizophora stylosa* for 63 days (DOY 223-285) on North-Stradbroke Island in Queensland, Australia. Both physiological and meteorological data were collected to acquire a clear view on how these trees respond to the prevalent conditions. The physiological measurements consisted of the continuous monitoring of the stem diameter, sap flux density and branch water potential and the manual measurements of the stomatal resistance and leaf water potential. The monitored meteorological variables were air temperature, atmospheric relative humidity, solar radiation and rainfall. Further, the vapor pressure deficit was calculated using the measured air temperature and relative humidity, and the soil osmotic potential was calculated using the measured soil water conductivity.

We investigated how the water status and physiological behavior of this mangrove species was influenced by the surrounding conditions. Differences between *R. stylosa* and other species were tracked down and these differences were explained. The diurnal pattern of the sap flux density was comparable to that of other species. This physiological variable was mostly influenced by the vapor pressure deficit. The water potential at the branches was also mostly influenced by the vapor pressure deficit and had a similar diurnal pattern compared to other species, however the values of the water potential were much lower. The typical observed water potential values would induce severe water stress in other plants, whereas mangroves, like *R. stylosa*, could maintain a water potential that is sufficiently low to pull water up from the saline soil. The most striking difference between *R. stylosa* and most other trees was the diurnal growth pattern, displayed by the stem diameter. An average growth pattern was constructed and *R. stylosa* exhibited an increase in the stem diameter between sunrise and noon and a decrease in diameter between noon and 20 h. The most intensive growth occurred around 8 h, 2 hours after sunrise, and the strongest shrinkage was situated around 16 h. The increase in the diameter was rapid and strong whereas the decrease in the diameter was more gradual. During the night, the growth dynamics were rather low.

The initial 40 days of the experiment, not a single rain event was registered, which was very exceptional and which gave the opportunity of monitoring these trees during a period of severe drought. Due to the drought, the trees exhibited an overall shrinkage during the first weeks of the experiment. This negative growth kept on going until new water reserves were provided due to rain events. In response to these rain events, large growth spurts were observed on all trees. This radial expansion was attributed to a decrease in the atmospheric water demand during the day and water uptake through the leaves and the bark during both day and night. The level of inundation did not appear to have a great influence on these growth spurts, so the moistening of the soil had little effect on the water uptake during the rain events. Only three rain events were observed and they occurred after a period of severe drought so these general conclusions should be confirmed by more research.

R. stylosa had a typical stomatal behavior including stomatal closure during the night and a partial midday stomatal closure. This kind of stomatal behavior is found in C3- and C4-plants, opposite to the nocturnal stomatal aperture of CAM-plants. In contrast, the growth pattern showed more resemblance with the growth pattern of CAM-plants than with the growth pattern of C3- and C4-plants. In the past, other researchers evaluated the photosynthetic metabolism of *R. stylosa* and concluded that *R. stylosa* is a C3-plant.

Eventually, the average growth pattern, combined with all the data gathered, led to the following preliminary hypothesis. *Under influence of light reception, osmotic substances are rapidly formed inside the tree cells lowering the osmotic potential*. This results in an influx of water inside the cells and consequently is observed as an increased stem diameter. Several hours later, this water uptake becomes lower because of the dilution effect and ceases when the water potentials are equalized again. Under influence of a rising water demand of the atmosphere, it becomes increasingly difficult for the cells to retain the water inside the cells. Next to this, it is expected that the concentration of osmotic substances lowers again throughout the day, due to the conversion to substances that are less osmotically active. This results in the gradual decrease of the growth figures, which become negative around noon and continue in becoming more negative until 16 h. At that time the atmospheric water demand is becoming lower and growth figures become less negative again and eventually neither growth nor shrinkage takes place during the night, when water is redistributed throughout the tree. Because the water uptake initiates when light reception starts, there is a possibility that the formation of these osmotic substances is part of the photosynthetic pathway. If this is the case, this could be a sign of a hybrid or even a new form of a photosynthetic metabolism.

Keywords: mangrove, *Rhizophora stylosa*, plant-water relations, growth, stem diameter variation, sap flow, plant water potential, osmotic regulation.

Samenvatting

Mangrovebomen fascineren wetenschappers al een hele tijd. Mangroves slagen erin om te overleven in het intertidaal van tropische en subtropische kusten. De zoute bodem die daar aanwezig is, zou voor andere boomsoorten een onoverkomelijke waterstress veroorzaken. Mangroves maken gebruik van één of meer van de volgende drie hoofdstrategieën om met deze waterstress om te gaan. Deze strategieën bestaan erin om (i) zout uit het water te filteren ter hoogte van de wortels, (ii) zout uit te scheiden door zoutklieren in het blad en (iii) zout te accumuleren in bladstructuren, zodat dit zout geen risico meer inhoudt voor de boom.

In dit experiment zijn drie bomen van de soort *Rhizophora stylosa* gedurende 63 dagen (DOY 223-285) onderzocht op het AustralischenNorth-Stradbroke Island in de staat Queensland. Zowel fysiologische als meteorologische gegevens werden verzameld om een inzicht te verkrijgen over de vraag hoe deze soort reageert op de heersende omstandigheden. De fysiologische metingen bestonden uit het continu meten van de stamdiameter, de sapstroomflux en de waterpotentiaal in de takken en het manueel meten van de stomatale weerstand en de waterpotentiaal in de bladeren. Wat de meteorologische gegevens betreft werden luchttemperatuur, relatieve luchtvochtigheid, zonnestraling en regenval opgemeten. Het dampdruktekort werd berekend aan de hand van de luchttemperatuur, de relatieve luchtvochtigheid en de relevante formules en de osmotisch potentiaal in de bodem werd berekend aan de hand van de gemeten bodemwaterconductiviteit.

Tijdens dit onderzoek werd nagegaan hoe de waterstatus en het fysiologische gedrag wordt beïnvloed door omgevingsfactoren. De verschillen tussen *R. stylosa* en andere soorten werden onderzocht en verklaard. Het dagelijkse patroon van sapstroom was vergelijkbaar met het patroon in andere soorten en werd voornamelijk beïnvloed door het dampdruktekort. De waterpotentiaal in de takken werd eveneens hoofdzakelijk beïnvloed door het dampdruktekort en ook deze patronen waren zeer vergelijkbaar met andere soorten, hoewel de waarden van de waterpotentiaal veel lager waren in vergelijking met andere soorten. Als deze waarden in andere boomsoorten zouden voorkomen, zou dit wijzen op zeer zware waterstress, in tegenstelling tot mangrovebomen, die deze sterk negatieve waarden nodig hebben om water te kunnen onttrekken aan de zoute bodem. Het meeste opvallende verschil tussen *R. stylosa* en andere boomsoorten was het groeipatroon dat de stamdiameter liet optekenen. Een gemiddeld groeipatroon werd opgesteld en dit vertoonde een stamdiameter die zwol gedurende de voormiddag, kromp tijdens de namiddag en avond en nagenoeg constant bleef tijdens de nacht. De sterkste groei werd gemeten rond 8 uur, 2 uur na zonsopgang, en de sterkste krimp vond plaats rond 16 uur. De groei gebeurde snel, terwijl de krimp veel geleidelijker was.

Tijdens de eerste 40 dagen van dit experiment werd er niet één regenbui waargenomen, hetgeen zeer uitzonderlijk was en de mogelijkheid gaf om deze mangrovesoort te bestuderen tijdens een periode van ernstige droogte. Door deze droogte kromp de stamdiameter op middellange termijn. Deze negatieve groei bleef aanhouden totdat regen de bomen bevoorraadde van extra water en de stamdiameter snel uitzette. Deze radiale uitzetting werd verklaard door een verlaagde watervraag van de atmosfeer overdag en wateropname doorheen de schors en door de bladeren, zowel overdag als tijdens de nacht. Het niveau van het zeewater bleek geen grote invloed te hebben op deze sterke groei en dus bleek de bevochtiging van de bodem niet belangrijk voor de wateropname van de boom tijdens regenbuien. Deze observaties zijn gebaseerd op slechts drie dagen met regenbuien en dus moeten algemene conclusies worden bevestigd door toekomstige experimenten.

De huidmondjes van *R. stylosa* waren gesloten tijdens de nacht, openden zich overdag, maar sloten zich opnieuw gedeeltelijk tijdens de middag. Dit is typisch voor C3- en C4-planten, in tegenstelling tot de huidmondjes van CAM-planten die open zijn tijdens de nacht. Nochtans vertoonde het groeipatroon van *R. stylosa* meer gelijkenissen met het groeipatroon van CAM-planten dan met die van C3- of C4-planten. In het verleden zijn andere onderzoekers echter tot het besluit gekomen dat *R. stylosa* wel degelijk een C3-plant is.

Uiteindelijk werd het gemiddelde groeipatroon gecombineerd met de andere gegevens die gemeten waren en dit leidde tot de volgende hypothese. *Onder invloed van licht worden osmotisch actieve stoffen snel gevormd binnenin de cellen, zodanig dat de osmotische potentiaal binnen deze cellen daalt.* Dit heeft als gevolg dat water wordt opgenomen door de cellen en bijgevolg de stamdiameter uitzet. Enkele uren later vermindert deze wateropname omdat de concentratie van osmotische stoffen daalt door de verdunning die wordt veroorzaakt door het instromende water. Uiteindelijk stopt de wateropname wanneer de waterpotentialen opnieuw in evenwicht zijn. Doordat op dit moment van de dag de watervraag van de atmosfeer nog steeds stijgt, wordt het voor de boom steeds moeilijker om het water binnenin de cellen te houden. Daarenboven wordt een verlaging van de hoeveelheid osmotische stoffen verwacht door de omzetting naar osmotisch minder actieve of zelfs inactieve stoffen. Hierdoor daalt het groeicijfer geleidelijk aan en wordt het negatief rond de middag. Deze groeicijfers blijven dalen tot ongeveer 16 uur, waarna de groeicijfers opnieuw naar 0 evolueren en ongeveer 0 blijven gedurende de nacht. Deze neutrale groeicijfers worden geobserveerd wanneer het water in de boom is herverdeeld en er geen gradiënt meer aanwezig is om een waterstroom te veroorzaken. Omdat wateropname samenviel met het eerste daglicht, werd er rekening gehouden met de mogelijkheid dat de vorming van osmotische stoffen deel uitmaakt van het fotosynthetische proces. Als dit effectief het geval zou zijn, zou dit een teken kunnen zijn van een hybride of zelfs een nieuwe vorm van het fotosynthetisch metabolisme.

Sleutelwoorden: mangrove, *Rhizophora stylosa*, plant-water relaties, groei, stamdiametervariatie, sapstroom, plant waterpotentiaal, osmotische regulatie.

Introduction

General introduction

A mangrove ecosystem is unique due to its trees that can withstand and thrive in the harsh conditions of the intertidal zone of tropical and subtropical coasts. These trees have to cope with a very high salinity, recurrent flooding and high temperatures. Although the area, suited for mangroves is limited and they cover less than 0.1 % of the Earths land coverage, mangroves are highly valuable and offer a lot of services to both humans and animals. Humans have been using resources from mangroves such as timber, fibers, food, medicines and chemicals since ages. Mangrove communities provide support for both marine and terrestrial food webs and as a result can generate human income. Besides goods, other services are provided by sheltering human settlements from tsunamis, sea-level rise and storms. Furthermore, coral reefs and seagrass beds are protected from siltation that originates from rivers. In the perspective of climate change, mangrove systems are important due to (i) their major sink capacity of atmospheric CO_2, (ii) their exceptional high primary production rates, and (iii) their source capacity of oceanic carbon. The clearing of mangroves for aquaculture, urbanization or other causes could release this CO_2 back into the atmosphere.

Yet, in spite of this great value, mangrove forest are disappearing at a disturbing rate of 1 to 2 % per year. Experts believe that at this rate the world will no longer be able to rely on the services provided by this exceptional environment, perhaps within 100 years. Despite this concern, only less than 7 % of the mangrove ecosystems are protected. In order to facilitate a good conservation management, proper knowledge is required and this dissertation contributes to fulfill this knowledge gap. Furthermore, the unique properties of mangrove trees and the surroundings in which they survive make the ecophysiological research important to complement the existing theories with new insights.

Justification

In previous ecophysiological research on a mangrove tree species, signs of special traits were discovered in *Avicennia marina* (Hoste 2011) whereby during rain events a negative sap flow had been observed. The hypothesis of foliar rain uptake was put forward in this research. The experiment of Hoste (2011) measured continuously the water potential, sap flow and stem diameter with a high time resolution and linked these variables with one another and with meteorological variables. A new experiment was suggested in order to gather new evidence for this foliar uptake and to acquire confirmation of the previous observations. To assess the possible differences between different mangrove species the experiment performed in this master dissertation was set up on another common mangrove species, namely *Rhizophora stylosa*. However, only few studies exist that measure diameter growth patterns of mangroves with band dendrometers (Day et al. 1982, Jintana et al. 1985, Krauss et al. 2007) and none exist that measures the stem diameter on a short term with high resolution on *R. stylosa.* Consequently, a new highly valuable dataset could be generated because of the differences between these species. In general, mangroves have been divided into three categories according to the prevailing salt eliminating mechanism, i.e. salt excluders, salt secretors and salt accumulators, although many species exhibit adaptations of several categories (Ball 1988). Salt excluders reject most of the salt at the roots through ultrafiltration, salt secretors use salt glands to remove excess salt and salt accumulators store excess salt in different plant parts to avoid salt damage. *R. stylosa* is a salt excluder, whereas *A. marina* is a salt secretor. Therefore, measuring and linking the same physiological and meteorological variables on a different species could possibly give rise to a new perception and understanding on how mangroves, in particular *R. stylosa*, cope with the challenging environment in which they thrive. Not only knowledge on how this mangrove species functions will be acquired but even more, the current physiological theories will be tested and even extended.

Objectives

The main objective of this master dissertation is to collect and interpret a first set of physiological data for the mangrove species *R. stylosa*, a salt excluder. The data are collected under natural conditions in a mangrove forest and provide a first glimpse on how this species deals with the extensive challenges associated with the intertidal zone.

Therefore the specific objectives are:

(i) To monitor the physiological variables (i.e. stem diameter variations, sap flux density and branch water potential) of *R. stylosa* at a high time resolution with a focus on the general diurnal patterns and their differences with non-mangal species.
(ii) To monitor the prevailing meteorological parameters (i.e. air temperature, atmospheric relative humidity, solar radiation, rainfall and vapor pressure deficit) and soil osmotic potential) with the purpose to link these parameters to the physiological variables.
(iii) To monitor the discrete events of rain and the response of *R. stylosa* to these events.
(iv) To physiologically explain the relationships between all the measured parameters and the patterns they exhibit.

Chapter 1: Literature review

1.1 Water in trees: a complex story

1.1.1 The function of water in trees

Water is an essential resource in trees for their survival, due to its important involvement in a broad range of vital functions (Coder 1999). For instance, water acts as a constituent, a solvent, a reactant and moreover water is responsible for the maintenance of cell turgidity (Kramer and Boyer 1995b). As a consequence, trees have developed a wide variety of strategies to optimize their hydraulic architecture to cope with all kinds of prevalent conditions (Tyree and Ewers 1991). Although it may seem that the water content in trees is constant, the opposite is true. Water storage and movement is a dynamic process in which water is continuously depleted and replenished on daily bases (Zweifel et al. 2000).

Water, stored and used by trees, can be divided into three categories (Zweifel et al. 2000). A first category is the capillary water, which is stored in intercellular pores and inactive xylem. This water is relatively weakly bound and is easily released at high xylem water potentials (depleted for $\Psi \approx -0.5$ MPa) (Zweifel et al. 2000). The second category is water in the xylem that can be used as an extra water source in case the water potential drops to a lower water potential. In case the water potential drops below a species-dependent threshold, cavitation of the xylem occurs (Zweifel et al. 2000). Cavitation or embolism is caused by high negative potentials (tensions) that can cause the rupture of the water column inside a xylem vessel which results in the infiltration of air in the vessel (Kramer and Boyer 1995c). When only a small amount of vessels is cavitated, a plant can recover rather easily. However, if too many vessels are cavitated, hydraulic conductance is reduced which leads to a further increase in water column tension and consequently a higher probability that more vessels will cavitate. This course of events, called runaway embolism, can propagate throughout the entire plant and can eventually result in the failure of water transport which will lead to a loss of functionality inside the plant (Tyree and Ewers 1991). A third category is water stored in living cells that can be utilized. This water can be withdrawn from the cells over the entire range of occurring water potentials in trees (Zweifel et al. 2000). The depletion of this water has a significant impact on the viability of the tree because the amount of water present in a living cell has a large influence on the performance of this cell (Porporato et al. 2001).

1.1.2 The Höfler diagram and water potential

The relationship between the amount of water in a living tree cell and the performance of this cell can be described by the Höfler diagram. Such a Höfler diagram shows different components of the water potential of a living cell (pressure and osmotic component) and their sequence with respect to changing relative water contents (Figure 1.1) (Hsiao and Acevedo 1974, Porporato et al. 2001). Figure 1.1 shows that the depletion of water in a living cell results in a decreasing pressure potential (positive turgor pressure, Π_p) and a decreasing (negative) osmotic pressure (Ω_p) due to an increasing solute concentration (Porporato et al. 2001). Obviously, also the total water potential decreases and the water will become increasingly unavailable. Plasmolysis occurs when turgor pressure becomes zero or negative. The phenomenon of the plasma membrane retracting from the cell wall in response to osmotic shock, can give rise to cellular injury (Oparka 1994). During the initial stage of plasmolysis, the cell can regain turgor when it takes water up again and then plasmolysis is reversible. However, when dehydration of the cell becomes too severe, plasmolysis is irreversible and the cell will lose its functionality (Porporato et al. 2001).

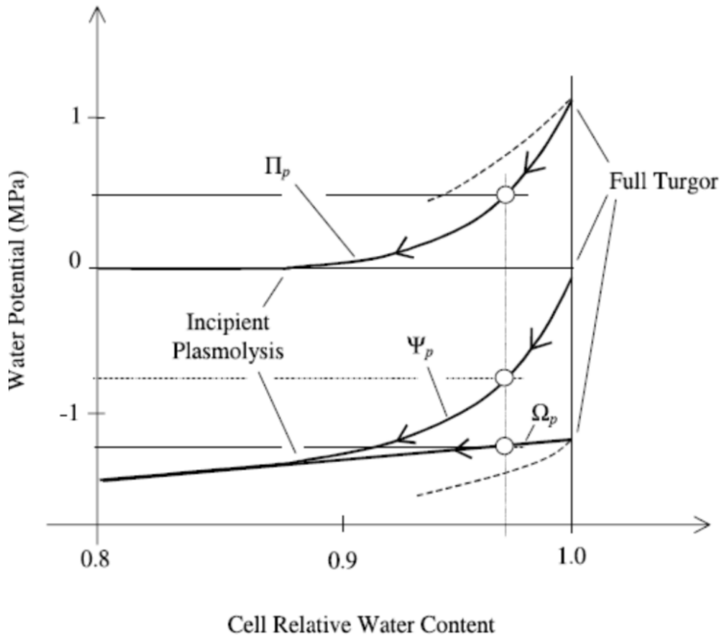

Figure 1.1 The Höfler diagram relates different components of the water potential to the relative water content (RWC) of the cell. The protopolast turgor pressure (Π_p) is maximum and at full turgor for a RWC of 1. When Π_p becomes 0 MPa or negative, plasmolysis of the cell occurs. The protoplast osmotic potential (Ω_p) is function of the solute concentration and the total cell pressure potential (Ψ_p) is obtained by adding the turgor and osmotic pressure (Porporato et al. 2001).

Another striking example of the importance of water shortage in living cells is presented in Figure 1.2 (Porporato et al. 2001). Figure 1.2 represents a list of different cell functions which fail given a certain loss of turgor pressure in comparison to full turgor (reference point 0), showing that even mild water stress affects the cell functionality. Not only growth but also the process of photosynthesis is affected fairly rapidly (Hsiao and Acevedo 1974, Porporato et al. 2001). It could be stated that water stress is the most important stress factor for trees (Bohnert et al. 1995, Coder 1999). Moreover, a shortage of water gives rise to many other types of stress. For instance, a decrease in cooling caused by a decrease in transpiration will lead to even more stress caused by heat and radiation (Hsiao and Acevedo 1974, Porporato et al. 2001).

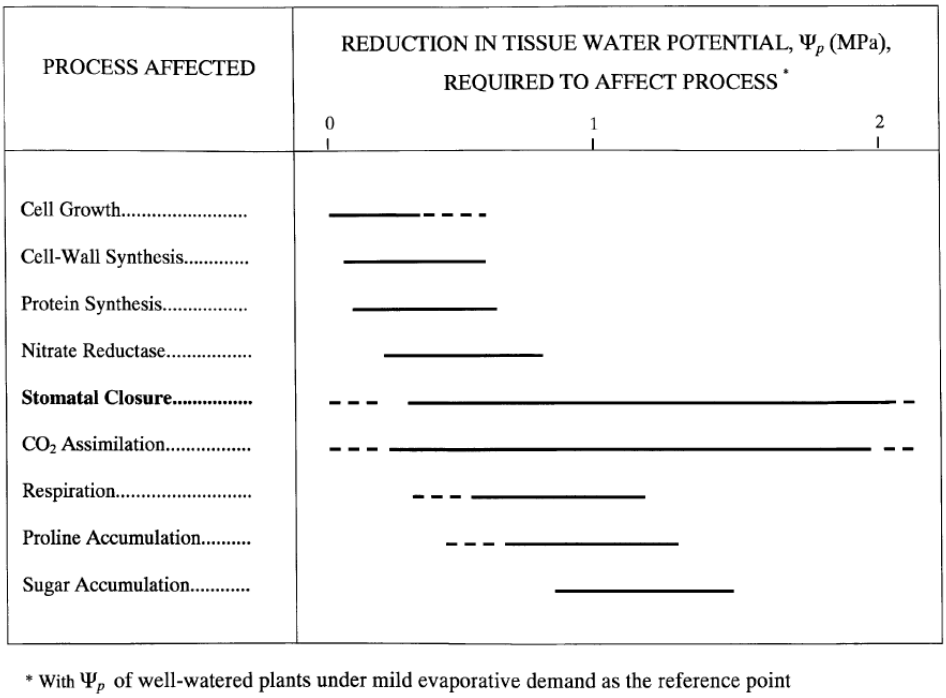

Figure 1.2 Range of water potential (relative to water potential of a well-watered plant) in which different cell processes and effects occur (Hsiao and Acevedo 1974, Porporato et al. 2001).

Figure 1.3 shows the variation in the soil water potential (Ψ_s), root water potential (Ψ_r) and leaf water potential (Ψ_l) in case of a soil that is drying out. Without drought, the normal daily variation of Ψ_l is a decline when transpiration commences. This is because the water demand of the atmosphere is exerting a force on the water column. Normally, i.e. without drought, a minimum Ψ_l is attained around noon, when the atmospheric water demand is highest and Ψ_l will rise again during the afternoon. During the night a more or less constant Ψ_l is maintained. However, with dry conditions and as a consequence a lower Ψ_s, the Ψ_l will gradually decline every day because the plant will not be able to replenish the entire water reserve. Furthermore, with severe drought, the nocturnal Ψ_l and Ψ_r will become lower as well and water stress will affect the plant (Boyer 1968, Slatyer 1969, Tardieu and Simonneau 1998, Kume et al. 2007). Plants will react to a lowered water potential in different ways. An example of a protection mechanism to retain more water inside the plant is stomatal closure. This phenomenon gives rise to small fluctuations in Ψ_l during the day (Slatyer 1969, Dolman and Van Den Burg 1988, Bond and Kavanagh 1999, Zweifel et al. 2002). Ψ_s is always higher than or equal to Ψ_r, which, in turn, is always higher than or equal to Ψ_l (Slatyer 1969).

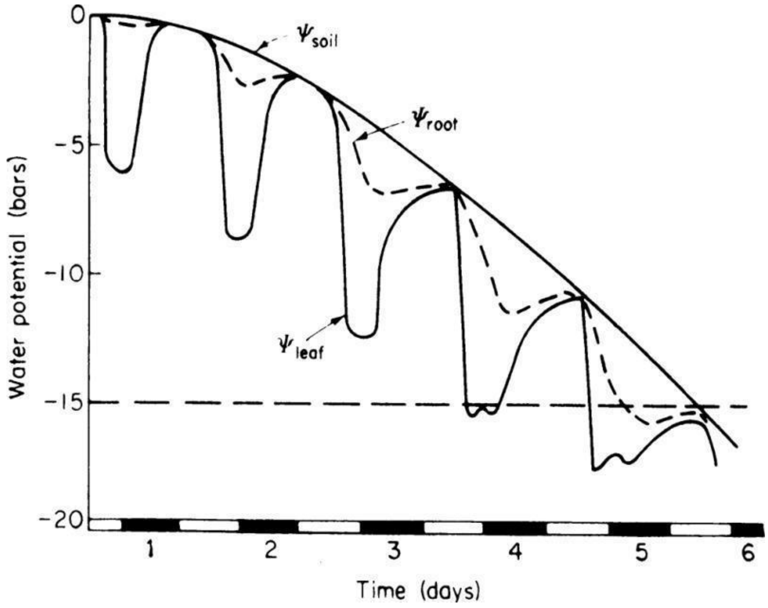

Figure 1.3 Typical course of the different water potentials (Ψ_s, Ψ_r and Ψ_l) affecting the plant. During the first days, the plant is not suffering from water stress but during the last days of the experiment, the soil potential drops rapidly and water stress becomes severe (Boyer 1968, Slatyer 1969).

1.1.3 Water movement in trees

As previously mentioned, water in trees is not stationary but dynamically, it moves bottom-up and is taken up and lost again every day. A brief overview of water movement can be illustrated by Figure 1.4 (Leuning et al. 2004). Figure 1.4 illustrates that firstly water is taken up at root level. Water is sucked into the roots as a result of the difference in water potential between the higher soil potential, Ψ_s, and the lower root potential, Ψ_r, as shown in the small diagram at the bottom of Figure 1.4. The soil surrounding the root will have a lowered water potential due to this water uptake. Secondly, inside the plant, water is drawn into the xylem and further transported to the upper part of the plant. Finally, water is lost to the atmosphere at the leaves, a process called transpiration (T) and it originates from the water demand of the atmosphere. When the water is transported from the xylem in the leaves to the stomata it passes leaf parenchyma, the substomatal cavity (sc) and it exits through the stomata, which is regulated by the guard cell (g) and companion cell (c). The water potentials important for transpiration in the leaf are the epidermal cell water potential (Ψ_e) and the guard cell water potential (Ψ_g). Transpiration through the other epidermal cells (e) is mostly prevented by a hydrophobic layer called the cuticle. The resulting water flux (J_W) is caused by the difference in water potentials which are becoming increasingly negative moving upward in the tree ($\Psi_s < \Psi_r < \Psi_e < \Psi_g$) (Kramer and Boyer 1995c, a, Leuning et al. 2004).

The cohesion-tension theory describes the physical force enabling this upward movement (Kramer and Boyer 1995c, a). This theory states that cohesion between water molecules (due to hydrogen bonds) in a confined tube, such as xylem vessels, is very strong and enables a water column to withstand pressures of several MPa without rupturing. A water column in plants consists of one continuous system from the roots to the transpiring leaves. As a result, water in xylem vessels is connected and will move together in one direction. The movement itself arises from the lowered water potential at leaf level, where transpiration takes place. This lowered potential gives rise to a tension on the water column and pulls the water up. Because of the cohesion throughout the entire plant, this pulling force at leaf height also pulls water up at root height and this eventually results in water uptake through the roots (Kramer and Boyer 1995b, c).

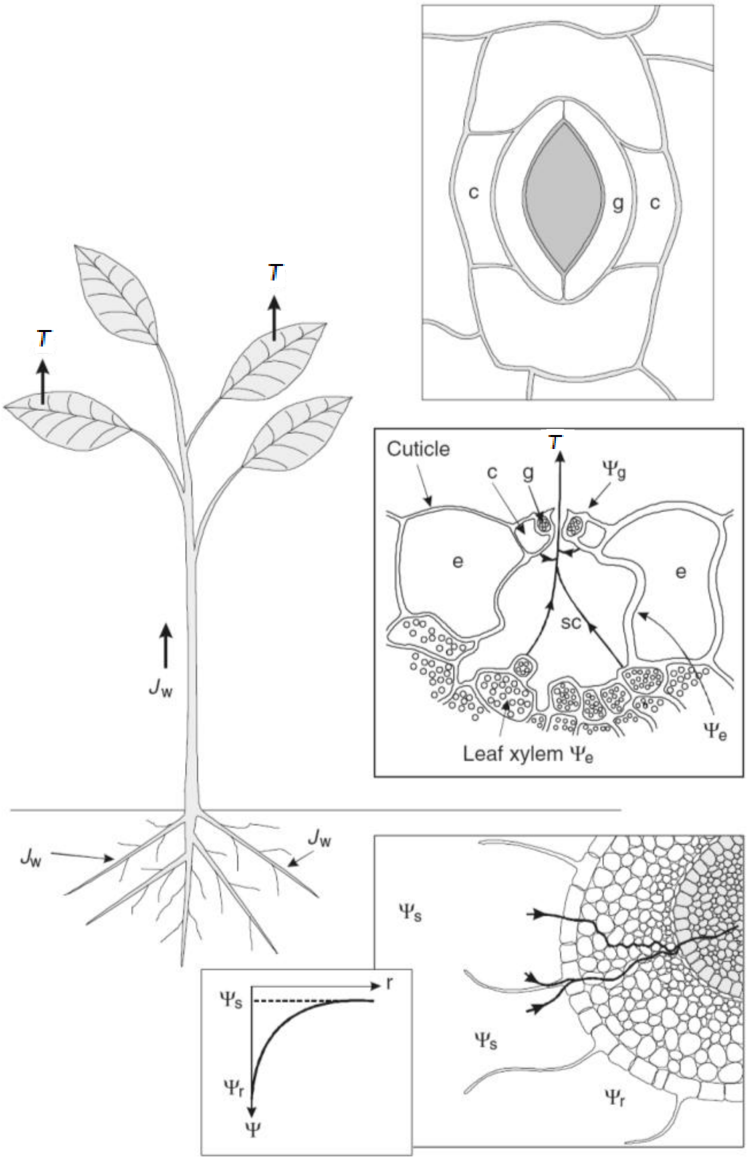

Figure 1.4 Schematic drawing of water movement in plants (Leuning et al. 2004).

1.1.4 Stomatal control on water loss from transpiration

Plants are able to actively regulate their water loss by transpiration through the control of stomatal aperture (Figure 1.4) (Mansfield 2004). This stomatal aperture is regulated by different factors of which the most important are soil moisture content and relative humidity (RH) and it induces both a loss of water and an increase of internal CO_2 concentration (Whitehead 1998, Porporato et al. 2001, Hosy et al. 2003, Leuning et al. 2004). Therefore, for a plant to thrive, it is important that it is able to open its stomata as freely as possible. If, due to water stress, the tree cannot freely regulate stomatal aperture, the tree will not be able to use its photosynthetic apparatus to its full extend.

The observation of stomatal resistance throughout the day reveals a lot about how a tree reacts to the prevalent conditions in function of both the environmental variables and the water status of the tree. Typically for C3- and C4-plants, stomatal opening occurs in the beginning of the day when light reception by the leaves is initiated and stomata are closed again when light disappears after sunset (Ibrahim et al. 2008). Throughout the day, stomata can react in different ways. Stomata can be fully opened when conditions are most interesting for photosynthesis, i.e. when light reception is high. However, when the water demand is too high, the tree can prevent excessive water loss by closing the stomata, partially or completely (Slatyer 1969, Dolman and Van Den Burg 1988, Zweifel et al. 2002, O'Brien et al. 2004). This phenomenon is called midday stomatal closure and is encountered in a wide variety of species (Dolman and Van Den Burg 1988, Bond and Kavanagh 1999, White et al. 2000, Zweifel et al. 2002).

Although the mechanism of stomatal regulation is still not completely understood, it is supposed that both feedback and feed-forward regulation exist (Porporato et al. 2001). The feedback control is induced when water stress is already present. The structure of the guard cells will cause a stoma to close when a loss of turgor occurs as a result of a lowered water content in the guard cells (Hosy et al. 2003, Leuning et al. 2004). The feed-forward control will initiate an action before water stress is present. The mechanism induces the formation of abscisic acid (ABA) at the level of the roots when a low level of soil moisture content is detected (Tardieu and Simonneau 1998, Porporato et al. 2001). However, in case of mangroves, it is not so much soil moisture content that matters for the water relations, but rather soil water availability because of the high salinity. ABA is transported to the leaves where it induces a decrease in guard cell turgor. Hence, the stomatal aperture is lowered and the water loss to the atmosphere decreases. Another feed-forward control is the reduced stomatal aperture in reaction to a decline in relative atmospheric humidity to prevent a sudden rise in transpiration and thus in water loss (Porporato et al. 2001).

1.1.5 The numbers tell the tale

It needs to be emphasized that water stress is the most prevalent stress (Bohnert et al. 1995, Coder 1999). Nevertheless, plants can suffer from many other stress factors, such as too much or too little light, low or high temperatures, drought and flooding, salinity, nutrient shortage or infection and predation (Bohnert and Sheveleva 1998). Therefore, a good water household is essential for the health of trees. In order to understand the physiological mechanisms of trees, knowledge and understanding of water relations is essential and this study aims to improve the understanding of the physiological behavior of the mangrove species *Rhizophora stylosa* with respect to water.

For a better understanding of these water relations, different techniques are required to measure several characteristics of the tree. Tree sensors have been developed and widely used since the previous century (Scholander et al. 1965, Boyer 1968, Kanemasu et al. 1969, Smith and Allen 1996, Drew and Downes 2009, Vandegehuchte and Steppe 2013). Sap flow velocity and sap flux density can be measured with sap flow sensors, water potential with psychrometers and pressure bombs, stomatal resistance with porometers and stem diameter changes with dendrometers.

1.2 Stem growth patterns

1.2.1 Diurnal growth patterns

The continuous measurements (e.g. every 10 minutes) of the stem radius comprises a lot of information. Both reversible shrinking and swelling as irreversible growth can be monitored (Kozlowski and Winget 1964, Irvine and Grace 1997, Deslauriers et al. 2007a, Scholz et al. 2008). Typical circadian patterns can be observed on a small time scale, these patterns typically consist of three distinct phases, namely the shrinkage phase, recovery phase and increment phase (Downes et al. 1999).

After dawn, when transpiration commences, a tree stem will start to shrink (Figure 1.5). Transpiration is located in the canopy of the tree (Figure 1.4) and regulated by stomata on the leaves (Lee 1967, Porporato et al. 2001, Mansfield 2004). As already mentioned, the phenomenon of transpiration consists of a trade-off between the loss of water and the uptake of CO_2 (Scarth 1927, Hosy et al. 2003, Leuning et al. 2004, Ainsworth and Rogers 2007, Katul et al. 2010). Due to the distance and hydraulic resistance between the canopy, where the loss of water is situated, and the roots, where the uptake of water occurs, daily stem growth is a dynamic process (Figure 1.4) (Herzog et al. 1995, Goldstein et al. 1998, Zweifel and Häsler 2001, Scholz et al. 2008). During the shrinkage phase, trees use their internal water reserves from storage tissues. The depletion of these reserves results in shrinkage of the stem diameter. The shrinkage phase will end when the water uptake equals the water demand needed for transpiration (Goldstein et al. 1998, Downes et al. 1999)

The next phase described by Downes et al. (1999) is the recovery phase (Figure 1.5). In this phase the water uptake at root level is higher than the water loss in the canopy. Hence, the depleted water reserves are replenished and simultaneously cell turgor is regained. The end of this phase is marked by a radial diameter equal to the diameter at the beginning of the shrinkage phase.

Typically, the third phase is the increment phase, in which the tree diameter exceeds the maximal diameter reached at the end of the previous circadian cycle (Figure 1.5) (Downes et al. 1999). In other words, during the increment phase stem growth occurs. Lockhart (1965) introduced a model of plastic growth in which a wall-yielding threshold value is defined. The turgor pressure inside the cells must exceed this value to be able to elongate and to result in net growth. Of course, net growth does not always occur and it is possible that the stem diameter is smaller the next morning. In this case the tree has not been able to replenish its entire water reserve, which indicates a bad water household (Herzog et al. 1995, Deslauriers et al. 2007a, Deslauriers et al. 2007b).

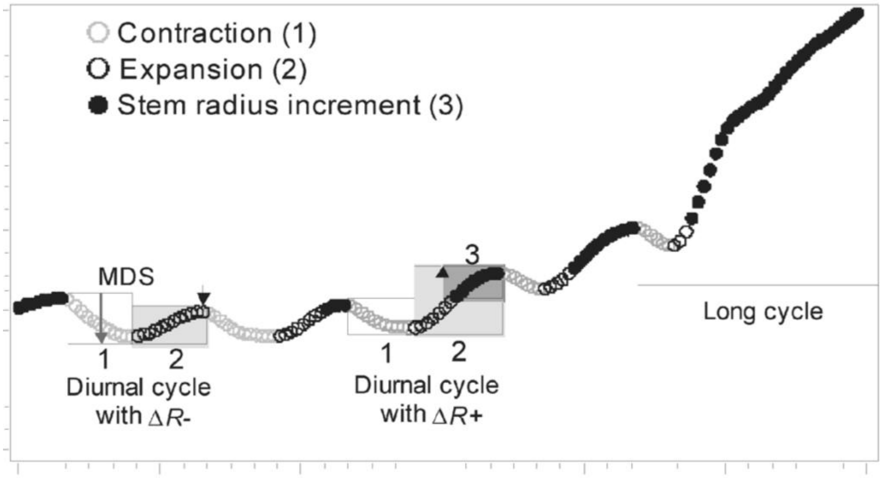

Figure 1.5 A typical circadian course of stem radius with a shrinkage phase (1), a recovery phase (2) and an increment phase (3). Rainfall induces a long cycle and then the typical circadian pattern is no longer visible for some time. Maximum daily shrinkage (MDS) is an important factor for analyzing dendrometer data. Both days with positive growth (ΔR+) as days with negative growth (ΔR-) are shown (Deslauriers et al. 2007a).

Hitherto, the experiments and measurements performed in literature all report the same course of diurnal growth patterns as previously described (Kozlowski and Winget 1964, Klepper et al. 1971, Brough et al. 1986, Herzog et al. 1995, Irvine and Grace 1997, Downes et al. 1999, Zweifel et al. 2000, Genard et al. 2001, Offenthaler et al. 2001, Perämäki et al. 2001, Sevanto et al. 2001, Zweifel and Häsler 2001, Deslauriers et al. 2003, McLaughlin et al. 2003, Bouriaud et al. 2005, Daudet et al. 2005, Steppe et al. 2006, Čermák et al. 2007, Deslauriers et al. 2007a, Deslauriers et al. 2007b, Xiong et al. 2007, Drew et al. 2008, Scholz et al. 2008, Drew and Downes 2009, Fernández et al. 2011). All foregoing research presents results which show the classical pattern on many different species. They describe the phases previously discussed, namely shrinking tree stems after dawn, a recovery phase when transpiration becomes less intensive (typically right after noon) and a nocturnal period of growth. This net growth will not occur in periods of bad water household during for instance drought or high temperature and can result in net shrinkage of the stem (Herzog et al. 1995, Deslauriers et al. 2007a, Deslauriers et al. 2007b). However, some researchers reported different stem growth patterns. Matimati et al. (2012) describes the growth pattern of plants using the crasulacean acid metabolism (CAM) that show growth initiated by sunrise, a maximum in stem diameter at noon followed by shrinkage until night or the next morning. Unfortunately, there have not been a lot of studies that focuses on gathering small time scale and high resolution stem radius data on CAM-plants. More studies on different species could expose more atypical stem growth patterns.

1.2.2 Sap flow and its influence on water depletion and replenishment

Daily fluctuations of the stem radius are mainly caused by differences in water content of the stem storage tissues. This indicates the utility of sap flow measurements because there is a clear diurnal relationship between sap flow and stem size (De Swaef and Steppe 2010). Both the period and the amount of sap flow can be related to stem diameter patterns (Herzog et al. 1995, Scholz et al. 2008). A good way to demonstrate this is by measuring sap flow in the canopy (through branches) and in the stem (Figure 1.6 a). In most cases the branch sap flow increases earlier than the basal sap flow which confirms that the take up of water lags behind the loss of water. The upper sap flow initiates earlier than the basal sap flow and therefore there is a net loss of water during the beginning of the day, which results in a decrease of the stem diameter. Some time period later, the basal sap flows begins to rise as well, mostly with the same sequence as the branch sap flow. When the basal sap flow becomes higher than the upper sap flow, the recovery phase is induced and the water storages are replenished again. A good way of coupling these sap flow and dendrometer data is by subtracting basal sap flow from branch sap flow (Figure 1.6 b). Doing so, the amount of water depleted and replenished is visualized (Schulze et al. 1985, Goldstein et al. 1998, Perämäki et al. 2001, McLaughlin et al. 2003, Meinzer et al. 2004, Steppe and Lemeur 2004, Čermák et al. 2007, Scholz et al. 2008).

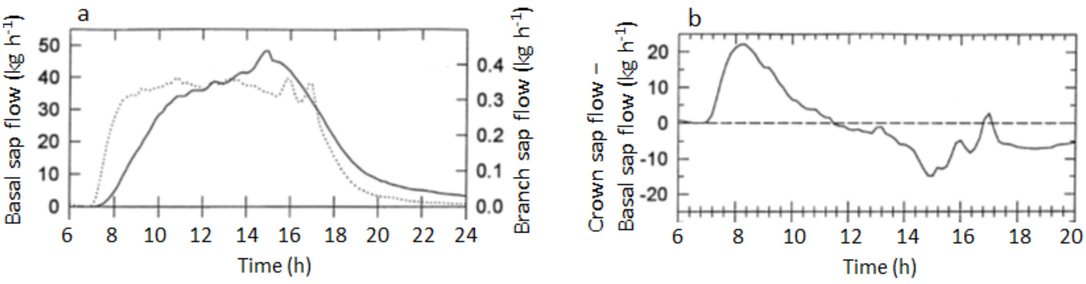

Figure 1.6 A typical curve of the branch sap flow (dotted line) and a lagging basal sap flow (solid line) (a). By subtracting the two different flows the water budget of the tree is visualized (b). A positive value represents a depletion of water storage, whereas a negative value indicates the replenishment of the water storage (Goldstein et al. 1998).

These diurnal patterns can be described as well by combining information gathered from sap flow and transpiration. The amount of transpiration can be calculated for instance by using stomatal conductance data (Schulze et al. 1985) or via measurements of water content of an air flow in a controlled measuring chamber (Steppe and Lemeur 2004). Plotting the transpiration to the average stem sap flow and connecting the successive points is an alternative for visualizing the daily cycle (Figure 1.7) (Schulze et al. 1985). In the morning the amount of transpirations rises quickly, whereas the stem flow remains low for quite a while. Later, transpiration stays roughly the same but the stem flow increases. When the transpiration begins to decrease, stem flow remains fairly high. As a result, a net water uptake takes place in the tree. The shrinkage phase and the recovery phase (in this case both recovery and increment phase) are distinguished by the identity line (transpiration equals stem flow). Shrinkage takes place at the points of time below the identity line and the recovery phase at the point in time above this line (Schulze et al. 1985).

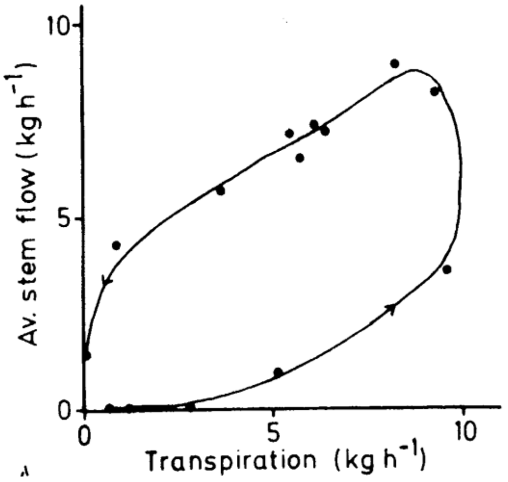

Figure 1.7 The relation between transpiration and stem sap flow changes throughout the day. The first phase indicates water depletion and the second phase water replenishment (Schulze et al. 1985).

1.2.3 Microclimatic factors are the main drivers for plant water household

The foregoing clearly shows that a relation must exist between stem radius dynamics and climatic factors influencing transpiration and soil dynamics. Therefore a lot of work has been put in the research of relating the variations in radial growth patterns to microclimatic factors (Downes et al. 1999, Tardif et al. 2001, Deslauriers et al. 2003, Mäkinen et al. 2003, Bouriaud et al. 2005, Zweifel et al. 2006, Deslauriers et al. 2007a). Nevertheless the interaction between weather conditions and the physiological activity are still not fully understood and are not self-evident. It has been found that the response to climatic variables changes from time to time (e.g. season to season) (Downes et al. 1999, Tardif et al. 2001, Bouriaud et al. 2005). Especially correlations on daily base are difficult to assess (Downes et al. 1999). When the different diurnal phases of stem growth (shrinkage, recovery and increment) are examined, many different factors come in play. Therefore, it is useful to analyze each phase seperatly (Downes et al. 1999, Deslauriers et al. 2003, Deslauriers et al. 2007a). This way, Deslauriers et al. (2003) found that prevailing weather conditions during the expansion and stem radius increment (SRI) phases, which take place from evening till morning, have a great significance to the extent and course of these phases. For both phases, they found significant positive correlations for the maximum air temperature and amount of precipitation, while a negative one was found for solar radiation. Precipitation had significant effects on the expansion phase, the SRI phases and the entire cycle. For the recovery phase it was shown that vapor pressure deficit (VPD) had a negative effect on the tree stem radius (Deslauriers et al. 2003). Other research (Tardif et al. 2001) showed other factors affecting the radial growth, such as, soil temperature, minimum air temperature and foliage water potential. Also soil water deficit influenced the daily stem radius dynamics because it prevented a fluent water uptake (Bouriaud et al. 2005). These findings indicate that microclimatic variables have a very complex way of influencing and interacting with tree water relations.

It is well known that rain has an extensive effect on trees (Downes et al. 1999, Drew et al. 2008, Zeppel et al. 2008). The influence of precipitation on most species is explained by Downes et al. (1999) by examining the effect of rain on the different phases of daily stem growth. When it rains, there is a swift radial expansion and a subsequent slower shrinkage phase. This response does not occur when irrigation is applied, which proves that not only the extra water availability in the soil is responsible for the radial increase. Downes et al. (1999) concluded that this response is caused by transpiration that is halted, while water availability at root level is high because of the moistening of the soil by rainfall. This ensures that the tree can operate at full turgor for a longer period than usual, which extends the growth period as depicted in Figure 1.2.

1.3 Mangroves

1.3.1 Introduction

Mangroves are a very unique group of trees that live in the intertidal zone of tropical and subtropical seas and oceans and that are confronted with recurrent flooding (Scholander et al. 1962, Lawton et al. 1981, Robert et al. 2009). These conditions have presented vegetation with great challenges, but mangroves have adapted to these harsh surroundings. Even in ancient times the harsh environments were already recognized to be very hostile towards plants (cf. citation of Plutarch, 70 AD).

> *"What is the reason that seawater nourishes not trees? Is it not for the same reason it nourishes not earthly animals?...Nor, though seawater be aliment to marine plants as to its fishes, will it therefore nourishes earthly plants, since it can neither penetrate the roots, because of its grossness, nor ascend, by reason of its weight...Or is it because drought is a great enemy of trees?"*
>
> Plutarch, 70 AD (translated by Bowman 1917)

The main challenges in these regularly flooded areas are anoxic conditions when flooded, high temperature and irradiance and high levels of salinity (Ball 1988, Medina 1999, Kathiresan and Bingham 2001, Robert et al. 2009). Most trees are not able to withstand high salt concentrations and are damaged or even killed when confronted with elevated salinity (Allen et al. 1994). (True) mangroves on the contrary thrive under conditions of elevated salinity and cannot survive in the absence of a certain amount of NaCl (Medina 1999).

Mangrove communities are not only fascinating because they can flourish despite these challenges, but at the same time they have a very important ecological function. This makes the research on how mangroves survive in these harsh conditions relevant in both a physiological and an ecological perspective.

A possible way of evaluating the importance of mangroves is by quantifying their economic value (Lal 2003). Mangroves can deliver certain services such as construction wood, fuel, tannins or medicines, local fisheries, nursery habitat and marine productivity. Their physical presence can stabilize the underlying land, buffer seagrass beds and coral reefs against river-borne siltation or offer protection for coastal areas against storms, sea-level rise and tsunamis (Kelly and Adger 2000, Kathiresan and Bingham 2001, Dahdouh-Guebas et al. 2005, Wells et al. 2006, Duke et al. 2007, Walters et al. 2008). Furthermore, mangal systems contribute significantly to both marine and terrestrial food webs and any decline in the functionality of marine food webs will, in turn, cause a decline in fishery yield. Finally, mangrove territory can be considered as an important CO_2 sink and carbon source for oceans because they have a very high primary productivity (Duke et al. 2007). All these services indicate that mangrove are valuable, with a valuation of US$ 200,000 - 900,000 per km² as calculated by Wells et al. (2006). Nonetheless mangrove areas are declining extremely rapidly at an alarming rate of 1 to 2% per year, according to Duke et al. (2007).

1.3.2 Classification

The classification of mangroves, according to Tomlinson (1995), consists of 8 families (which are mostly not closely related phylogenetically), 13 genera and 39 species and are presented in Table 1.1 (Blasco et al. 1996, Medina 1999). Throughout this elucidation on mangroves, there will be special interest for *Rhizophora stylosa*, the tree on which the experiments in this study were conducted.

Table 1.1 Classification of mangrove tree species. R. *stylosa* is underlined (Lugo and Snedaker 1974, Tomlinson 1995, Medina 1999).

Family	Genera	Species
Anniaceae		
	Avicennia	9
Combretaceae		
	Conocarpus	1
	Laguncularia	1
	Lumnitzera	3
Meliaceae		
	Xylocarpus	3
Myrsinaceae		
	Aegiceras	2
Pellicieraceae		
	Pelliciera	1
Plumbaginaceae		
	Aegialitis	2
Rhizophoraceae		
	Bruguiera	6
	Ceriops	2
	Kandelia	1
	Rhizophora	3 (*stylosa*)
Sonneratiaceae		
	Sonneratia	5

1.3.3 Distribution

The distribution of mangroves is shown in Figure 1.8 and mangroves are situated on the coast lines of tropical and subtropical areas. As Giri et al. (2011) ascertains, Australia has an area of 977,975 ha that is covered with mangroves. This represents 7.1 % of the total area of mangroves in the world, which makes Australia the country with the second biggest area of mangrove communities.

Indonesia is the country with the largest surface area covered with mangroves, with 3,112,989 ha or 22.6 % of the world total (Giri et al. 2011).

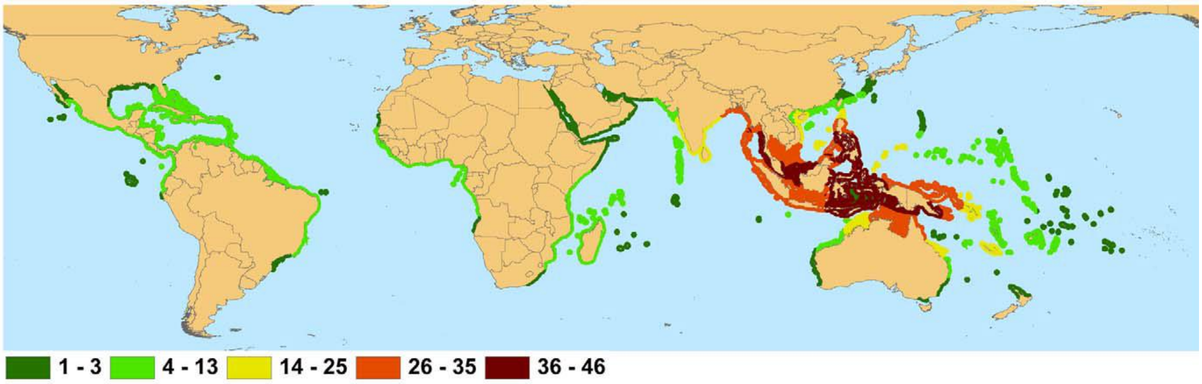

Figure 1.8 The colored bands represent the amount of mangrove species that are found at that location. Mangrove communities are situated around tropical and subtropical latitudes (Polidoro et al. 2010).

The species *Rhizophora stylosa* is situated in Northern Australia and Southeast Asia. The distribution of *R. stylosa* and other species of the genera *Rhizophora* in the Indo West Pacific is presented in Figure 1.9. *R. stylosa* is present in the area roughly between 23.5°N - 23.5°S and 100°E - 190°E (Duke et al. 2002).

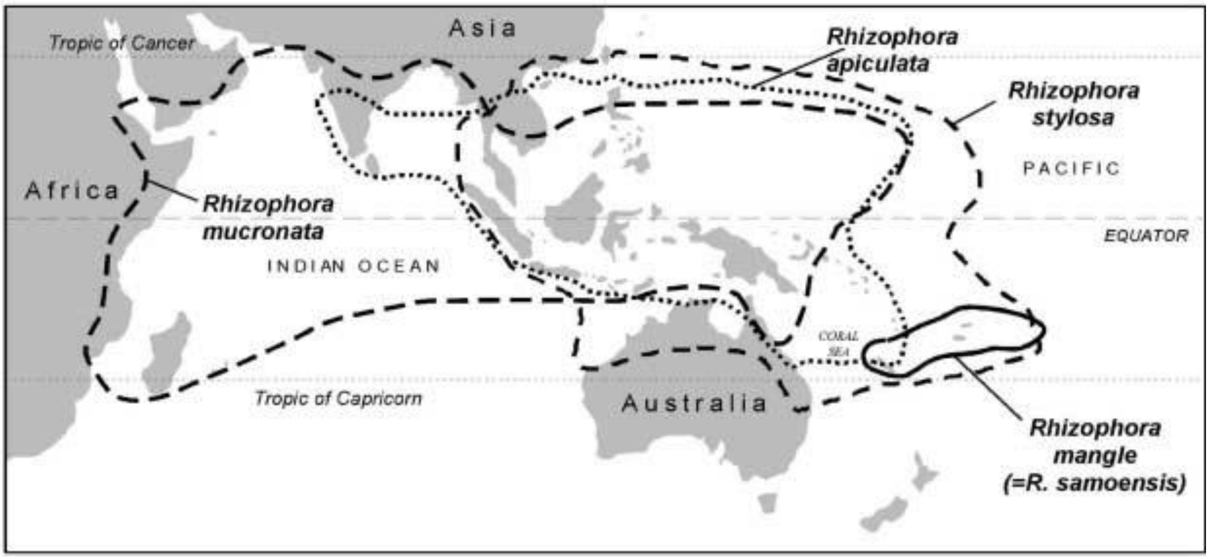

Figure 1.9 Areas where different *Rhizophora* species, including *R. stylosa*, can be found in the Indo West Pacific (Duke et al. 2002).

1.3.4 Root system

Because mangroves are flooded on a regular base, the oxygen supply to the roots is limited. This can interfere with the respiratory metabolism in root cells because diffusion of oxygen is 10,000 times slower through water than through air (Ball 1988). To have as much oxygen as possible to their disposal most species produce strongly aerenchymatic aerial roots. Mangrove species have come up with several solutions such as pneumatophores (e.g. *Avicennia marina,* Figure 1.10a) and stilt roots (e.g. *Rhizophora stylosa,* Figure 1.10b) (Scholander et al. 1955, Tomlinson 1995, Medina 1999). Root "extensions" make sure that the tree can take up enough oxygen and dispose of the produced CO_2 when the roots are exposed to air (Medina 1999).

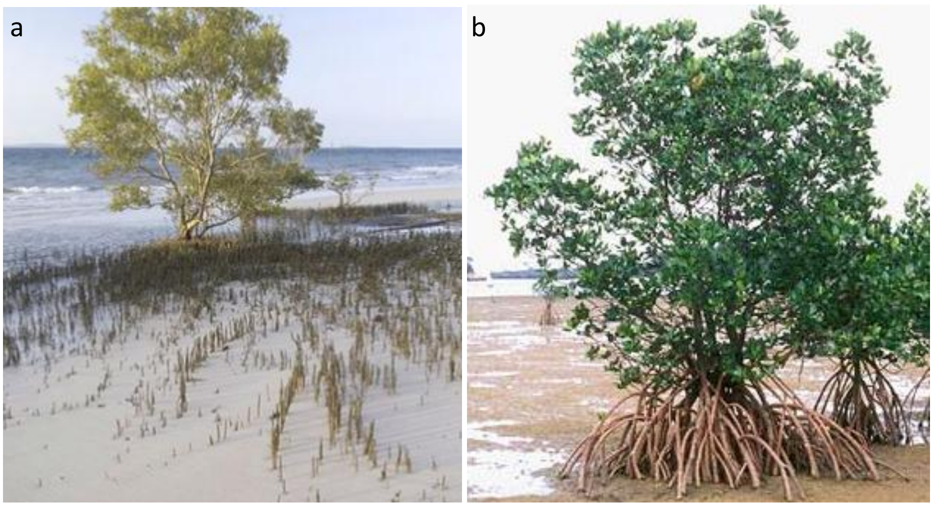

Figure 1.10 *Avicennia marina* (a) with a lot of pneumatophores and *Rhizophora stylosa* (b) with stilt roots.

1.3.5 Mangroves have to face many challenges

Although water is present in large quantities and it might not be expected that mangroves encounter water stress, this water is not easily available. The high salinity of seawater is responsible for the strong osmotic potential of seawater and results in a negative water potential (Ω ≈ -2.5 MPa). If trees want to use this water, they need to be able to pull the water up through the roots and into the xylem vessels, which implies they need to maintain water potentials even lower than -2.5 MPa (Scholander et al. 1964, Scholander 1968). Xylem pressures in *Rhizophora* spp. range from -3.0 to -4.5 MPa as reported by Scholander (1968) and Aziz and Khan (2001) demonstrated a xylem pressure of about -2.7 MPa in *R. mucronata* and a water potential of approximately -5.5 MPa in the leaves which are low values compared to non-mangal species. The review on whole-plant water use composed by Wullschleger et al. (1998) describes normal water potentials between 0 and -2 MPa and describes xylem dysfunction for certain species for water potentials below -2.5 to -2.8 MPa. This clearly demonstrates that mangroves operate at extremely negative water potentials without deterioration of the tree. Lacking proper adaptations, mangroves would never be able to sustain positive turgor inside living cells. Therefore, cell turgor in mangroves is dependent on a very high solute pressure inside the cell, often exceeding the seawater pressure by -1 to -3 MPa (Scholander 1968, Ball 1988).

Mangroves are often divided into two types, as proposed by Scholander et al. (1962), namely salt excluders (or non-secretors) and salt secretors. The former type mainly uses the process of ultrafiltration at root level to maintain a relatively low salt concentration in the sap. This concentration is a lot lower compared to pure sea water, though still a lot higher than in other tree species (Scholander et al. 1964, Scholander 1968, Parida and Jha 2010). The latter type filtrates less salt at root level (because of a less efficient ultrafiltration), resulting in higher sap concentrations, but these mangroves secrete salt at leaf level through specially designed salt glands. The salt concentration in xylem sap in mangrove species is determined in the range of 0.2 to 0.5 g NaCl/L in salt excluders and 0.8 - 8.0 g NaCl/L in salt secretors (Scholander et al. 1962, Popp 1984, Medina 1999). It is clearly demonstrated that root ultrafiltration is performed at a high efficiency if these sap concentrations are compared to the sea water concentration, which is about 36 g NaCl/L (Scholander et al. 1962, Scholander et al. 1964, Scholander 1968, Lawton et al. 1981, Popp 1984, Ball 1988, Medina 1999, Parida and Jha 2010). Further, a third major tactic is displayed by mangroves, namely the accumulation of salt in their leaves and other tree parts (Scholander 1968, Popp 1984, Parida and

Jha 2010). Older leaves have a higher salt concentration and in response, these leaves will increase their succulence in order to maintain a constant salt concentration inside the leaves, more specific, inside the vacuoles of leaf cells (Popp 1984, Ball 1988, Medina 1999). But even an increasing succulence cannot account for dealing with all the salt entering the tree. Therefore a dilutionary effect is proposed by Popp (1984) in which not only leaves accumulate ions but also transport them to other parts of the tree for accumulation. Many species use a combination of the foregoing tactics, summarized in the review by Parida and Jha (2010). *Rhizophora* is a salt-excluder and accumulator.

Another typical challenge mangroves need to cope with is the combination of high temperature and high irradiance originating from their (sub)tropical location. These conditions result in a high atmospheric water demand and consequently in the risk of damaging the photosynthetic apparatus and failure of the leaf functions due to overheating. Next to the variable control of stomatal regulation, as previously described, mangroves have developed some anatomical changes in their leaves to deal with possible overheating (Medina 1999). An increased leaf angle reduces the projected area, hence, reduces the incident radiation per area leaf. Another adaptation of mangroves is the production of small leaves which results in an enhanced boundary layer conductance and therefore, a smaller temperature difference between ambient air and leaf temperature and thus reducing the chances of overheating. Finally, mangroves have high heat capacities per leaf area. This helps reducing the temperature differences between the leaf and ambient air. This higher heat capacity is obtained by producing leaves with a high succulence (Ball 1988), such as the leaves of *Rhizophora stylosa*.

1.3.6 Anatomical adaptations make mangroves less vulnerable to cavitation

Previously, it is mentioned that mangroves need to maintain very negative water potentials in order to transport water up to the leaves. Obviously, these very negative water potentials create a very severe tension on the water column. Therefore, the prevention of cavitation is an important issue for mangroves and this has resulted in different strategies concerning hydraulic architecture. Trees can vary their vessel radius and their vessel density. A higher vessel density creates more possible bypasses in the event of cavitated vessels and gives the tree the opportunity to produce vessels with a lower radius which are less prone to cavitation, as proven by Lo Gullo et al. (1995). Robert et al. (2009) explained the zonation of *Avicennia marina* and *Rhizophora mucronata* based on differences in their hydraulic anatomy. They showed that on the one hand *A. marina* had a much safer hydraulic architecture because its vessels were narrower and more abundant. On the other hand, the hydraulic architecture of *R. mucronata* was much more efficient. The safer architecture of *A. marina* made this species able to thrive under more saline conditions. On the locations where salinity was low enough *R. mucronata* was the stronger competitor, due to the less safe but more efficient architecture, and barely any *A. marina* was found. (Robert et al. 2009). The final distribution for this case is presented in Figure 1.11.

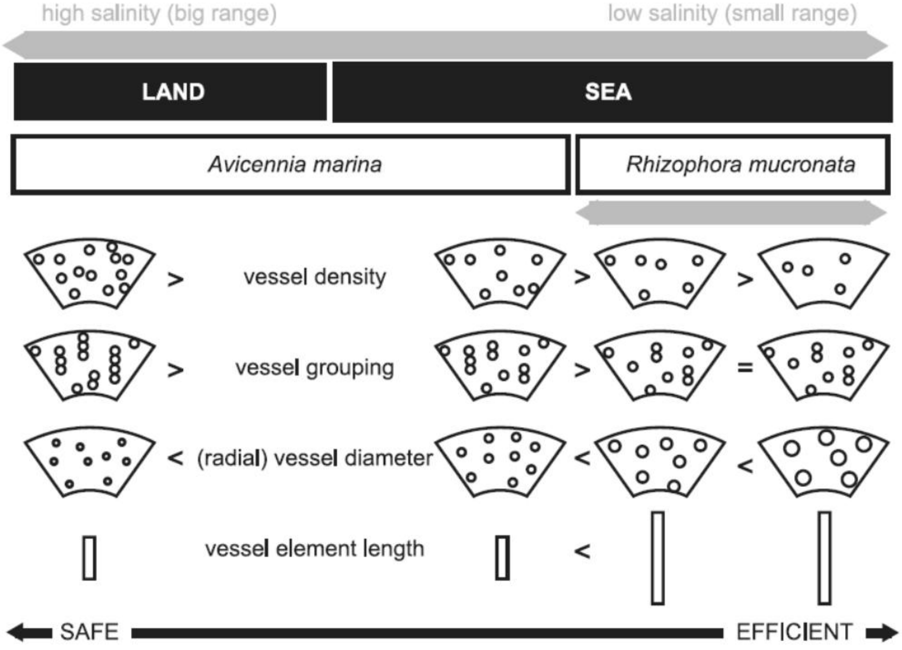

Figure 1.11 Zonation of *Avicennia marina* and *Rhizophora mucronata* linked with several possible vessel designs. Safer and less efficient hydraulic structure is found in more saline, in general more inland, regions. The safer vessels are less prone to cavitate, hence they are located in more saline places. Possible safety features are (i) a higher vessel density and (ii) high vessel grouping, both offering more possible bypasses in the event of cavitation, (iii) a smaller vessel diameter and (iv) a smaller vessel element length. (Robert et al. 2009)

The zonation of different species is typical for mangroves because most species are very sensitive to the rapidly environmental changes such as inundation frequency, waterlogging, nutrient availability and soil salinity (McKee 1993, Blasco et al. 1996). Intuitively, it might be expected to find the highest soil salinity closest to the sea and the lowest salinity furthest from the sea. In reality, however, those locations that are inundated every day will have a nearly constant salinity while salt concentrations in regions that are less frequently flooded fluctuate much more due to evaporation. This evaporation process removes water from the soil but leaves salt particles behind, increasing the salt concentration (Robert et al. 2009). This creates a very distinct transition between mangal vegetation and the more inland vegetation which typically is a mudflat, a salt marsh, a brackish forested wetland or a dryland forest (Adam 1994).

1.3.7 Mangrove response to climate change

Mangrove systems have a great ecological importance. They serve as a habitat for a large number of molluscs, crustaceans, birds, insects, monkeys, and reptiles, trap pollutants and sediment and contribute to human services (as depicted in 1.3.1 Introduction). Therefore it is meaningful to prospect how and in what extent climate change could affect mangroves. The most important direct effects of climate change on ecosystems, as determined by McLeod and Salm (2006) and Field (1995), are changes in temperature, CO_2 concentration, hurricane and storm frequency and intensity, precipitation and sea-level. The temperature is expected to rise but it is not expected that this will harm mangroves. Mangroves might even be able to extend their region of occurrence to areas further away from the equator (both southward as northward) (McLeod and Salm 2006). Another prospect is a rise in CO_2 concentration caused by a massive anthropogenic input of additional CO_2 in the atmosphere, caused by the usage of fossil fuels. A possible effect of such a rise is that photosynthesis enhances and the level of stomatal aperture needed for adequate CO_2 uptake reduces and consequently, the amount of water that transpires will reduce and growth will increase (McLeod and Salm 2006, Ainsworth and Rogers 2007, Alongi 2008, Taub 2010). Ball et al. (1997) demonstrated enhanced growth on *R. stylosa* under conditions of low salinity. However, in the review of Alongi (2008) on the response of mangroves to climate change, it was predicted that the primary production will not or hardly change. Augmented water use efficiency and an advanced flowering period are forecasted as the positive effects of a CO_2 concentration rise. The main outcome would probably be the alteration of species patterns and occurrence. An indirect effect of rising temperature and rising CO_2 levels is the bleaching and reduced growth of coral reefs (Hoegh-Guldberg 1999). These reefs shelter mangroves against damage induced by waves and a decline of reef area will cause an adverse effect on mangrove population (McLeod and Salm 2006). In case of increased precipitation, mangroves are expected to be more successful and vice versa (Alongi 2008). The net effect of change in precipitation due to climate change is difficult to foresee because the prediction about precipitation is location dependent. For some regions an increase in precipitation is expected, whereas other regions are expected to receive less precipitation, and furthermore predictions on future precipitation have turned out to be very difficult and error-prone (Hughes (2003) made projections for the Australian climate). Hurricanes and storms will probably increase in frequency and these events can cause grave damage to mangrove systems. Not only physical damage but also indirect effects such as waterlogging and inundation, changes in salinity or even altered soil structure can lead to the deterioration of mangroves (McLeod and Salm 2006). The heating up of seawater and the melting of glacial ice will both lead to a rising sea-level. This will be the most radical challenge mangroves have to cope with, because of the sensitivity towards sea-level rise induced changes, such as salinity and inundation. This will create threats, causing mangrove areas to disappear, and opportunities for expansion, however to profit from these opportunities, the rise should be slow enough in order for mangroves to adapt (Field 1995, McLeod and Salm 2006).

It can be concluded that mangrove systems contribute significantly to the well-being of the earth. These systems may be relatively small qua coverage, but they are very important in both aquatic and terrestrial processes and equilibria. Furthermore, mangrove systems are extremely sensitive to changing conditions and are decreasing at an alarmingly rate. Proper knowledge and extensive research and surveying could help to gather more information on mangroves, on how to prevent further destruction and it could even help researchers in proposing adequate restoration strategies.

Chapter 2: Materials and Methods

2.1 Study area

Different sensors were installed on three trees of the species *Rhizophora stylosa*. These trees were located on North Stradbroke Island, an Australian island, 30 km southeast of Brisbane, the largest city and capital of the state of Queensland. North Stradbroke Island is the largest island in the Moreton Bay and is the second largest sand island in the world. It is one of the islands that acts as a barrier between the Pacific Ocean and Moreton Bay.

The study area was located on the bay side of the island between the towns Dunwich and Amity. The mangrove forest was sheltered from strong waves because of the presence of sand banks near the shore and its bayside orientation. More specifically, the research site was located 2,100 m north of the river mouth of Myora Spring, at 27° 27' 3.25"S and 153° 25' 47.70"E.

In the study area, the three trees were located in the central part of a mangrove forest strip. The elevation of the land was approximately 1.8 m above sea level. The studied site was a less dense part of the mangrove forest with a mixture of *Rhizophora stylosa* and *Avicennia marina*. Adjacent to this less dense part there were dense mangrove forest which consisted of only *R. stylosa*. The trees were labeled from 1 to 3 as represented in Figure 2.1.

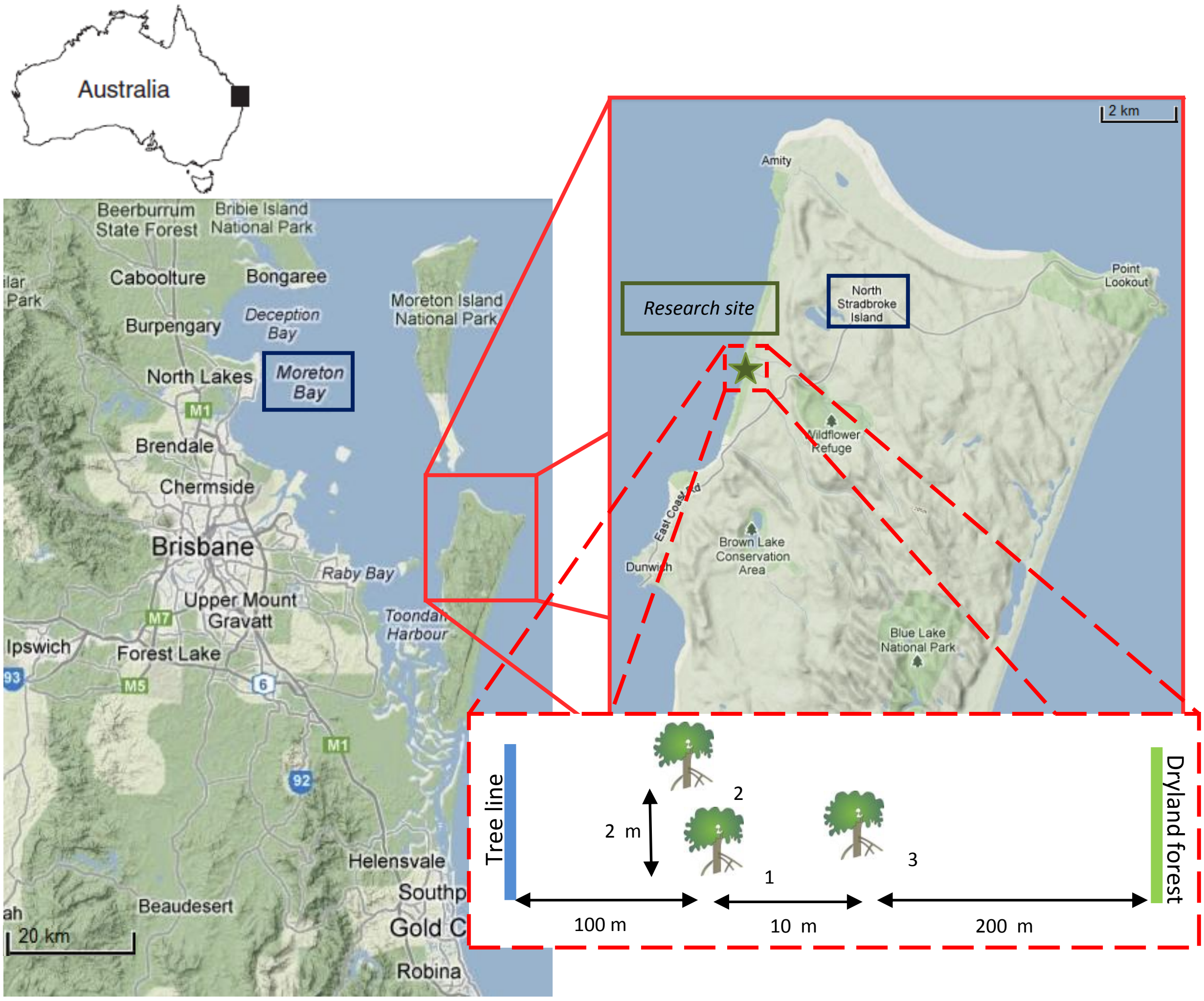

Figure 2.1 Overview of the study site location. The research site is represented by a star. A detailed schematic of the site is represented in the lower box and the trees are labeled with their according number.

Details of the dimensions and placement of the sensors are shown in Table 2.1 and the position of the trees is shown in Figure 2.2. The trees were similar in size and thickness, although *R. stylosa* 2 was somewhat less thick than the other two (Table 2.1). The field experiment was conducted during a period of approximately two months (from 10 August 2012 to 12 October 2012) (day of year (DOY) 223-286).

Table 2.1 Details of the position of the roots and tree sensors. The psychrometers were reinstalled several times so those values are rather indicative.

	R. stylosa 1		*R. stylosa* 2		*R. stylosa* 3	
	Height (cm)	Circumference (cm)	Height (cm)	Circumference (cm)	Height (cm)	Circumference (cm)
Highest stilt root	80 ± 1	-	64 ± 1	-	50 ± 1	-
Dendrometer	145 ± 1	59 ± 1	143 ± 1	35 ± 1	160 ± 1	54 ± 1
HRM 1	138 ± 1	59 ± 1	136 ± 1	35 ± 1	152 ± 1	54 ± 1
HRM 2	260 ± 1	53 ± 1	217 ± 1	34 ± 1	300 ± 1	45 ± 1
Psychrometer	350 ± 1	8.0 ± 0.1	290 ± 1	16.0 ± 0.1	260 ± 1	6.2 ± 0.1

Figure 2.2 Picture of the research site with three *Rhizophora stylosa* trees that were equipped and that are indicated by arrows. The black cases that are visible in some trees that are not measured are Pelican cases, used for protecting the

2.2 Meteorological data

Two meteorological stations were installed in the vicinity of the research site. These station were geared with different types of meteorological sensors in order to measure environmental variables. The first station was placed inland some distance from the site, in the transition zone, characterized by juncus vegetation, between the mangrove forest and the dryland forest. This EnviroStation, constructed by ICT International (Armidale, New South Wales, Australia), was provided with sensors to measure solar radiation, air temperature, atmospheric relative humidity and rainfall. Solar radiation could be measured in the range 0 – 2,000 W m^{-2} with a resolution of 0.1 % and an accuracy of ± 5 % of the measured value. Air temperature could be recorded between -20 and 60 °C with a resolution of 0.01 °C and an accuracy of 0.1 °C. The relative air humidity could be determined in a range of 0 - 99 % with 0.1 % resolution and ± 2 % accuracy. The rain gauge was only used in the period DOY 222 - 245, when no rainfall occurred and so further specifications are not necessary. Readings on all these parameters were taken every 15 minutes, during DOY 222 - 285.

The second meteorological station, on site, was a HOBO Weather Station Starter Kit made by MicroDAQ.com Ltd. (Contoocook, New Hampshire, USA) and measurements were obtained during DOY 245 -285 (Figure 2.3). The station was placed in a forest gap to prevent influence from vegetation on radiation measurements. This station measured radiation with 2 silicon pyranometers, both measuring in the range of 0 to 1,280 W m^{-2} with a resolution of 0.1 W m^{-2} for light with a wavelength of 300 to 1,100 nm and an azimuth error of ± 2 % at 45° from vertical (this error is the result of differences between measurements before noon and after noon). A 12-bit temperature RH smart sensor was mounted inside a radiation shield and could measure temperatures from -40 to 100 °C attaining an accuracy of at least ± 0.2 °C, a resolution of 0.001 °C and it could also measure relative humidity (0 - 100 %) with ± 2.5 % and a resolution of 0.1 %. For precise rain measurements, a rain gauge smart sensor was installed on top of the meteorological station. This rain gauge had a tipping bucket mechanism that could measure up to 10 cm of rain per hour with a resolution of 0.2 mm and a maximum of 4,000 tips per interval. For measurements below 2 cm an accuracy of ± 1 % is achieved. A measurement interval of 10 minutes was chosen to gather sufficient weather data.

Derived from these measured variables (RH and air temperature) the VPD was calculated. The calculation of the VPD was based on the equations presented in Allen et al. (1998) and Buck (1981). The vapor pressure deficit (VPD, kPa) is the subtraction of the actual vapor pressure (e_a, kPa) from the saturated vapor pressure (e_s, kPa). First the saturated vapor pressure is calculated using equation 1. For the calculation of the actual vapor pressure, the dewpoint temperature (T_{dew}, °C) needs to be determined using the relative humidity (RH, %), the air temperature (T_a, °C), and a set of constants presented in equations 2 and 3. T_{dew} is used to compute the actual vapor pressure (eq. 4) and the VPD isdetermined using equation 5.

$$e_s = 0.6108 exp\left(\frac{17.27T_a}{T_a + 237.3}\right) \tag{1}$$

$$\gamma = \ln\left(\frac{RH}{100} exp\left[\left(18.678 - \frac{T_a}{234.5}\right)\left(\frac{T_a}{T_a + 257.14}\right)\right]\right) \tag{2}$$

$$T_{dew} = \frac{257.14\gamma}{18.678 - \gamma} \tag{3}$$

$$e_a = 0.6108 exp\left(\frac{17.27T_{dew}}{T_{dew} + 237.3}\right) \tag{4}$$

$$VPD = e_s - e_a \tag{5}$$

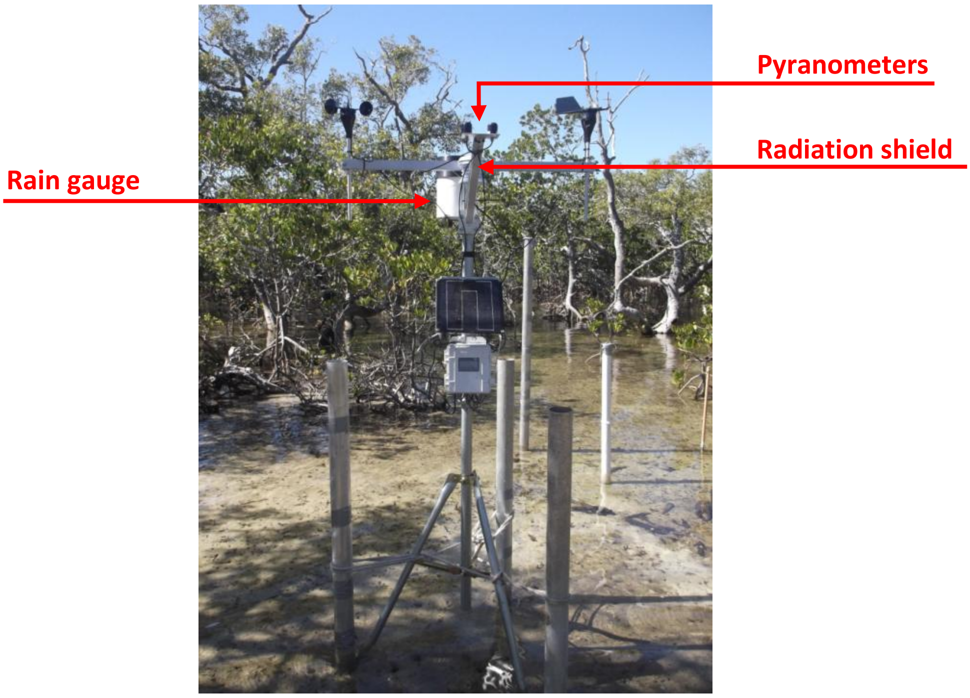

Figure 2.3 A picture of the meteorological Hobo station. For the sake of stability three pipes were drilled into the soil and the tripod was fastened to these pipes. Relative humidity and air temperature are measured with sensors inside the radiation shield.

2.3 Tree sensors

In this experiment three tree variables were measured continuously (every 15 minutes). Variation in stem radius was measured using dendrometers (DRL 26 - Logging Band Dendrometer, ICT International), sap flow data was obtained with HRM sap flow meters (ICT International) and water potential in the branches was determined with the use of smart stem psychrometers (ICT International). Stomatal resistance and water potential in the leaves were also measured, but with non-continuous readings. The sensors used were a porometer (AP4 porometer, Delta-T Devices Ltd) for the stomatal resistance and a Scholander pressure bomb (3005F01 Plant Water Status Console, Soil Moisture Equipment Corp.) for the water potential at the leaves.

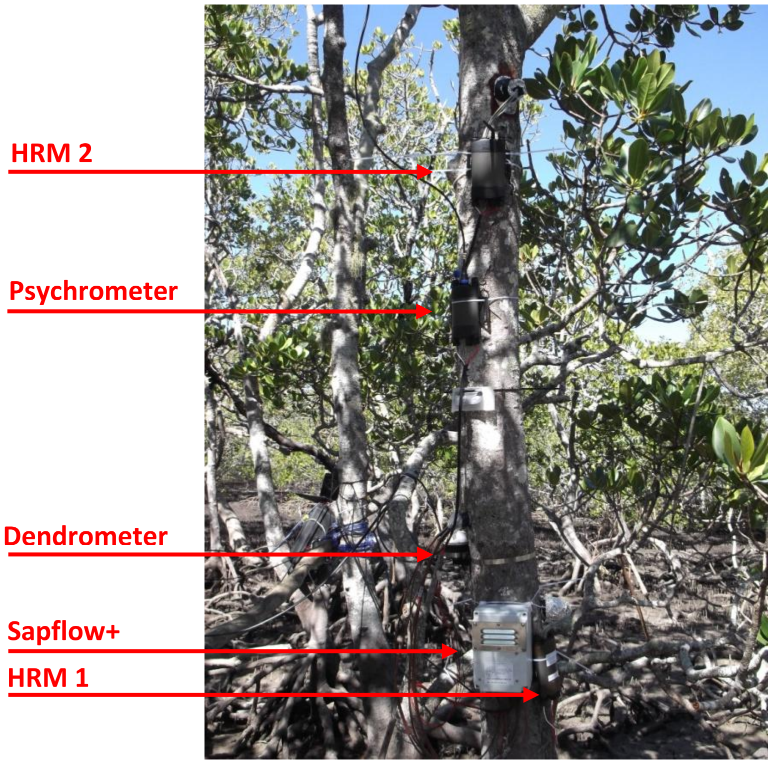

Figure 2.4 A fully equipped tree. A dendrometer, psychrometer and 2 HRMs are visible on the picture. Also a Sapflow+ (Vandegehuchte and Steppe 2012), used for another research, can be seen. Only the psychrometer recorder is visible, the measuring device itself is installed in the canopy on a branch.

2.3.1 Dendrometer: band dendrometer

A dendrometer is a useful instrument for scientists calculating tree growth. It measures the stem diameter on a fixed height and is able to elucidate long term growth patterns (days, weeks, years) as well as short term patterns (hours or even minutes). Obviously, the smaller the time period between two consecutive measurements, the larger a resolution is necessary to be in order to receive useful data. All dendrometers have the advantage of using non-invasive techniques, hence minimizing the disturbance on the tree. There are different types of dendrometers available on the market. They can be divided in contact dendrometers and non-contact dendrometers (Drew and Downes 2009). The first high-resolution dendrometers were developed in the early 1900s. These high-resolution dendrometers can be divided into three classes. The first type is the radial type which measures changes by monitoring the radius, the second type is the diametral type which measures changes by monitoring the diameter and the third type is the circumferential type which uses bands around the stem to measure changes in the circumference. The latter type, Introduced by Hall (1944), is the most frequently used in forest research and was used in this experiment. The advantages of using dendrometers in physiological science are quite broad. Not only are they relatively cheap and very easy to install and maintain, they also give fairly straightforward and easily interpretable information about the tree behavior, unlike many other tree sensors. In other words, stem diameter changes represent the result of a lot of different physiological processes. An important feature of band dendrometers is their low susceptibility to disturbance because they are fixed tightly to the tree which is an important condition for field experiments with a lot of activity during the experiment and where the wind can blow freely.

At the site each tree was equipped with one dendrometer (Table 2.1). The dendrometer type used was the DRL 26 - Logging Band Dendrometers and manufactured by ICT International (Armidale, New

South Wales, Australia). This type has a measuring resolution of 1 μm over an unadjusted range of 65 mm. A measurement was logged every 10 minutes. This type of dendrometer has an infrared communication system, whereby data is collected by holding the infrared device close, without making physical contact. As a consequence, unintentional disturbance of the very sensitive meter is prevented. Prior to installation, the bark was smoothened by scratching unevenness with a knife. The dendrometers were installed two days before the starting of the experiments in order for the band to settle.

Figure 2.5 A band dendrometer attached to a *R. stylosa* with dendrometer tape.

For the evaluation and interpretation of the dendrometer data, two different sets of time periods were defined. The first set divides the day in two equal parts in which the first part covers the time period between 0 and 12 h and the second part between 12 and 24 h. For the second set, the first timeframe is taken from 6 to 12 h and the second from 12 to 20 h. Subsequently, some different parameters are determined within these time periods and defined in Table 2.2 and Figure 2.6. The parameters are defined so that a positive value always represents growth and a negative one shrinkage. These parameters were calculated for every tree on every day and the average and the corresponding standard deviation were computed.

Table 2.2 Definition of different parameters used for the growth pattern characterization.

Period	Abbreviation	Time frame (h)	Calculation (see Figure 2.6)
Growth first half of the day	Gr1H	0 - 12	C-A
Shrink second half of the day	Sh2H	12 - 24	E-C
Growth period	GrP	6 - 12	C-B
Shrink period	ShP	12 - 20	D-E
Growth per day	GrD	0 - 24	E-A

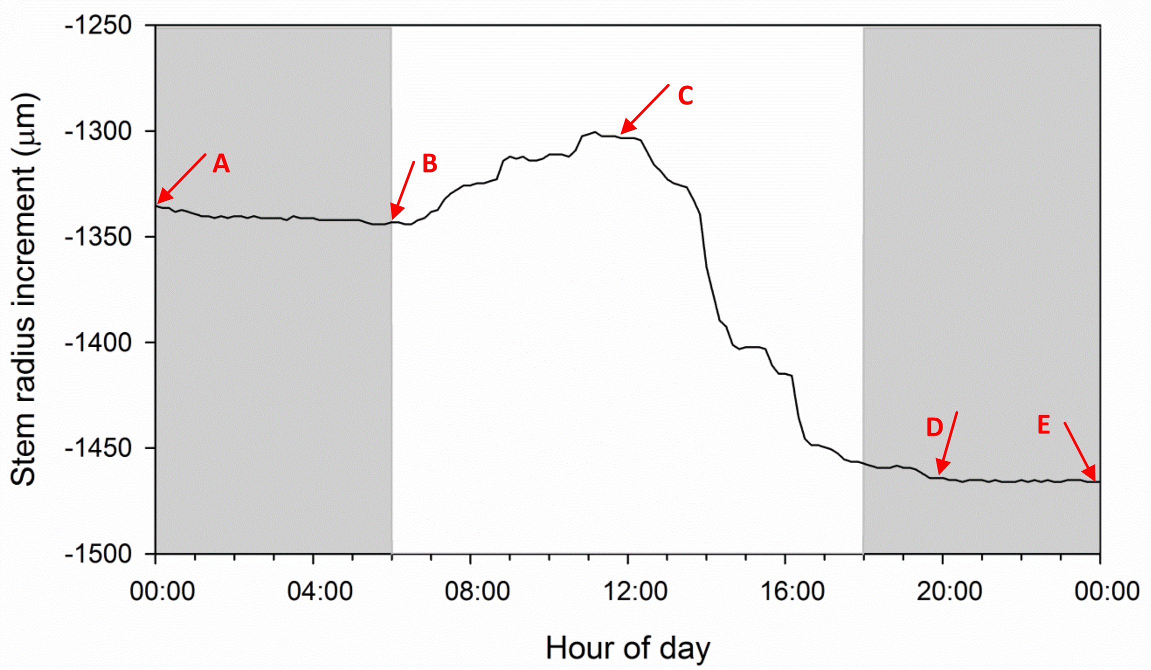

Figure 2.6 A typical daily growth pattern of *R. stylosa* (on DOY 266). On this graph, the stem radius values used are highlighted with arrows and a corresponding letter. Shaded areas represent nighttime and unshaded area represents daytime.

2.3.2 Sap flow sensor: heat ratio method (HRM)

Measurements of sap flow can reveal a lot of information on the physiological behavior of trees. A broad range of techniques exists to acquire data on sap flow, however each technique has its own set of advantages and disadvantages. Each technique is based on the usage of heat, transported by the sap, to detect the movement of the sap. In general, three categories of sap flow sensors are distinguished. Sap flow can be measured using (i) heat pulses in the sap, (ii) a controlled heat source or (iii) empirical relationships which describe a relation between heat dissipation and sap flow (Smith and Allen 1996). The former category is often preferred due to simple instrumentation and lower required energy input. A short non-exhaustive list of possible sap flow sensor techniques is presented. Constant heat sources are used with the stem heat balance method and the trunk sector heat balance method. Methods that rely on empirical relationships are the thermal dissipation method and the heat field deformation method. Techniques that obtain data by pulsing heat into the sap flow are the compensating heat pulse method, the Tmax method, the heat ratio method (HRM) and the recently developed Sapflow+ method (Smith and Allen 1996, Burgess et al. 2001, Steppe et al. 2010, Vandegehuchte and Steppe 2012). For more detailed information on these techniques papers such as Smith and Allen (1996), Burgess et al. (2001), Steppe et al. (2010), Vandegehuchte and Steppe (2012) and Vandegehuchte and Steppe (2013) are recommended.

In this field trial, the HRM method was used because of its sensitivity and ability to record low and negative sap flow, which is a great advantage and could be convenient for mangrove tree measurements, because of the extreme low soil potential, which could possibly result in negative sap flow. HRM sensors fabricated by ICT International (Armidale, New South Wales, Australia) were used. Burgess et al. (2001) described this method in detail. The HRM uses different measuring points to acquire a more reliable value for sap flow. However, a disadvantage of this method is its limitation to measure high sap flux densities correctly (V_s > 30 cm^3 cm^{-2} h^{-1}) (Bleby et al. 2008). In this experiment, such high velocities of sap flow were not expected (Hao et al. 2009). The HRM sensor consists of three vertically aligned needles. The middle needle is the heater, the other two, placed equidistant (x = 0.5 cm) above and beneath the heater, are the temperature probes. The heat pulse velocity (V_h) is calculated by using the ratio of temperature increase in the upflow and downflow needle and some constant parameters (eq. 6).

$$V_h = \frac{k_r}{x} \ln(\frac{v_1}{v_2}) \cdot 3600 \tag{6}$$

With v_1 and v_2 (°C) the increase in temperature downstream and upstream respectively, measured by the temperature probes, k_r is the reference thermal diffusivity (default setting: $k_r = 0.0025$ cm² s^{-1}) and x is the distance between the temperature probes and the heater, fixed at 0.5 cm. Each temperature probe is provided with measuring points at a depth of 0.75 cm and 2.25 cm. These two measurements of sap flow give the opportunity to create a radial profile as well. The ratio v_1/v_2 becomes linear 60 s after the heat pulse (25 J, 2.5 s), therefore the ratio is taken between 60 and 100 s after the pulse and the readings are averaged. Each tree was equipped with two HRM sensors on different heights (Table 2.1) and measurements were taken every 15 minutes. Unfortunately, only the measurements on the lower position and at a depth of 0.75 cm yielded usable data. For the installation, three holes were drilled with a drill bit which had a diameter of 1.35 mm. These holes needed to fit needles that were 1.3 mm in diameter. For a smooth insertion of the needles and a good thermal contact between the needles and the wood, a small portion of silicon grease was used. For the conversion from heat pulse velocity to sap flux density (V_s) the software Sap Flow Tool (Phyto-IT BVBA, Mariakerke, Belgium and ICT International, Armidale, New South Wales, Australia) and the appropriate parameters were used in equation 7.

$$V_s = \frac{k}{0.0025} \cdot B \cdot \frac{\rho_b(c_w + m_c c_s)}{\rho_s c_s} V_h \tag{7}$$

With k (cm² s^{-1}) the thermal diffusivity, as can be calculated using the proper equations presented in Burgess et al. (2001), 0.0025 the default thermal diffusivity, B (-) the wound correction factor, calculated as in Burgess et al. (2001) with a wound diameter of 0.18 cm, ρ_b and ρ_s, the basic density of wood calculated as the ratio sapwood dry weight/sapwood fresh volume (kg m^{-3}) and the density of water (1,000 kg m^{-3}), c_w and c_s, the specific heat capacity of the wood matrix (1,200 J kg^{-1} °C^{-1}) and the specific heat capacity of the sap (4,182 J kg^{-1} °C^{-1}) and m_c (kg kg^{-1}) the water content of sapwood (fresh weight of sapwood minus dry weight of sapwood divided by sapwood dry weight).

At the end of the experiment the tree vessels were cut in order to attain zero readings. This enabled a linear transformation, which provided a better estimation of the absolute values, although the measurements taken after cutting contained a lot of noise and thus the new zero line still included an error.

The parameters required to calculate the thermal diffusivity and the sap flux density were calculated by determining the fresh weight of sapwood, the dry weight and the volume of a core sample. Dimensions were measured with a digital Vernier caliper with an accuracy of ± 0.02 mm and with an analytical balance with an accuracy of 0.001 g and are presented in Table 2.3. Besides these measuring errors, some small errors were induced by handling the samples and drying them.

Table 2.3 Wood properties calculated from wood cores. These properties are used to determine the thermal diffusivity and sap flux density.

	Fresh weight (g)	Dry weight (g)	Volume (cm^3)
R. stylosa 1	0.624 ± 0.001	0.525 ± 0.002	0.79 ± 0.03
R. stylosa 2	0.778 ± 0.001	0.586 ± 0.002	0.83 ± 0.04
R. stylosa 3	1.075 ± 0.001	0.869 ± 0.002	1.13 ± 0.04

Figure 2.7 Picture of an installed HRM sensor. The needles are shielded from radiation with some insulation and reflective aluminum foil to prevent temperature gradients influencing the sap flow measurements.

2.3.3 Water potential: Stem psychrometer

The water potential is measured continuously and in a non-destructive manner with stem psychrometers, mounted on every tree (Table 2.1), based on the technique described by Dixon and Tyree (1984). The psychrometers automatically correct for temperature gradients and they provide data on water potentials on a small time scale (several minutes), which enables the detection of water potential responses towards changing conditions rapidly. Although it is the most suitable sensor to measure water potentials in-situ and continuously, this technique has some drawbacks. First of all, it has a high sensitivity towards temperature gradients (Comstock 2000) making proper insulation indispensable for correct measurements. For longer experiments, the psychrometer should be inspected regularly for fouling or malfunction, which can be done by checking the Peltier cooling curve. This curve should have a distinctive shape with two plateaus and in between a very swift decline (Figure 2.8a). When fouling occurs, first the decline will become less steep and the plateaus will be much less pronounced and eventually the curve will be reduced to a straight line (Figure 2.8b). When fouling arises, a reinstallation of a cleaned psychrometer is necessary. Reinstallation was required, in most cases, about four weeks after installation. This breaks the continuous measurements and also obliges to replace the sensor on another suited spot on the tree which makes the linkage of the data series somewhat error-prone. The new suitable spot for reinstallation was always near the previous spot or on a similar branch. For this reason the water potential data will mainly be used to assess relative changes on a smaller time scale. A final drawback of the psychrometer is that the junctions are vulnerable to damage when installing them on a tree.

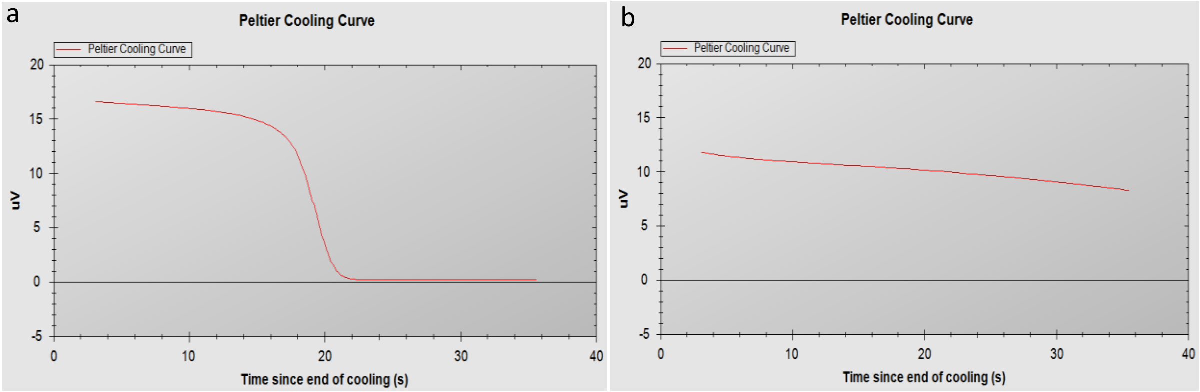

Figure 2.8 An example of a good Peltier cooling curve (a), measured with a recently cleaned psychrometer, immediately after a reinstallation. Peltier cooling curve after a reading with a fouled psychrometer (b). Such curves indicate that the psychrometer needs to be reinstalled.

For the installation of the smart stem psychrometers (ICT International, Armidale, New South Wales, Australia) the bark, phloem and cambium was removed until the xylem was reached. The surface was then flattened out by gently abrading the surface, which appeared to be very important for the proper operation of the psychrometer. The spot was rinsed thoroughly with distilled water and dried. The psychrometer was attached to the spot with a clamp and the space between the psychrometer chamber and the xylem was made airtight with high-vacuum grease. The installation was completed after insulating the psychrometer head with minimum 10 cm of expansion foam. The psychrometers were first calibrated with NaCl solutions in the range from 0.5 to 2 M (4 measuring points) in the laboratory. Peltier cooling times of 5 to 20 s were applied, in order to obtain a satisfying Peltier cooling curve. Measurements of water potential were taken every 15 minutes.

Figure 2.9 An insulated stem psychrometer (a). The Insulation needs to be of sufficient thickness to prevent temperature influencing the measurements. An aluminum foil surrounding the insulation foam provides extra shelter from radiation. The stem psychrometer head (b), attached to a branch of another mangrove species (*Avicennia marina*) with a clamp. The grease surrounding the head is high-vacuum grease to create an air-sealed space.

2.3.4 Stomatal resistance: Porometer

A porometer measures the stomatal resistance of plant leaves, which is a non-continuous measurement. Herewith, an assessment of the stomatal response of the tree to environmental factors and its water household is possible. Using the cycling diffusion principle, the AP4 porometer, fabricated by Delta-T Devices Ltd (Burwell, Cambridge, United Kingdom) is able to give values for stomatal resistance within 15 to 60 s. This technique was developed by Van Bavel et al. (1965), improved by Kanemasu et al. (1969) and devised by Stiles et al. (1970). Before the introduction of porometers, only indirect measurements (such as visual observation of stomata or the slow, subjective and error-prone cobalt chloride field technique) of stomatal resistance were possible (Van Bavel et al. 1965). The AP4 porometer operates as follows. Firstly, ambient RH is measured as an input "set RH". Secondly, the cup is clamped on a leaf surface which encloses a specified area of the leaf. The small cuvette is humidified by the flow of vaporized water through the stomata (and cuticle) during transpiration. This humidification increases the relative humidity inside the cup, which is measured. One measuring cycle starts with pumping dry air over the leaf surface in order to decrease the RH till a specified value is attained (for the AP4, -5 % RH compared to the ambient "set RH"). Subsequently, the measuring time begins and when the RH reaches another preset value (+2.3 % for the AP4) the elapsed time is registered. The elapsed time is then compared with the calibration curve and stomatal resistance is determined and recorded. These cycles are repeated until two consecutive readings are acquired which differ less than 2 %.

During the field work, the porometer was used during seven days with similar weather conditions, which were sunny days with clear skies. Of those seven days, three days fully covered an entire day cycle, which includes the opening of the stomata at dawn and the complete closure after dusk. First measurements were taken around 5 to 6 h, including some predawn measurements, and continued throughout the day until 18 to 19 h, when complete stomatal closure was observed and the resistance did no longer change. For each tree, three successive measurements on the underside of different representative leaves were obtained and one measurements on the upper side, since barely any stomata were expected on the top of the leaf whereas a lot were expected on the bottom of the leaf (Hetherington and Woodward 2003).

Resistances could be recorded in a range from 20 to 4,000 s m^{-1} with a resolution of 0.01-0.1 s m^{-1}, with lower resolutions for lower resistances. The accuracy was ± 20 s m^{-1} in the range 20 - 50 s m^{-1} and ± 10 % for the range 50 - 4000 s m^{-1}.

Measurements were divided in periods of one hour and averages of measurements within these periods were calculated as weighted averages and also their corresponding errors were computed, both with equation 8. $r_{s,avg}$ is the weighted average of the stomatal resistance in the time period, $r_{s,I}$ is the average stomatal resistance for 3 consecutive measurements, SD_i is the standard deviation on $r_{s,I}$ and $error_{rs,avg}$ is the error on the weighted average $r_{s,avg}$.

$$r_{s,avg} = \frac{\sum_i \frac{r_{s,i}}{(SD_i)^2}}{\sum_i \left(\frac{1}{SD_i}\right)^2} \; and \; error_{r_{s,avg}} = \sqrt{\frac{1}{\sum_i \left(\frac{1}{SD_i}\right)^2}} \tag{8}$$

Figure 2.10 The porometer consists of a logger, a cup which needs to be clamped on a leaf to measure stomatal resistance and a calibration plate in a pouch. The end of the tube enters a container tube, filled with silica gel used for drying the air.

2.3.5 Water potential: Pressure bomb

The pressure bomb, also known as pressure chamber or Scholander pressure bomb was already used to measure negative hydrostatic pressures in mangroves since the very beginning of the usage of this technique by Scholander et al. (1964). Later, it was generalized for other plants by Scholander et al. (1965). The principle of the pressure bomb is rather straightforward. When a plant segment is cut (a leaf or a small branch), the tension in the xylem vessels is lost and the water column recedes in the plant segment. The original tension can be measured by placing the segment under pressure and registering the pressure when sap reaches the cut surface, the pressure whereby the water column is back in its original position, hence it is again under the same tension as before the segment was cut. This last operation is performed in a pressure chamber, which is a closed and sealed chamber in which the pressure can be increased to high pressures (several MPa). The cut surface is visually monitored and the hydrostatic pressure is registered when water appears at the surface. (Scholander et al. 1964)

The disadvantage of this non-continuous technique is that correct visual observations of the cut surface are needed. Another drawback is that only hydrostatic pressure can be measured, which means that osmotic potential is not included (Scholander et al. 1964). In most cases hydrostatic sap pressure is quite close to the total water potential, but for measurements on mangroves this can cause some small errors. For this experiment a 3005F01 Plant Water Status Console, assembled by the Soil Moisture Equipment Corp. (Santa Barbara, California, USA) was used with a read out resolution of 0.05 MPa, a range of 0 - 8 MPa and an accuracy of 0.25 %. Measurements were taken on the same days as for the porometer, unfortunately only one day of usable data was retained because of some initial problems with fluid, other than sap water, appearing at very low pressures. This problem was overcome by wiping of this initial fluid and carrying on until xylem sap appeared. Measurements were obtained every hour for two trees and two leaves were cut per tree. The trees used for this experiment were other trees than the trees equipped with sensors, in order to prevent wounding of the examined trees.

Figure 2.11 The pressure bomb has a pressure chamber in which the leaf or branch is exposed to elevated pressures. A lead cover is used to make the chamber airtight. The pressure gauge is used to read hydrostatic sap pressures. By using magnifying glasses, a higher accuracy and consistency can be achieved.

2.4 Soil salinity

To acquire information on soil salinity, two water sensors were placed, hanging in two drilled tubes. One was placed 15 cm below the surface, in order to measure soil salinity near the surface, the other was installed at a depth of 1.5 m to assess whether salinity had a different pattern at a higher depth (e.g. due to the infiltration of ground water). Two Aqua TROLL 200s from the company In-Situ Inc. (Fort Collins, Colorado, USA) were used. The deep Aqua Troll was lowered in a piezometer, the other, more shallow, troll was lowered in an aluminum tube. In order to measure salinity, the actual conductivity was determined. This was possible in a range of 5 to 100,000 μS cm^{-1} with a resolution of 0.1 μS cm^{-1} and an accuracy of ± 0.5 % for an actual conductivity lower than 80,000 μS cm^{-1}. Actual conductivity is a parameter which can be used to calculate total ion concentration and osmotic soil potential, which is very useful for plant measurements. An equation to convert actual conductivity to osmotic potential proposed by McIntyre (1980) was used (eq. 9). In this equation Ω_s is the osmotic potential of the soil and κ is the measured actual conductivity.

$$\log \Omega_S = 1.111 \log \kappa - 0.512 \tag{9}$$

The water level in the deep tube immediately rose to the same level as the shallow tube and the water level fluctuated at the same levels as the water observed in the tube for surface water. This indicated that the drilling of the deep tube caused an inflow of surface water towards deeper levels and that the assessments on the level and salinity of ground water was not possible. Furthermore the measurements in the deep tube were unreliable due to sudden changes in the recordings and consequently these data were not used.

Chapter 3: Results

As the literature review already emphasized, stem radius data contains a broad range of information on different physiological features of trees. The overview of the physiological measurements starts with the dendrometer data and attempts afterwards to link these data to other physiological and meteorological data in order to acquire insights in the processes and behavior of this exceptional species, *Rhizophora stylosa*. The main objective is to interpret results on a broader scale, even though some figures and data shall be discussed on individual scale. Some comparisons are made with typical patterns observed in other species, enabling the proposal of some new hypotheses and theories on how different tree species cope with a set of typical conditions in which they thrive. Before focusing on the physiological data, a short representation of the meteorological conditions is given.

3.1 Meteorological data

Figure 3.1 represents meteorological information during the experimental period. As shown, the first 40 days of the measuring campaign no rainfall occurred. In general, average temperature gradually increased. All daily averages of the variables fluctuated throughout the period (Figure 3.1a). In the more detailed graph, typical daily curves can be seen for the period DOY 248-262 (Figure 3.1b).

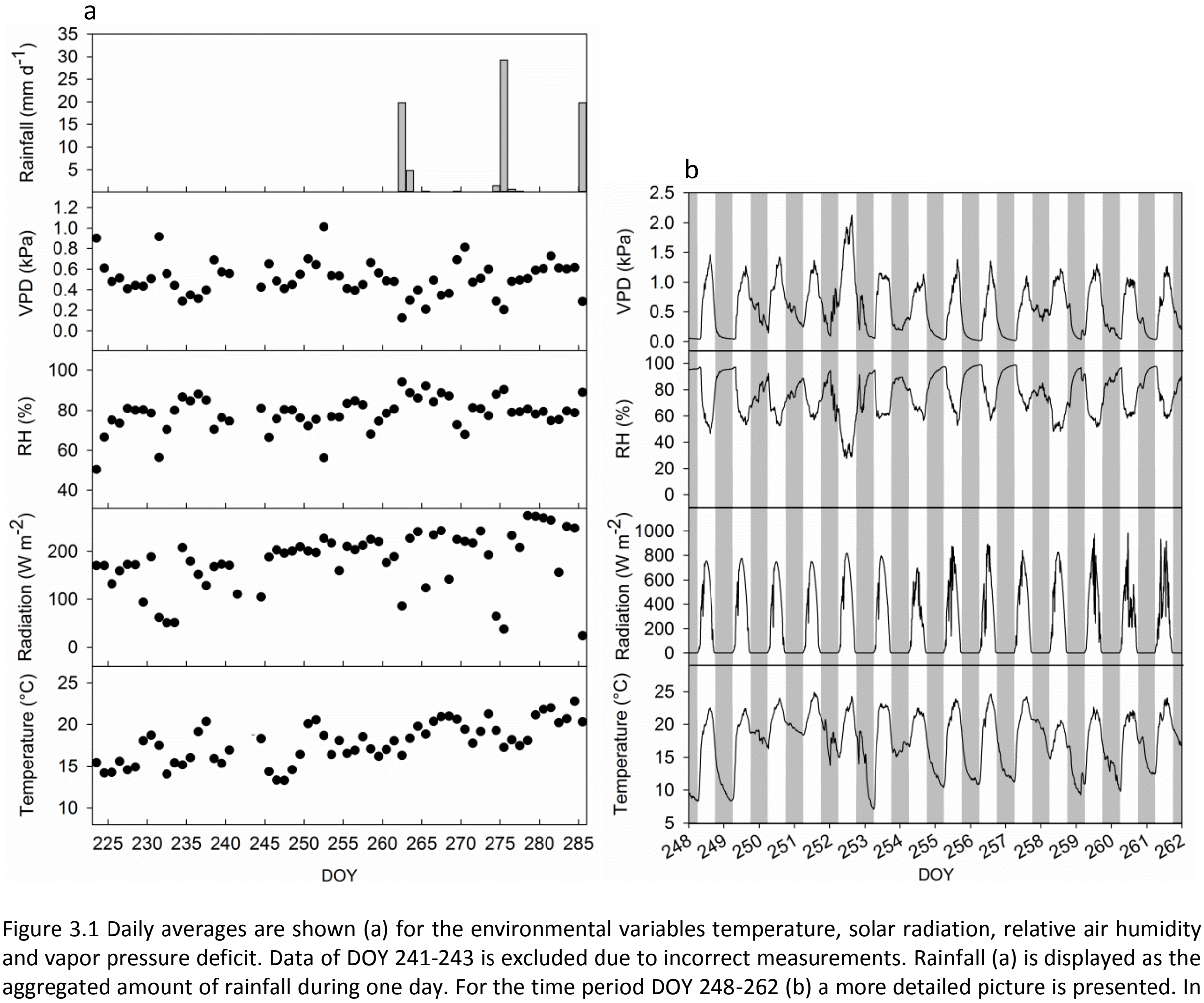

Figure 3.1 Daily averages are shown (a) for the environmental variables temperature, solar radiation, relative air humidity and vapor pressure deficit. Data of DOY 241-243 is excluded due to incorrect measurements. Rainfall (a) is displayed as the aggregated amount of rainfall during one day. For the time period DOY 248-262 (b) a more detailed picture is presented. In this graph each measurement is displayed (interval of 15 minutes) to outline the daily curves of the weather variables and the fluctuations between different days. The same variables are displayed, expect rain, because no rainfall occurred in this time period. Shaded areas represent nighttime and unshaded areas represent daytime.

3.2 Stem radius changes

The visualization of all kinds of processes and reactions that occur inside the tree are represented by the stem radius changes and its daily and long term patterns. In Figure 3.2 the patterns of stem radius increment are represented for the entire experimental period. The stem increments are shifted to zero for the first measurement. Therefore, long term growth or shrinkage of the stem radius between the different trees could be assessed. The periods of growth and shrinkage are similar, however the extent of growth and shrinkage was not the same for all the trees. For *R. stylosa* 1, the short term shrinkage periods resulted in a much larger decrease of the tree diameter than in trees 2 and 3. To assess the magnitude of the radius increment, reference is made to the circumference of the trees as illustrated in Table 2.1. *R. stylosa* 2 had a smaller diameter, while the diameters of *R. stylosa* 1 and 3 were comparable.

The conducted experiment took place during 2 months and yet 2 out of 3 trees were not able to enlarge their stem radius during this time period. Weather data showed that the last rain event in that region occurred on DOY 208, after which a completely dry period of 58 days followed (Bureau of Meteorology 2012). Therefore, a period of severe drought could be observed which is unusual for this region that normally has an average of 5 to 10 days of rainfall and more specific, 61 mm of rain in August, compared to none in 2012 (Bureau of Meteorology 2012). These conditions are likely to cause stress to the trees and can be the reason for the severe shrinkage during the first 20 days of the experiment and the status quo in stem diameter during DOY 246 - 262.

The more pronounced shrinking of tree 1 originated from the much greater decline in stem diameter during some time periods, whereas the difference in positive growth periods between tree 1 and the other trees was smaller. Some recognizable patterns are observed in Figure 3.2 (e.g. DOY 245 - 252). These patterns, thoroughly described in literature, show a daily decline and increase and the result of these dynamics is the steady increase or decrease of the stem radius (Downes et al. 1999, Deslauriers et al. 2007b). Generally these patterns do not exhibit many sudden drops or increases, but rather gradual increments of daily growth or shrinkage (Downes et al. 1999, Deslauriers et al. 2003, Deslauriers et al. 2007a, Deslauriers et al. 2007b). In the case of *R. stylosa* however, periods of relative growth in the time frame of several days (most clear for *R. stylosa* 2 and 3) were followed by the rapid and strong decrease of stem radius, while this was not the case for growth, with the exception of intensive radial expansion after rain events. When the meteorological data will be used for analysis, the events of sudden contraction will be of extral interest because they had a serious impact on the water household of the trees (4.6.2 Periods of growth and shrinkage).

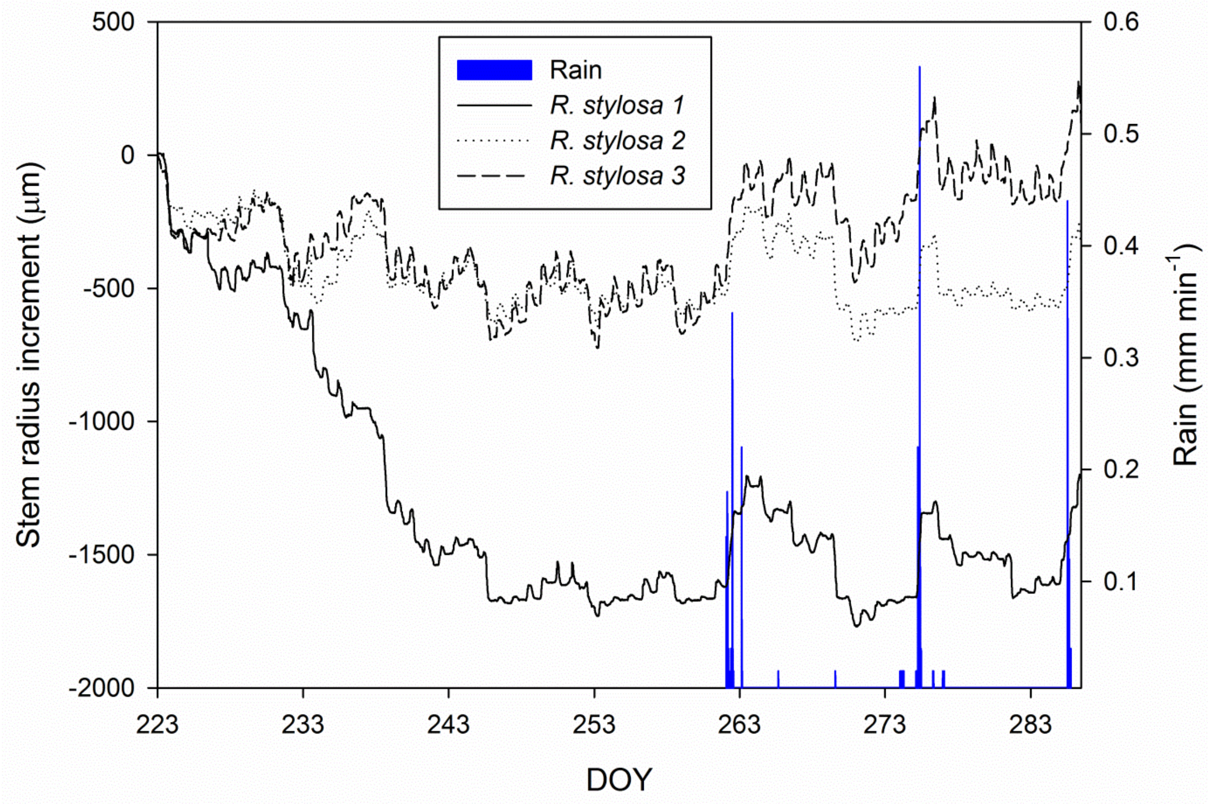

Figure 3.2 Overview of the stem radius increment patterns throughout the duration of the experiment, for each individual tree. Gray bars represent the amount of rainfall.

The longer term pattern exposes some peculiarities in the stem radius patterns of *R. stylosa*. However, the patterns on a daily scale display exceptional diurnal patterns. Figure 3.3 represents a time period of 2 weeks (DOY 248-262) indicating clear daily fluctuations of stem radius. During the period of field work (Figure 3.3), *R. stylosa* showed a different typical day and night cycle compared to other tree species. This pattern is consistent throughout the entire period, for almost every day.

The growth pattern of *R. stylosa* can be described in three phases which were observed during most days. The first phase started at sunrise whereby the stem radius expanded until noon. The second phase was in the afternoon when the tree diameter started to shrink until some period after dusk. During the third phase, after dusk, *R. stylosa* did not swell or shrink a lot during most nights. The growth figures in the morning were the highest around the first hours after sunrise. After some hours the radius increased less and it gradually altered in shrinkage, which occurred after midday. The shrinkage figures increased after noon until shrinkage became less again, and the stem diameter remained nearly constant after dusk. Because the growth pattern deviates from other tree species, the other measurements are compared with the common patterns encountered on other species in the literature. This might enable the proposition of an hypothesis that could explain these growth patterns.

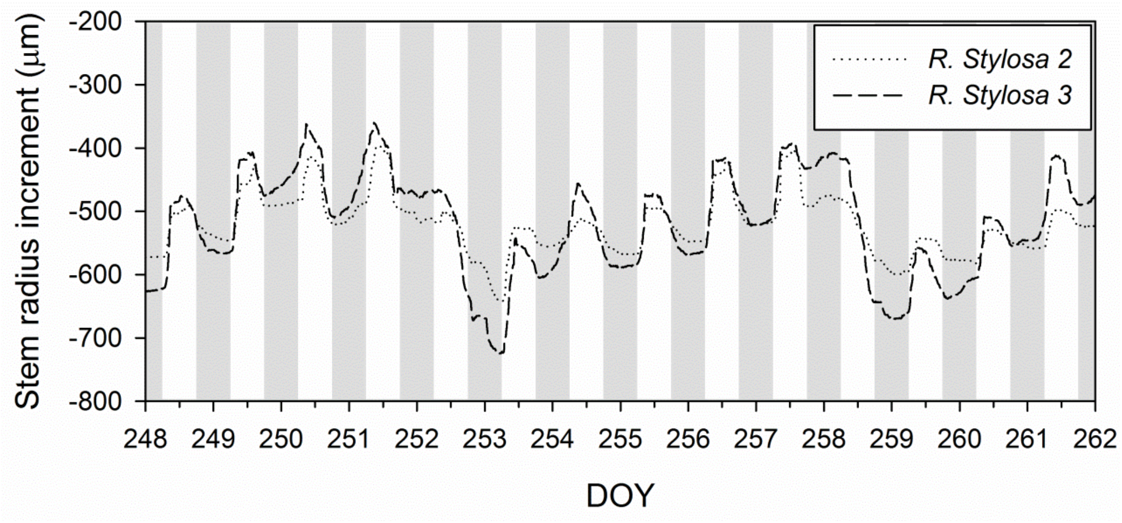

Figure 3.3 Typical circadian growth patterns for *R. stylosa*. This species exhibits a unique pattern of stem radius increments. Shaded areas represent nighttime and unshaded areas represent daytime.

3.3 Sap flow

Figure 3.4 represents the sap flux density of each individual tree on the lower position, at a depth of 0.75 cm. The values depended on different anatomical traits, which caused some differences in the absolute values between the trees (Wullschleger and King 2000). However, the measured patterns were the same for all three trees and the pattern consisted of a rise in sap flux density in the morning, typically a maximum around noon and a decreasing sap flux density in the afternoon. Usually a daily minimum was reached right before sunrise. During the night values of sap flux density were usually a little bit higher that zero.

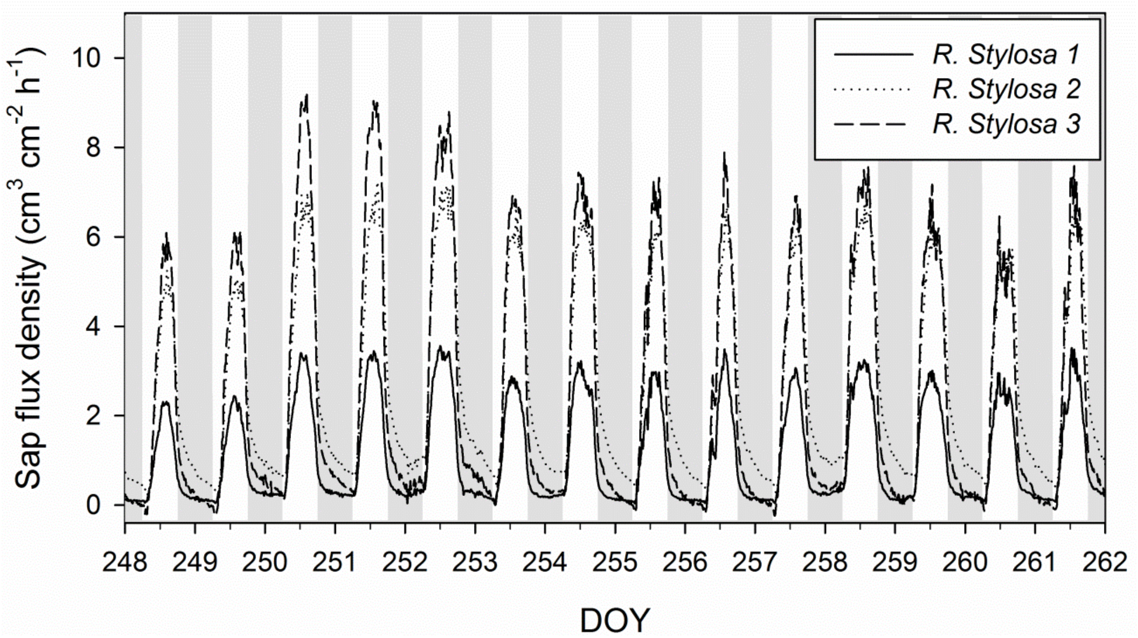

Figure 3.4 Course of the sap flux density, presented for each individual tree. The sap flux density data originates from the lowest HRM on each tree measured at 0.75 cm depth. Shaded areas represent nighttime and unshaded areas represent daytime.

As already mentioned, some meteorological variables were monitored during the experiment. The correlation between these variables and the average sap flux density for the three trees is quite high

(Figure 3.5). The correlation coefficient is the highest for VPD (0.870), but still a moderate correlation of about 0.7 is found for temperature (positive), radiation (positive) and relative humidity (negative). The sap flux density, which is proportional to the amount of water transported inside the vessels, is closely related with the amount of water that is transpired. Transpiration on its turn is closely related to stomatal aperture. The amount of transpiration and stomatal aperture are strongly linked to microclimatic variables, hence the high correlation between sap flux density and meteorological variables is not unusual. The two variables with the highest correlations, temperature and VPD, are elucidated in Figure 3.6. Rain is not strongly correlated, which is probably a distortion because of the small number of rain events. The effect of rain will be dealt with in detail in a later section (3.6 Rain and salinity).

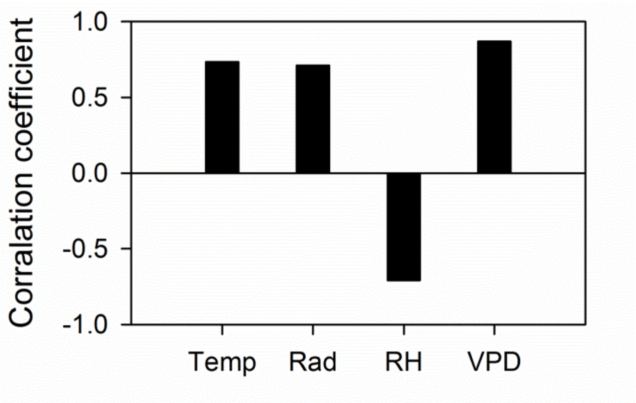

Figure 3.5 Correlation coefficients for the different meteorological variables with sap flux density.

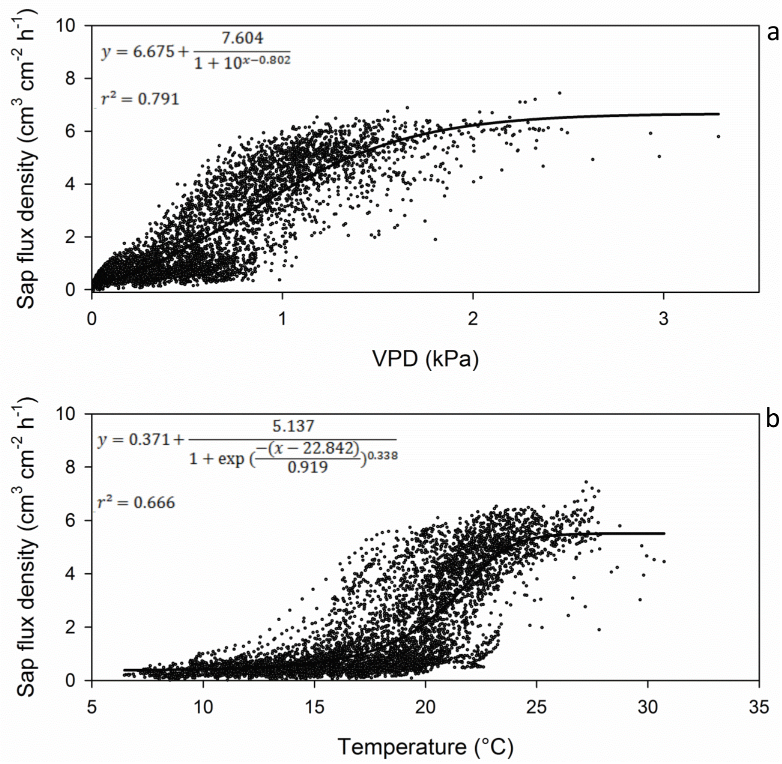

Figure 3.6 Regression between sap flux density and the two highest correlated meteorological variables, VPD (a) and temperature (b). For VPD, a ligand binding was chosen and for temperature a sigmoid relation.

3.4 Water potential

The course of the water potential in the branches (Ψ_b), as recorded by the psychrometers, is displayed in Figure 3.7, representing each tree. A similar course can be observed for all trees. A water potential as low as -4.28 MPa was recorded and as high as -0.56 MPa. Although the course of each individual tree was similar, the extent of the fluctuations were different. The variation of the distance from the leaves and the diameter of the branch on the spot where the psychrometers were installed caused the difference. The common pattern that is described in literature (Kume et al. 2007) is characterized by a decline in the water potential when transpiration started after sunrise. The decline implies that the force exerted on the water column, due to transpiration, increases. A minimum value is attained around noon and afterwards, the water potential starts to rise again. This rise means that the force on the water column is lowering due to the atmospheric water demand that is lowering as well. Throughout the night, the water potential keeps on rising, but at a lower rate until a new day starts and another cycle is initiated. Indeed, these patterns were mostly the same for *R. stylosa*. However, during some nights, the water potential tended to react differently than the common pattern with some sudden drops and rises.

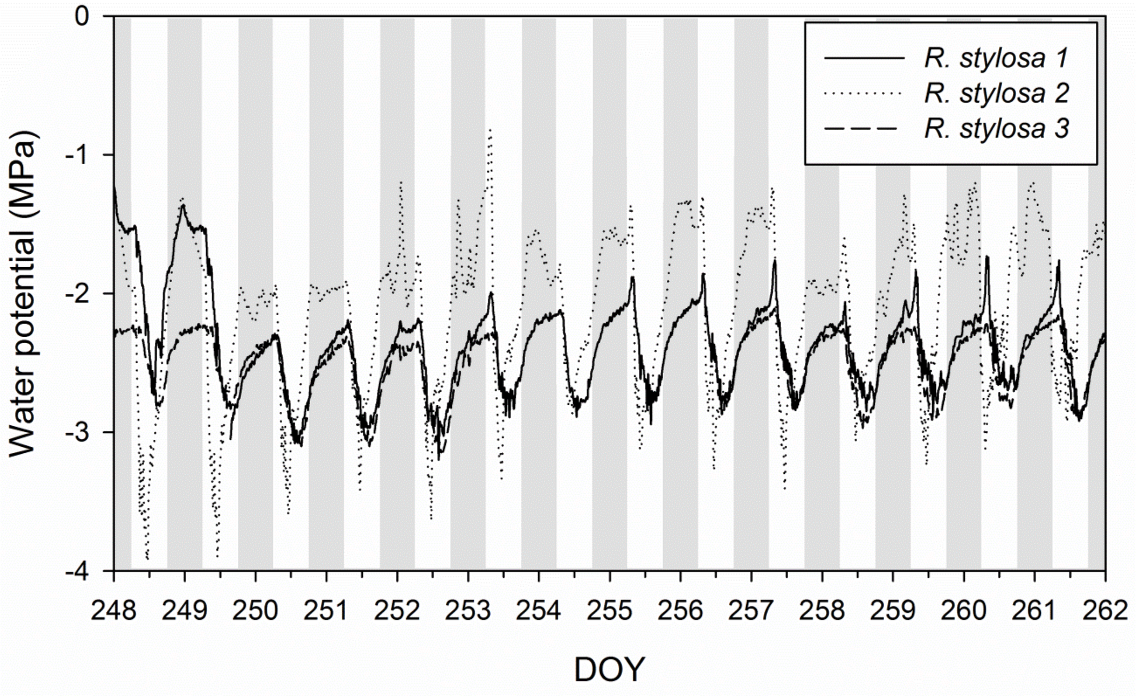

Figure 3.7 Course of the water potential in the branches for each individual tree. Shaded areas represent nighttime and unshaded areas represent daytime.

For *R. stylosa* the correlation coefficients are displayed in Figure 3.8 and the highest correlation was found between Ψ_b and VPD (-0.796). A quadratic relation was found for Ψ_b and VPD and a linear one for Ψ_b and RH (Figure 3.9). Temperature and radiation had a similar correlation coefficient of about -0.6. Again, rain will be dealt with in a different section because there were only a limited amount of rain events.

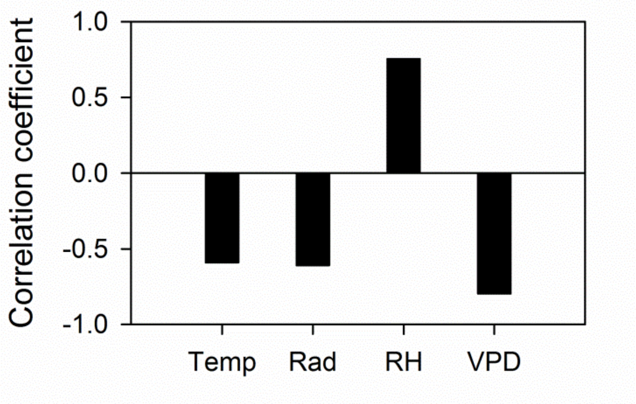

Figure 3.8 Correlation coefficients for the different meteorological variables with Ψ_b.

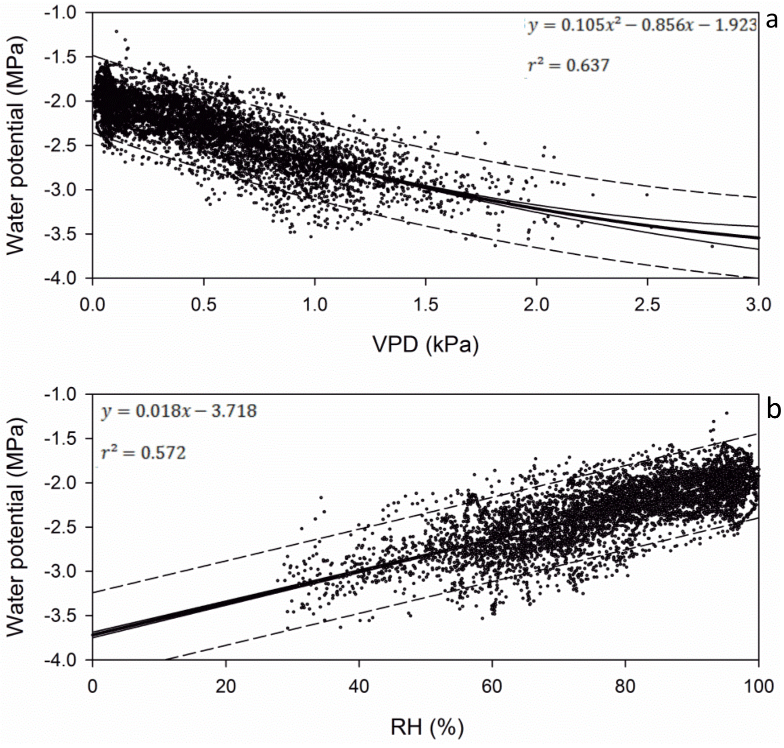

Figure 3.9 Regression curves which relates Ψ_b with VPD (a) and RH (b). The thick, thin and dashed lines are the regression curve, 95 % confidence band and 95 % prediction bands, respectively.

The water potential was also measured in the leaves (Ψ_l) with a pressure bomb on DOY 261. Both methods are represented and compared in Figure 3.10, where each point represented four measurements, two leaves on two trees. The error bars were calculated as the standard deviation on the four measurements. The methods differed in the plant segment that could be measured. A pressure bomb needs segments with a small diameter such as a leaf petiole or a thin branch, whereas a psychrometer needs a tree segment with a diameter that is large enough to hold the psychrometer head. Because transpiration takes place in the leaves, this is the first place were water is lost. Therefore, the strongest force on the water column is exerted here and the strongest fluctuations (difference between night and day water potential) in Ψ_l and the lowest values of Ψ_l were expected here (Begg and Turner 1970, Williams and Araujo 2002, Kume et al. 2007). The error bars in Figure 3.10 are relatively large for some measuring points, which made the interpretation of the pressure bomb data fairly uncertain. In Figure 3.10, the average Ψ_b (of the 3 trees) is represented, with its corresponding standard deviation. The first value for Ψ_l obtained with the pressure bomb was low and much lower than Ψ_b. Later, Ψ_l and Ψ_b was approximately equal for a couple of hours, after which Ψ_l declined more than Ψ_b. Both Ψ_l and Ψ_b were minimal around 15 h, when transpiration had been high for a while and still was.

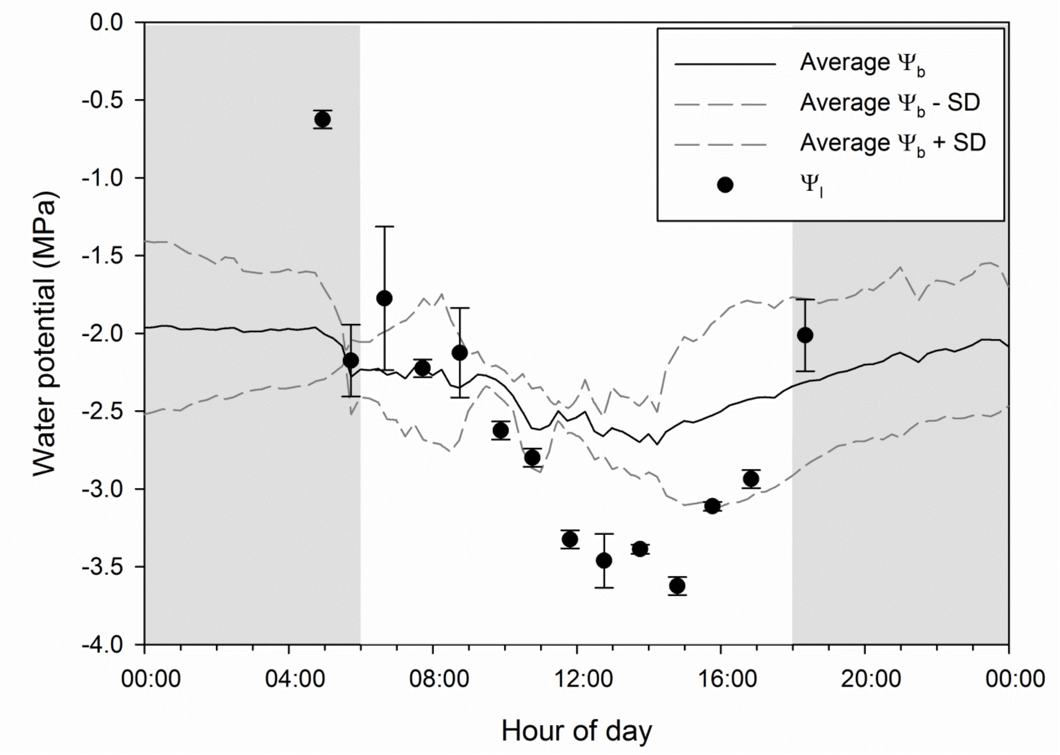

Figure 3.10 Comparison of two methods to measure water potential. The point measurements are taken with the pressure bomb and the continuous measurements (each 15 minutes) with psychrometers. The measurements on the 3 trees are displayed as an average and standard deviation. Shaded areas represent nighttime and unshaded area represents daytime.

3.5 Stomatal behavior

In Figure 3.11, the stomatal resistance pattern throughout the day is plotted. Each data point is the calculated weighted mean of a number of measurements on different days. Each measurement consisted of three successive readings taken with a porometer within a few minutes of each other. The standard deviation of these successive readings was calculated and used as a weight as displayed in equation 8. The number of measurements used is also shown in Figure 3.11. The stomatal pattern for *R. stylosa* was quite consistent over the 7 measuring days. According to the findings presented in Figure 3.11, *R. stylosa* showed a typical diurnal stomatal resistance pattern for C3- and C4-plants and signs of midday stomatal closure for a better water management (1.1.4 Stomatal control on water loss from transpiration). This pattern consisted of a rapid stomatal opening, right after sunrise, followed by a partial stomatal closure around midday and a gradual closing of the stomata during the afternoon and full closure was observed after dusk. The stomatal resistance was lower in the morning than in the afternoon after stomatal closure.

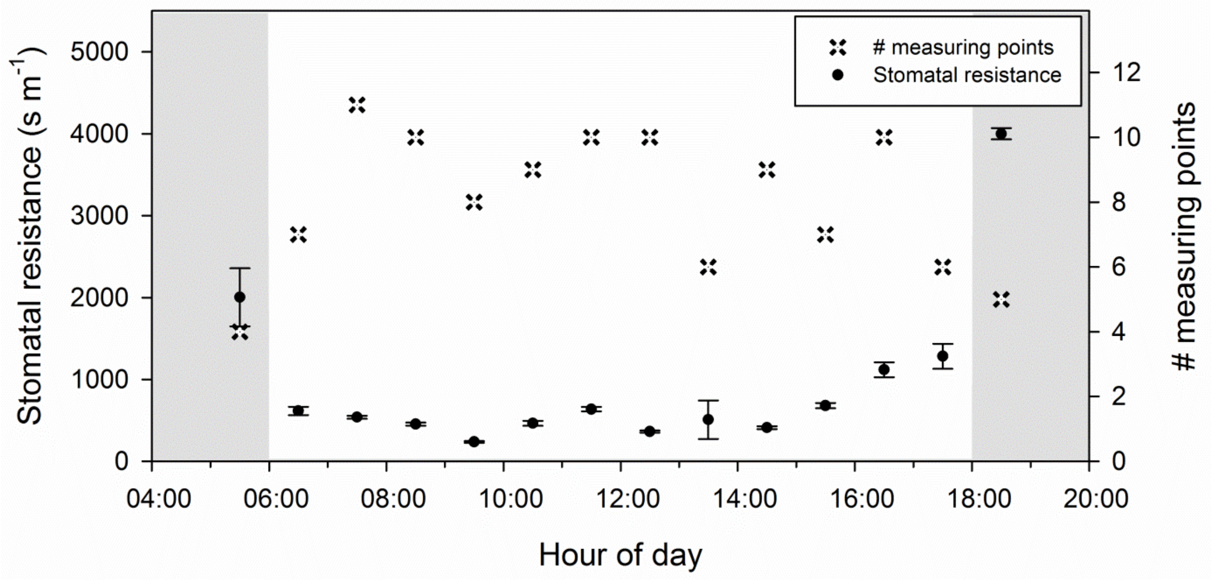

Figure 3.11 Stomatal resistance is represented with black circles. Each data point originates from several measuring points. The number of measuring points for each value is represented with crosses. The maximum resistance that can be measured with the AP4 is 4000 s m^{-1}. Shaded areas represent nighttime and unshaded area represents daytime.

3.6 Rain and salinity

All rain events took place during the period DOY 262-285, as illustrated in Figure 3.12. This graph clearly shows that intensive rain gave rise to large growth spurts. The overall shrinkage of the trees, situated in the first period of the experiment (DOY 223-262), was halted due to rain (Figure 3.2). Moreover, this clearly demonstrated that *R. stylosa* made use of this extra water supply. Although the trees always grew in a water saturated soil, they still took advantage of this fresh water source, which was not surprising because, notwithstanding that they grow in wet soils, the soils have a high salinity and thus a low osmotic water potential and low water availability, opposite to the fresh water in rain.

The first two intensive rain events (DOY 262 and 275) took place during the morning at high tide when the trees were inundated, whereas the third heavy rain event (DOY 285) took place in the afternoon while the tide was low and the trees were not inundated. These days will be the only considered when handling the influence of rain, and the smaller rain events will not be taken into account and will not be discussed because no immediate or strong effect was visible.

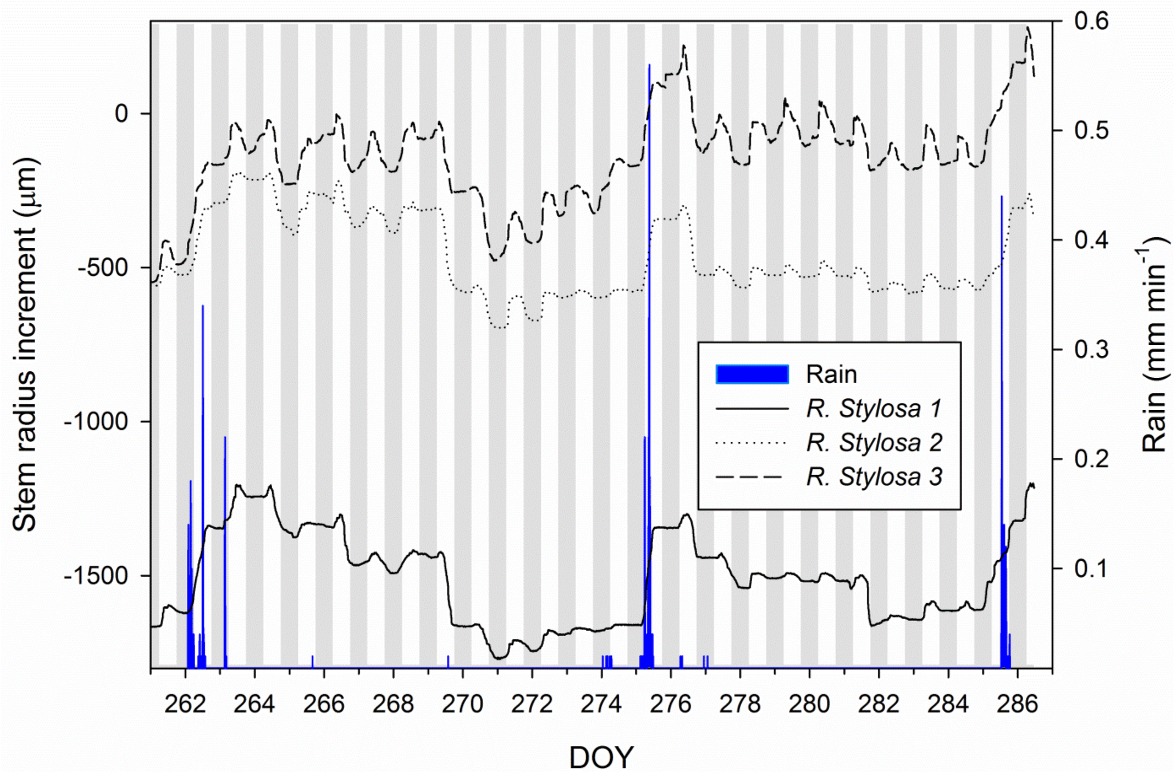

Figure 3.12 Stem growth patterns during the period in which rainfall occurred. Shaded areas represent nighttime and unshaded areas represent daytime.

The influence of rainfall on sap flow is demonstrated in Figure 3.13. In response to rainfall, the sap flux density and subsequently the daily flow was lowered. During the 2 first days with rain (DOY 262 and 275), rain fell during the morning, which resulted in a sap flux density of almost 0 cm^3 cm^{-2} h^{-1} during the rain, and when rainfall ended, the normal course resumed, but the maximum sap flux density attained that day was lower. When rainfall occurred in the afternoon (DOY 285), the increase of the sap flux density was halted and its value dropped closely to zero. In general, sap flux density was lowered to 0 cm^3 cm^{-2} h^{-1}, whenever intensive rain occurred. Consequently, daily sap flow rates were lowered in response to rainfall.

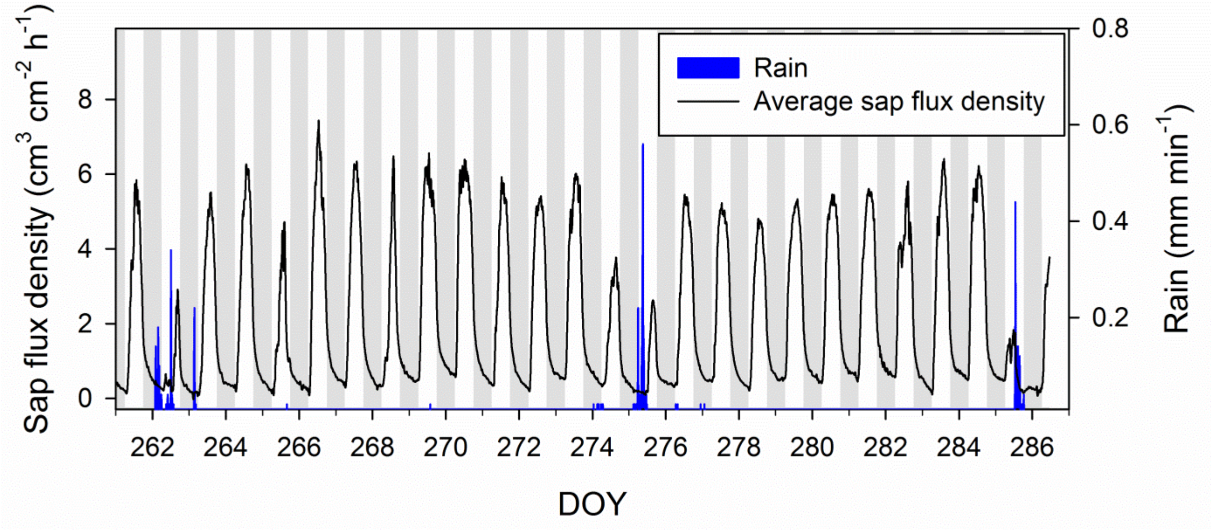

Figure 3.13 The course of sap flux density and its response to rainfall. The average of measurements of sap flux density on the three trees is displayed. Shaded areas represent nighttime and unshaded areas represent daytime.

The course of the Ψ_b for *R. stylosa* in the event of rainfall is displayed in Figure 3.14. When rainfall occurred the typical drop in Ψ_b, observed during the dry days, was postponed and therefore less negative values were attained that day. Rainfall that occurred on a soil that was not inundated, gave rise to an additional effect. In this case Ψ_b was elevated to values clearly exceeding the water potential of the soil.

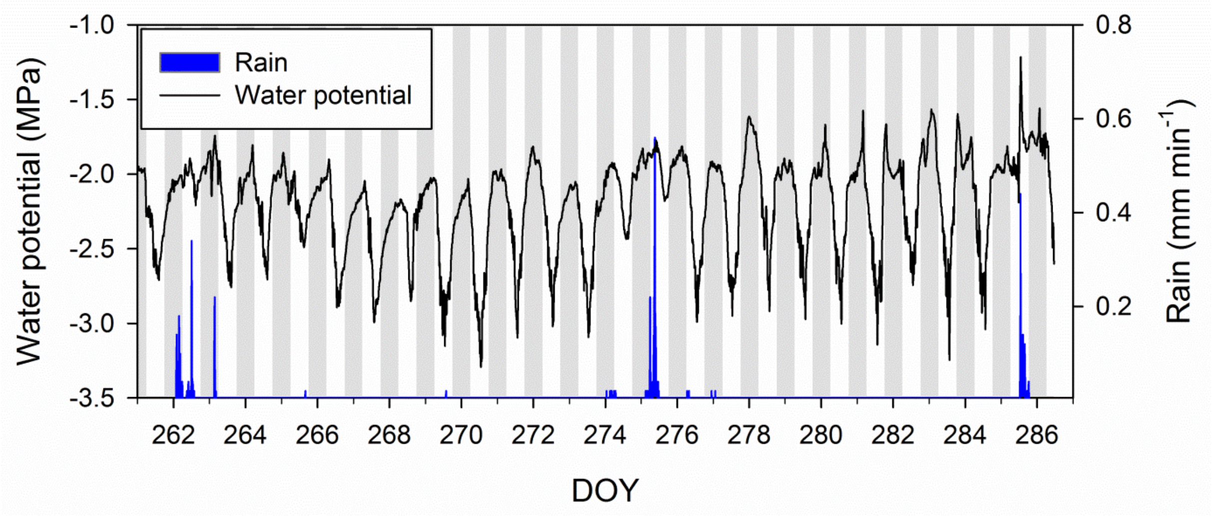

Figure 3.14 The curve of the water potential of *R. stylosa*, represented as the average of the three trees, in the time frame in which rain fell. Shaded areas represent nighttime and unshaded areas represent daytime.

In Figure 3.15 the osmotic soil potential (Ω_o), calculated with equation 9 is represented. The potential at the surface fluctuated according to the movement of the tide. This confirmed that fluctuations in surface soil potential were directly caused by the tide. When it was high tide, the soil potential reached the lowest values and vice versa. Thus, salinity was lowered when the soil was not inundated. In the time period shown, all three days with rain were included (DOY 262, 275 and 285). The effect of rain during the first and second rain event was not directly observable in the soil potential. The third rain event had a much clearer effect on the soil potential. Visual observations of the roots showed that the most developed roots were situated between 0 and 60 cm depth and the hardly any roots were present at a depth lower than 80 cm, indicating that roots were not able to reach ground water and that they were not dependent on such a fresh water sources.

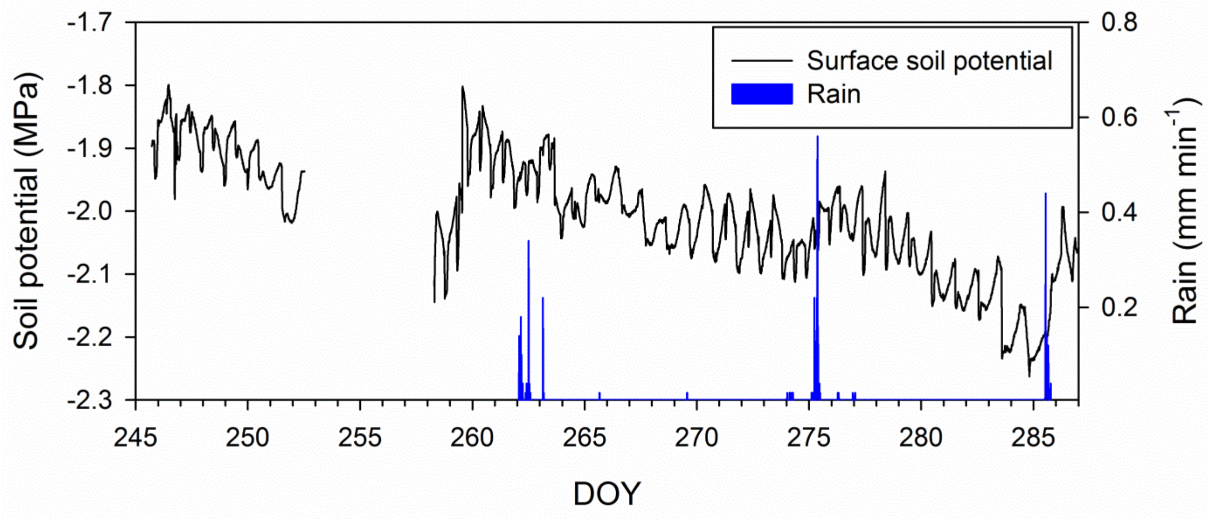

Figure 3.15 The soil potential calculated from the actual conductivity on a depth of 15 cm. During DOY 252 - 258 no measurements were obtained.

3.7 Growth pattern characterization

In a previous section (3.2 Stem radius changes) the growth patterns of *R. stylosa* were described. It was clear that the pattern displayed by this species is somewhat deviating from other species. In this section the growth curve of the entire experimental period is analyzed and characterized in order to discover some commonalities that are representative for this species. In a first phase, the objective is to distinguish the growth and shrinkage phases. Starting from the periods defined in Table 2.2, it will be analyzed whether these classification is valid.

The calculated growth and shrink for the corresponding period is presented in Figure 3.16. Figure 3.16a displays the growth (positive) or shrinkage (negative) per day. In most cases, days with very negative growth values were followed by positive growth figures. Days with highly negative values were quite often isolated and preceded by days with values that did not differ that much from each other. This is similar to the observation in Figure 3.2 that the diminutions in stem radius were mostly caused by large diameter decreases on single days. As regards positive growth, three outliers are visible, present on the days intensive rainfall was observed. This depicts the importance of rain for the trees. Figure 3.16b and c plot the amount of growth and shrinkage in the previously defined periods, which were 0 - 12 h and 12 - 20 h for Gr1H and Sh2H, and 6 - 12 h and 12 - 20 h for GrP and ShP. A first observation shows that for most days the periods called growth did show positive growth values and the periods defined as shrinkage did exhibit negative growth values. This was valid for both the large time frame definition (Gr1H and Sh2H) and the smaller time frame definition (GrP and ShP). A closer look at the data shows that both types of time frame definition had a lot of correspondence with each other. This indicated that the more specific time frame definition (i.e. growth from sunrise till noon and shrinkage from noon till a bit after sunset) might be satisfying in order to characterize the growth patterns of *R. stylosa*.

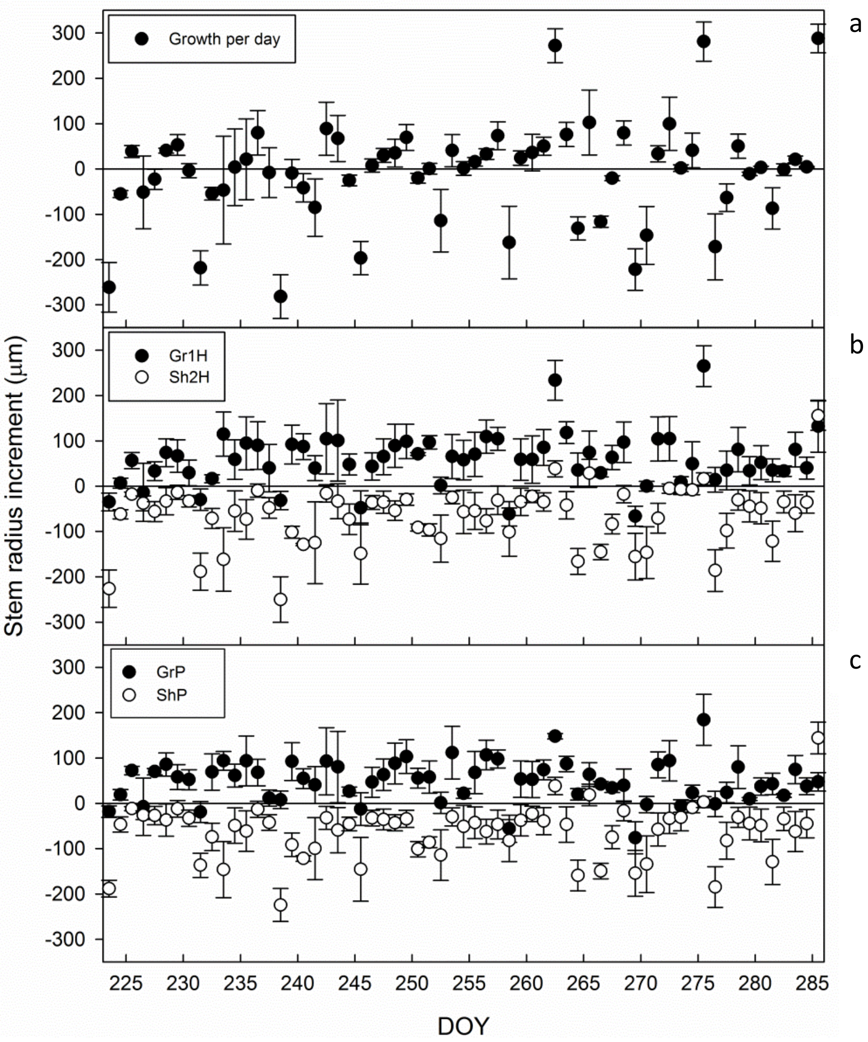

Figure 3.16 In this graph growth and shrinkage are presented in different time intervals. In (a) the growth between 0 h and 24 h is calculated. In graphs (b) and (c) the black circles represent the periods before noon and the white circles periods after noon. In (b) the intervals cover the entire day and in (c) only from 6-20 h.

Two tests were performed to confirm the accuracy of this characterization. In a first test, the correspondence between the large time frame definition and the small time frame definition was examined. This was performed by plotting the two variables to each other and by assessing whether a proper regression could be found. Such a regression was found in Figure 3.17. The correspondence between the two time frames shows that in the time interval 6 - 20 h most of the growth and shrinkage occurred and that growth (positive or negative) in this interval could be used to characterize the entire growth pattern of *R. stylosa*. Two curves were created, one in which the days with heavy rain were included and the other one that did not include these days with rain. This distinction was made because growth on a day with intensive rain will no longer be time dependent but depends on the period in which rain falls. If rainfall occurred between 20 h and 6 h in the night, it is logical that the intervals not including this time period (GrP and ShP) would show an underestimation of the total growth. The slope of the curve including the rain events was 1.109, which indicated that about 90 % of the growth and shrinkage took place in the intervals 6-12 h and 12-20 h, respectively. Analogously, when rain was not included about 93 % of the stem growth was included in the shorter time frame and the predictive force of this regression was somewhat stronger (with an r^2 of 0.954 compared to 0.947). It can be stated that the period between 6 and 20 h was the most important for the growth curve of *R. stylosa* and that there were not a lot of growth dynamics during night time.

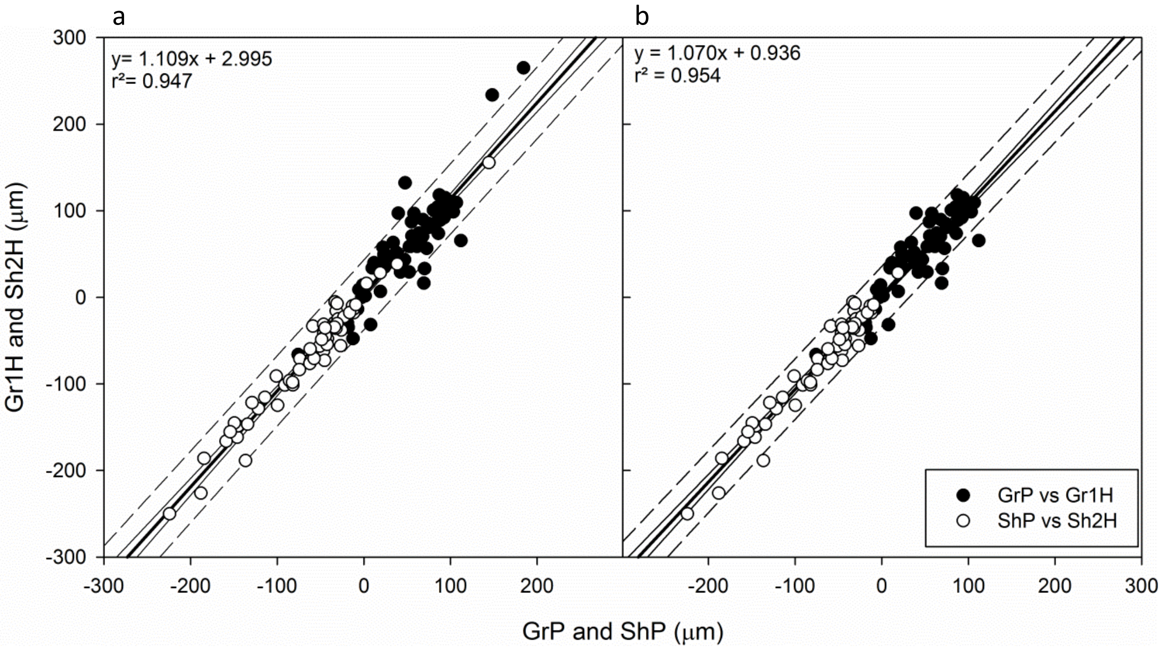

Figure 3.17 The relationship between the small time interval covering 6 - 20 h and the large interval covering the entire day with (a) rain included and (b) rain excluded. Black circles cover the period before midday and the white circles the period after midday. The regression line is applied for both periods and is presented with the thick line. 95 % confidence lines and 95 % prediction lines are shown with a thin black line and a dashed line, respectively.

In a second test, growth over an entire day was compared with growth during daytime (6 - 20 h) (Figure 3.17). Similarly, two situations were tested, one that included and one that excluded rain. When rain was included, the slope was 1.192, which indicated that both growth and shrinkage were underestimated in the smaller time interval. When rain was excluded, a similar image was acquired. The slope was a bit lower, with 1.108, which was logical because the days with a lot of growth, which were the days with rain, were not dependent on the time of the day but on the timing of the shower (which caused growth during both day and night).

Both Figure 3.17 and Figure 3.18 led to the same interpretation and growth dynamics could be appropriately analyzed by focusing on the growth patterns during the daily interval (6 - 20 h) and moreover, the effect of rain should be considered independently.

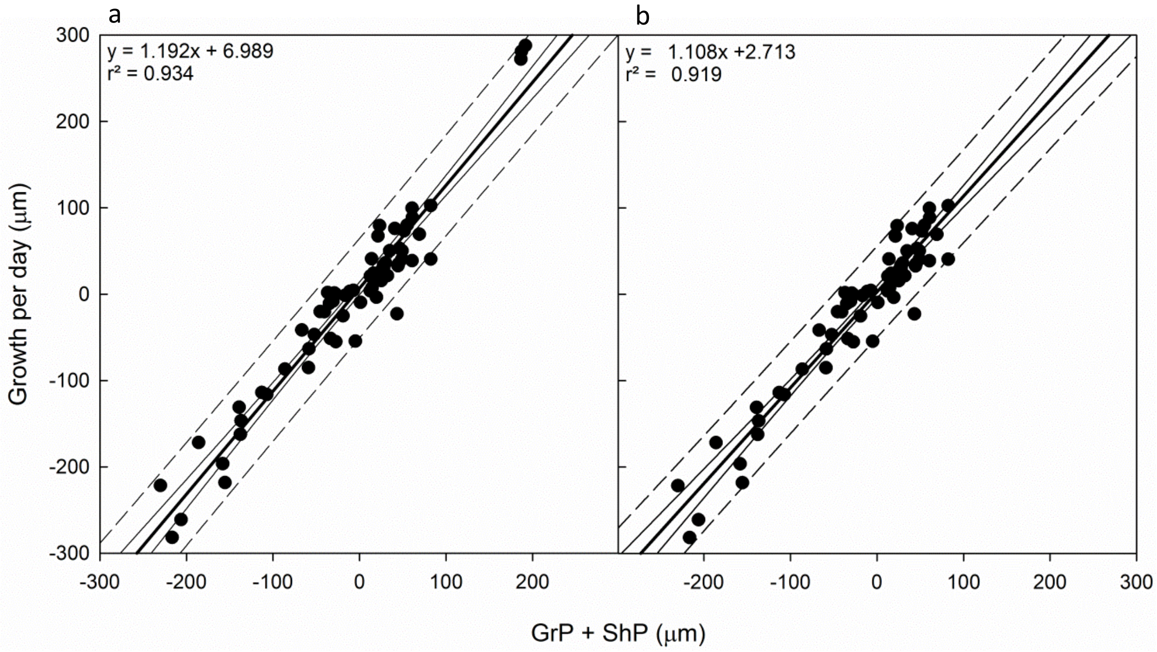

Figure 3.18 Comparison between the growth over an entire day and growth during the daytime, from 6 to 20 h. In graph (a) rain events are included, contrary to (b). The thick, thin and dashed lines are the regression line, the 95 % confidence lines and the 95 % prediction lines, respectively.

Lastly, Figure 3.19 represents a final way of visualizing the average growth dynamics of *R. stylosa*. In this graph the average growth during the corresponding time interval of one hour is plotted without taking days with rain into account. This graph confirmed the previous observations, which were a strong growth the first hours after sunrise, between 6 and 9 h, then around noon the growth curve showed a sort of a plateau and strong shrinkage occurred between 14 and 18 h. The initiation of growth in the morning was much more sudden and larger differences between consecutive time periods were recorded in contrast to a more gradual increasing and decreasing shrinkage in successive time intervals after 9 h. The shrinkage kept on continuing several hours after sunset. Figure 3.19 also represents the average diurnal growth curve by plotting the cumulative curve of these hourly growth figures. Important to mention is that this curve was based on growth data of only part of a year. During this part of the year these trees were confronted with severe drought, which was reflected in the negative growth value at the end of the average day. Besides this, days with rain were not taken into account, whereas rain contributed significantly ($P < 0.001$) to the growth figures. When rain would have been taken into account the negative growth per day would be -8 μm, compared to -22 μm without rain. This means that without rain the average growth for the trees would have been -1,373 μm per tree, whereas with rain the average growth during this experiment was -474 μm per tree.

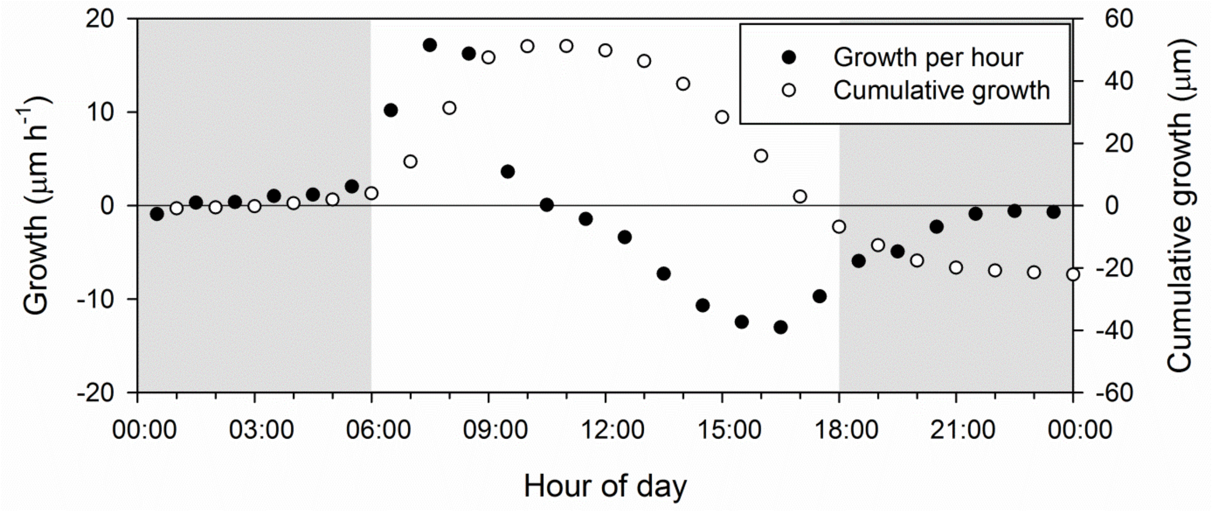

Figure 3.19 Average growth per hour is represented with black circles. Cumulative growth is displayed with white circles and shows the typical average growth curve of R. *stylosa*. Growth per hour and cumulative growth values are displayed at different axes. Shaded areas represent nighttime and unshaded area represents daytime.

3.8 Physiological effects on the growth pattern

Since the growth pattern could be approximated by growth from sunset to noon and by shrinkage from noon till 2 hours after sunset, these patterns were related to the other physiological observations. Firstly, it was analyzed which physiological variables could be correlated to the amount of growth for the different time periods. For this correlation study GrP, ShP and GpD were taken into account (Figure 3.20). Different choices of the appropriate variables were studied. For each variable, both the average over an entire day and the average over the studied time period were examined. For example, for a correlation between growth during the morning and the water potential, correlations were tested using the average daily water potential on the one hand and the average water potential in the morning period (6 - 12 h) on the other hand. For each of the three periods, the variables with the highest correlation were used for the further correlation study and are shown in Table 3.1. For sap flux density, the cumulative sap flux density for the respective period was used, which is referred to as sap flow.

The correlation between the growth dynamics and Ψ_b were rather low, but were higher for the afternoon period and the full day period than for the morning period. For sap flow, the correlation was lower in the morning as well, but these correlations were all higher than correlations with the water potential (Figure 3.20). In combination with the information from Table 3.1, for both Ψ_b and sap flow, the average values during 12 - 20 h had the largest influence on the growth dynamics. The correlations implied that an elevated Ψ_b resulted in an increased growth and that an increased sap flow decreased the amount of growth.

Table 3.1 For each variable the average value from the period depicted in this table is used. In these periods the correlation with the corresponding growth period is highest. The morning period is from 6 - 12 h, the afternoon is from 12 - 20 h and the day period takes the entire day into account.

	GrP	ShP	GpD
Water potential	morning	afternoon	afternoon
Sap flow	morning	afternoon	afternoon

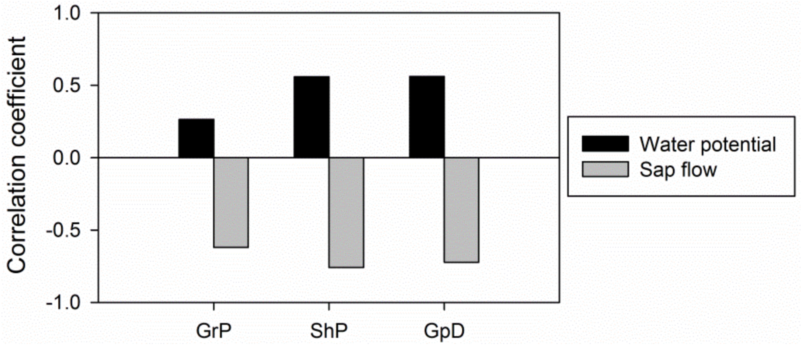

Figure 3.20 Correlation analysis of different growth periods with water potential and sap flow.

Chapter 4: Discussion

4.1 The diurnal physiological patterns of *R. stylosa*

So far only few studies use band dendrometers to quantify mangrove growth (Day et al. 1982, Jintana et al. 1985, Krauss et al. 2007) and none of these studies measured short-term diurnal growth patterns. The long term pattern revealed a stem diameter that barely or not expanded during the course of the experiment (Figure 3.2), which is uncommon for tree species, including mangrove species (Downes et al. 1999, Schöngart et al. 2002, Krauss et al. 2007). This study indicates that the trees had some sort of stress during the experiment, especially during the first 20 days.

R. stylosa did not have the typical sequence of shrinkage and growth (as described in 1.2.1 Diurnal growth patterns). The phases monitored during the day were opposite to the phases defined by Downes et al. (1999) or Herzog et al. (1995). The diurnal patterns of sap flux density (Goldstein et al. 1998, Fernández et al. 2001, Perämäki et al. 2001, Kume et al. 2007, Scholz et al. 2008) and water potential (Klepper 1968, Klepper et al. 1971, Acevedo et al. 1979, Offenthaler et al. 2001, Kume et al. 2007, Zufferey et al. 2011) were comparable to the observations in several other species. For the related *Rhizophora mangle*, a typical basal sap velocity has been recorded by Hao et al. (2009), which is very similar to the pattern of *R. stylosa* found in this study. The registered values of Ψ_b were within the range that has been encountered in other mangrove species (Scholander 1968).

4.2 The influence of meteorological variables on *R. stylosa*

For sap flux density, the vapor pressure deficit (VPD) and temperature could be related to the amount of sap transported through the tree (Figure 3.5). Firstly, for VPD, a ligand binding relation (Figure 3.6a) showed the best fitting relation ($r^2 = 0.791$). The curve rises towards a plateau, which is logical because a tree is limited by the anatomy of the xylem vessels and will not be able to exceed a certain maximum sap flux density. A rising VPD causes the xylem vessels to transport more water to the canopy according to the cohesion-tension theory. Secondly, for temperature, a sigmoid relation was found (Figure 3.6b, $r^2 = 0.666$). Again, this relation rises asymptotically to a maximum, representing the anatomical restriction of exceeding a certain amount of sap transported. Although VPD is a more accurate indicator for the water demand of the atmosphere than temperature (Ortuño et al. 2006b), lower temperatures resulted in a sap flux density of nearly 0 $cm^3 cm^{-2} h^{-1}$ and higher temperature resulted in a higher sap flux density. Both relations can be linked to the evaporative demand of the atmosphere. In the past, high correlations between VPD and sap flux density had already been found in other species (Ortuño et al. 2006a, Kume et al. 2007, Oguntunde and Oguntuase 2007). According to the findings of Ortuño et al. (2006b), similar relations were found between sap flux density and the meteorological variables VPD and air temperature.

Next to sap flux density, the Ψ_b was also linked to meteorological variables, although the correlations were weaker. The variables VPD and RH were most strongly correlated to Ψ_b (Figure 3.8). In other experiments the changes in Ψ_b were in response to VPD and linear (McCutchan and Shackel 1992, Fereres and Goldhamer 2003, Ortuño et al. 2006a), hyperbolic (Kume et al. 2007) and logarithmic (Elfving et al. 1972) relations were observed. However, in this experiment, a quadratic relation was found (Figure 3.9a, $r^2 = 0.637$). For a low VPD and consequently a low atmospheric water demand, the Ψ_b will be highest because a low force is exerted on the water column. When the atmospheric water demand rises, more tension on the water column arises and Ψ_b will become more negative.

The more negative the Ψ_b, the higher the VPD must be to lower Ψ_b with one incremental unit. The relation has a limited validity linked to the interval of VPD as shown in Figure 3.9, namely for higher VPD values the slope would be positive for an increasing VPD, which is physiologically not sound. The linear relation between Ψ_b and RH (Figure 3.9b, $r^2 = 0.572$) can be explained by the response to a higher relative atmospheric humidity resulting in a lower water demand from the atmosphere (eq. 2 - 5) and therefore a higher Ψ_b is expected.

In general, the sap flux density was more directly linked to micro climatic conditions than Ψ_b, as also seen in other research (Ortuño et al. 2006b). Especially VPD is an important meteorological variable with a high influence on the plant water relations of *R. stylosa*. The diurnal course of both sap flux density and Ψ_b were found to be very similar to what has been observed on a wide variety of species (Ortuño et al. 2006a, Ortuño et al. 2006b, Kume et al. 2007, Oguntunde and Oguntuase 2007). For Ψ_b, the values were low indicating the typical mechanism developed by mangroves in order to take up water in an environment where water in the soil has a low osmotic potential (Scholander et al. 1964, Scholander 1968).

4.3 Branch and leaf water potential

Not only Ψ_b was measured with stem psychrometers, but also Ψ_l was measured with a pressure bomb. The measurements of Ψ_l were only performed on one day, so general conclusions are difficult to make. Overall, the range of Ψ_l, which was -1.78 to -3.63 MPa (without the early measuring point), was rather high in comparison to the range of -3.0 to -4.5 MPa registered by Scholander (1968). The Ψ_b and Ψ_l were plotted in Figure 3.10 and unexpectedly, the first measuring point of Ψ_l was higher than Ψ_b, although more negative water potentials in the branches in comparison to the leaves were not expected as no reversed sap flow was measured. Normally, pre-dawn water potentials are either equal in the entire plant body or the water potential declines from root to stem to leaf (McCully 1999, Donovan et al. 2001, Kume et al. 2007).

Initially, differences between Ψ_l and Ψ_b were small, which is uncommon. Therefore, a rise in the concentration of osmotic substances in the cells is put forward as the main hypothesis. A rise in osmotic concentration results in a lower osmotic potential and consequently an influx of water in the cells. In this case, less water is available for transpiration and therefore less water is lost, postponing the typical drop in Ψ_l after sunrise. Later, the influx of water decreases because the osmotic substances are diluted and the amount of osmotic substances declines. Eventually, in response to a rising atmospheric water demand, Ψ_l and Ψ_b decrease and the difference between both water potentials becomes higher. The rise in osmotic substances is situated shortly after sunrise and the concentration during the night should be comparable to the levels of the previous night in order to have a daily cycle.

The recorded growth pattern was linked to the difference between Ψ_b and Ψ_l (Figure 3.19 and Figure 3.10) which can be divided in three phases. In the first phase, during the first hours after sunset, as a response to the rise in osmotic substances, an influx of water into the cells was created, which is reflected in the growth pattern (Figure 3.19). In a second phase, starting at 9 h, the atmospheric water demand increased and the osmotic substances were partly diluted and reconverted to less active substances lowering the water potential. The growth figures made a sudden drop and gradually, positive growth altered to negative growth reflecting the second phase in the growth pattern. In a third and final phase, after 16 h, the difference between the water potentials became smaller again (but Ψ remained lower at the leaves) and the negative growth became less as well. A lowered transpiration and therefore a lowered efflux of water from the cells caused this stagnation. Expect for the first measuring point, all the water potential data points could be linked with the overall growth pattern and the correspondence was striking. However, the data presented in Figure 3.10 is only based on a single day of measurements. In order to acquire a more definite answer on the gradient present in the tree, repeated measurements on more days should be carried out in coming research. If the predawn Ψ_l would be consistently higher than Ψ_b, this could indicate foliar water uptake from dew, as recorded by for instance Burgess and Dawson (2004) on *Sequoia sempervirens*.

4.4 Stomatal behavior

The regulation of the stomatal aperture is an essential mechanism for plants to control its water status. The combined measurements of seven days resulted in the circadian stomatal resistance curve presented in Figure 3.11. Evidence for midday stomatal closure was observed in the small dips in the stomatal resistance around noon. Midday stomatal closure was also visible as dips in the sap flux density and water potential on many days (Figure 3.4 and Figure 3.7). During stomatal closure, the force exerted on the water column declines because transpiration is lowered which results in a rise of the water potential (Brodribb et al. 2003) and a drop in the sap flux density (Zweifel et al. 2002). The diurnal stomatal resistance pattern and the midday stomatal closure were comparable to other tree species (Tardieu and Simonneau 1998, Romero and Botía 2006). Stomatal opening in the morning was rapid, while the stomatal closure was rather gradual, which is not uncommon for tree species (Cuevas et al. 2006, Romero and Botía 2006). Consequently a lower CO_2 assimilation was expected in the afternoon. A reason for this behavior could be a water conservation tactic or could originate from a lower need for CO_2 assimilation in the afternoon after a high production of photosynthetic assimilates in the morning.

Stomatal aperture throughout the day is typical for C3- or C4-plants and this eliminates the possibility of *R. stylosa* of being a CAM-plant (Ting et al. 1985, Knapp 1993).

4.5 Rain and salinity

The soil potential reacted different to the various rain events, because during the third rain event the osmotic soil potential rose more (Figure 3.15). Two possible explanations for the strong rise are the low tide on that time or the low soil potential before the rain event. In the latter case the soil potential simply recovered to similar values as after the other rain events.

The most important growth spurts occurred during periods of heavy rain (Figure 3.2 and Figure 3.12). During the three days with rain, 19.8, 29.2 and 19.8 mm rain fell, respectively. The first two rain events occurred during a period of high tide when the trees were inundated, whereas the third rain event occurred during low tide. Yet, all three days the growth per day was very similar (281 ± 21 μm) and thus the moistening of the soil did not appear to have a large influence as no larger growth was observed during the third rain event. Moreover, this result indicated that in the event of heavy rain the tree was able to take up water until a saturation point. The smaller rain events did not induce a visible effect of the stem diameter which could be due to a certain threshold which must be exceeded before direct visible effects can be monitored (Zeppel et al. 2008).

The sap flux density was lowered or even halted in response to rain (Figure 3.13), which is the same response as has been described in literature (Becker 1996, Motzer et al. 2005, Kume et al. 2007). For most species, rainfall goes hand in hand with a subsequent lowered water potential in case water stress is present (Poole and Miller 1975, Kume et al. 2007). This is due to a lowered atmospheric water demand and a moistening of the soil (Downes et al. 1999). After rainfall, the positive effect on the plant, i.e. a higher water potential, can last for several days or weeks, until water reserves can no longer be replenished from the soil (Boyer 1968, Poole and Miller 1975, Kume et al. 2007). In contrast, for mangrove species, the fresh water only infiltrates the soil when the soil is not inundated. If the soil is not inundated, the effect of rain on the soil will be mostly eliminated when it is inundated again.

For *R. stylosa*, rainfall induced a clear effect (Figure 3.14), indicating the usage of the fresh water source originating from rain by *R. stylosa*. Overall, rain lowered the average and minimum Ψ_b on those days. Furthermore, the third rain event gave rise to an additional elevation of Ψ_b above the levels reached during the night. The dissimilarity between the different days with rain was likely generated by the level of inundation on the time of the rain event. Rainfall resulted in a decreased or even halted sap flux density because the driving force for sap to rise was no longer present (Figure 3.13).

Two main effect have been described in literature to cause such significant growth spurts observed in the stem diameter, namely enhanced water uptake through the roots and foliar water uptake. The first effect describes an augmented water uptake through the roots in response to rain for two reasons. Firstly, transpiration is reduced because the leaves are wet and the atmospheric water demand is low (because of an increased RH, lowered temperature and radiation) and secondly the soil is moistened which increases the water availability in the soil (Downes et al. 1999, Burgess and Dawson 2004). In other tree species the effects of a moistened soil and a halted transpiration explain a swift diameter increase for both daily and nocturnal rain. During the night, rain will provide additional water to increase the growth and during the day the shrinkage will be avoided due to a halted transpiration (Downes et al. 1999, Sevanto et al. 2001).

Contrary, nocturnal growth dynamics are rather low for *R. stylosa* (3.7 Growth pattern characterization), although this species still exhibited a strong response to nocturnal rain. However, this study monitored no sap flow during nocturnal rain events so water uptake originating from other places than the roots was hypothesized. Confirmation was found by the high tide during the two nocturnal rain events, which made the uptake of fresh rain water from the roots highly unlikely. Subsequently, an explanation would be water uptake from the canopy or the bark, which is the second effect that could cause these growth spurts. In fresh water, a water potential of 0 MPa is expected and in *R. stylosa* a maximum average Ψ_b of -1.2 MPa was measured during rainfall resulting in a strong potential for water uptake in the event that water entrances were present in the plant body.

These kinds of entrances are certainly not self-evident, because trees are developed in such a way that water exits (or entrances) are avoided as much as possible when this is not wanted. An example of this feature is stomatal closure at nighttime. On the surfaces where no stomata are situated, a hydrophobic layer, the cuticle, is present to avoid nocturnal transpiration as much as possible (Burghardt and Riederer 2003). Nevertheless, Dawson et al. (2007) recently observed nighttime transpiration on a wide variety of species thriving in all types of ecosystems. Causes for nighttime transpiration were allocated to stomata that were not fully closed (wanted by the plant or unwanted) and to water loss through the cuticle, especially in older leaves. Besides nighttime transpiration, they also reported an elevated nocturnal stomatal conductance in response to rain for several nights after the rain event.

The results for *R. stylosa* provided a somewhat contradictory proof of the presence of nighttime transpiration. On the one hand the sap flow data showed the presence of nighttime sap flow ($V_s \neq 0$) on many nights (Figure 3.4 and Figure 3.13). On the other hand the aggregated stomatal resistance curve indicated full stomatal closure before sunrise and after sunset (Figure 3.11). Stomatal resistance recordings were analyzed on a daily basis but no linkage was found between pre-dawn and post-dusk stomatal resistances and elevated nightly sap flow. Neither could a relation be found between the amount of sap transported during the night and the prevalent VPD. Besides, the determination of nocturnal sap flow depends on the identification of the zero-sap-flow line, which is error-prone. Therefore, it could be stated that no considerable nighttime transpiration is present in *R. stylosa*. Another explanation for the nighttime sap flow could be hydraulic redistribution inside the tree.

In literature, a pathway for rain or fog uptake repeatedly proposed is water uptake through the cuticle and this pathway has been monitored on a wide variety of species (Yates and Hutley 1995, Gouvra and Grammatikopoulos 2003, Limm et al. 2009, Simonin et al. 2009). For mangroves, it could be possible that nighttime transpiration through the cuticle is prevented by the strong retention of water inside the tree due to the relatively low nocturnal water potential. Furthermore, this could enable the uptake of fresh water into the tree because a large gradient exists between fresh water on the outside of the leaf with a high water potential and a low water potential at the inside of the leaf. Such an uptake could cause growth spurts in response to nocturnal rainfall as observed during the conducted experiment. This would confirm the observations of responses to both daily and nocturnal rain events.

The response of the stem diameter of *R. stylosa* to rain events is almost immediate, which makes it remarkable if water uptake in response to rain would only be situated at the leaves. Water uptake by the bark is one of the possibilities that could explain the rapid response of the stem diameter (Katz et al. 1989, Oren and Pataki 2001). Oren and Pataki (2001) reported small annual rates of water loss through the bark and a much higher annual uptake after rain events, which was about a threefold of the losses. No relation was found between nightly growth figures and relative humidity or VPD, so water loss through the bark could be negligible due to the low water potential present inside the stem cells. However, when rain events occur, actual water drops come in contact with the bark which could enable the uptake of water through the bark (for instance through lenticels). Water uptake through the bark would also explain why no negative sap flow was observed during rainfall, while the stem clearly swelled. For such a water uptake only a radial water stream needs to be present to supply the adjacent cells with water.

The possibility exists that the bark exhibited hygroscopic swelling, without the water really passing the bark into the storage tissue of the stem. If this was the case, a more severe reduction of the stem diameter was expected when the moisture dried during the following days. However, the response to the first rain was a strong diameter increase which remained for several days (Figure 3.12).

Definitely, more research needs to be carried out to investigate the entire pathway of water in the tree in response to rain. For example, isotope analysis, dyed water or isotopic labeled water could be used to trace water in the tree.

4.6 The extraordinary growth pattern of *R. stylosa*

4.6.1 Is *R. stylosa* a CAM-plant?

In Figure 3.19, the general growth pattern is shown for *R. stylosa*. Net growth was situated in the morning and net shrinkage was set in before noon, which is a deviating pattern compared to other species. Nevertheless, deviating growth patterns for other species have been registered in literature before. Matimati et al. (2012) described a comparable course of diurnal stem growth pattern for South African succulent shrubs, which use the CAM pathway for the fixation of CO_2. Although the nocturnal stem diameter variation differs, the daily course is very similar. Explanations of the pre-noon swell and post-noon shrinkage in CAM-plants were proposed by MacDougal (1936) and Chen and Black (1983) and were based on the stomatal opening during the night and stomatal closure during the day. Moreover the leaves of *R. stylosa* are succulent leaves which has been described as a typical morphological feature for CAM-plants (Lüttge 2004). In CAM-plants, the acids formed during the night are osmotically active, which enables the acquisition of extra water, particularly towards the end of the night (Acevedo et al. 1983, Lüttge 2004).

One hypothesis could be that *R. stylosa* is a CAM-plant, but water uptake was not situated before dawn but immediately after dawn. Although CAM-plants are known to occur in areas with water stress, generally halophytes are not equipped with the CAM-metabolism (Lüttge 2004). Furthermore, Andrews et al. (1984) performed experiments on *R. stylosa* and concluded that this species photosynthesizes via the C3-mechanism. Also Martin and Loeschen (1993) did not find evidence for CAM-cycling in the related species *R. mangle*. Moreover, the conducted experiment in this master dissertation performed measurements on stomatal resistance (Figure 3.11) and observed typical stomatal patterns that are found in C3- or C4-plants.

In this study, a sudden increase in osmotic substances, shortly after sunrise, was hypothesized for *R. stylosa*. If these osmotic substances are photosynthetic assimilates, they are rapidly formed, whereas the formation of photosynthetic assimilates in C3-plants is rather gradual and continues throughout the day (Upmeyer and Koller 1973, Mitchell et al. 1992). It may be concluded that *R. stylosa* exhibited traits of CAM-plants but does not use the CAM-metabolism.

4.6.2 Periods of growth and shrinkage

Figure 3.17 and Figure 3.18 showed that most growth occurred in the morning, between 6 and 12 h, and most shrinkage in the afternoon, between 12 and 20 h. which were the most important growth dynamic periods. While morning growth only varied between -5 and 90 μm (10th and 90th percentile), the afternoon shrinkage varied between -150 and -15 μm, which is considerably more. For growth per day a lot of periods of several days with a little bit of net growth were followed by one day of strong shrinkage. A possible cause is the replenishment of water reserves on days with more favorable atmospheric conditions which resulted in the presence of more easily available water in the trees. When atmospheric conditions turned worse again for the tree, the readily available water was easily withdrawn from the tree. While daily growth spurts were only observed in the event of rainfall, extensive daily shrinkage was observed much more frequently. Most (80 %) of these extensive shrinkage events (> -100 μm) could be linked to a large drop in the average RH (> -5 %) and a large increase in the average VPD (> 0.2 kPa) the next day (Figure 3.1a and Figure 3.16a). Herewith, evidence that extensive shrinkage was mainly linked with easily available water that was taken up on previous days and was lost again when atmospheric conditions became less favorable is provided.

The amount of growth and shrinkage was positively affected by an increase in Ψ_b and negatively affected by an increase in sap flow (Figure 3.20). The correlation was stronger for sap flow than for Ψ_b. The positive correlation between Ψ_b and the growth dynamics indicates that a higher water potential increases growth. In other species, Fereres and Goldhamer (2003) found rather low correlations between these two physiological variables, Klepper et al. (1971) clearly showed a diurnal relationship between the water potential and stem diameter variations and Ortuño et al. (2006b) linked the maximum daily shrinkage to stem water potential. The amount of sap transported had a greater influence on the amount of growth and a larger sap flow resulted in a reduced growth. In literature, the relations tested between sap flux density and stem diameter on other species yielded high correlation coefficients (Herzog et al. 1995). Ortuño et al. (2006b) showed a strong correlation between the maximum daily shrinkage and sap flow and De Swaef and Steppe (2010) revealed a close diurnal relationship between sap flow and stem diameter variations. This experiment showed that growth per day and shrinkage in the afternoon was more directly influenced by the sap flow and Ψ_b than the morning growth. A possible explanation is that the water uptake in the cells, which causes the morning growth, is more closely related to the amount of osmotic substances that is formed during the morning. The amount of these substances is hypothesized to decline in the afternoon, hence the retention of the water inside the tree is less related to the amount of osmotic substances in the afternoon, but more related to the prevalent conditions during that time period.

4.6.3 An osmotic regulated growth pattern

The mechanism hypothesized to declare the observed growth pattern is an osmotic regulated rapid uptake of water in the morning and a gradual loss of water throughout the day. The mechanism is mainly driven by the increasing and decreasing concentration of osmotic substances. Our results showed that nocturnal growth dynamics and sap flux densities were rather low and therefore a state of equilibrium throughout the tree is supposed during the night, certainly just before dawn. During the first hours of daylight, the most intensive growth was observed. A sudden increase in the amount of osmotically active substances in the tree cells is hypothesized. The formation of such osmotic substances could be driven by photosynthesis, because they would have been formed on the same time as when photosynthesis is initiated. The increase in osmotic substances would lower the water potential of the cells, which would cause an influx of water and increase turgor in the cells. The increased water content of the cells would dilute the osmotic substances and lower the concentration and consequently cause the osmotic potential inside the cells to become less negative again. Furthermore, competition for the water inside the canopy increases due to the rising atmospheric water demand throughout the morning period. Right before noon, stem diameter reached a maximum value and the influx of water was gradually changing in an efflux of water.

The reasons for the efflux of water were twofold. On the one hand the water demand of the atmosphere remained fairly high during the afternoon and on the other hand a decrease of the osmotic substances is hypothesized. This requirement is necessary because the patterns are repeated every day and a decline to the predawn concentration is needed to obtain similar diurnal patterns. A possible explanation is that the substances that are osmotically active are converted into substances that are osmotically less active or even inactive.

Two possible pathways are proposed that could change the amount of osmotic substances. A first possible pathway is the active involvement of osmotic substances in the formation of sugars by the process of photosynthesis. These substances would be converted into building stones required for growth and maintenance inside the tree. A second possible pathway is the formation of the substances under influence of photosynthetic energy during the morning and a gradual conversion back into their original state in which they were not osmotically active. The reconversion could be initiated by the influx of water. The rapid formation of these substances and the more gradual conversion to other substances would explain the rapid swell monitored during the morning and the gradual decrease of the growth figures after 9 h. However, in this dissertation, no chemical analysis was performed, which could provide confirmation of the process. Information about the diurnal concentration curves of substances formed during photosynthesis in *R. stylosa* could be very valuable. Such a further research would possibly provide some additional evidence to explain the unique growth pattern of *R. stylosa*.

While in other trees the lagging (tens of minutes - several hours, see Phillips et al. (1997)) sap stream near the roots causes these trees to shrink during the first moments of transpiration, *R. stylosa* did not shrink in early morning. In other trees the shrinkage phase is caused by the depletion in the canopy due to transpiration, while water uptake at the roots does not follow immediately causing a net decrease of the water inside the tree. In *R. stylosa* however, when transpiration should initiate, the increase in osmotic substances causes water to preferentially flow to the cells because a gradient between the cells and the xylem vessels is present. This prevents a shrinkage in the morning and would also prevent the Ψ_l to decline considerably during the first hours of the morning (Figure 3.10). During a day with a higher VPD, the demand for transpiration would increase, less water would be supplied to the cells, and a higher amount of sap would be transported, which would decrease the morning growth and increase the afternoon shrinkage (Figure 3.20).

An overview of the foregoing hypothesis can be summarized with Figure 4.1. In Figure 4.1 a comparison is made between the five phases that can be monitored in other species, displayed in Figure 4.1a, and the different phases of water movement in the stem of *R. stylosa*, according to the hypothesis, shown in Figure 4.1b. The figure and description of the classic pattern is based on the work done by Herzog et al. (1995) and is discussed firstly. The first phase (I) is the nightly phase in which the water reserves of the stem are replenished by water that is taken up from the soil. The second phase (II) describes the delay period between the increase of sap flow and the shrinkage of the stem. The third phase (III) is the period when stem shrinkage is the strongest and when sap flow is reaching its maximum values. Phase IV is the delay period between maximum flow and the minimum stem radius. Finally, phase V describes the period in which the sap flow is lowering and the radius increases again. The same phases are depicted in Figure 4.2 on the classical growth curve.

As already explained, the growth pattern of *R. stylosa* is different and can be described in five other phases (Figure 4.1b). The first phase (1) is the nightly phase in which no or a low sap flux density is observed. Small amounts of water could be transported caused by hydraulic redistribution inside the tree. Phase 2 starts when daylight is intercepted by the canopy and photosynthesis is initiated, which provides energy for osmotic substances to become active. During this phase, sap flow is initiated and water is taken up at the roots and delivered to the cells because of their low osmotic potential. A strong water stream into the storage tissues results in a swelling of the cells and a strong increase in the stem diameter. The strong influx of water causes the concentration of osmotic substances to decline and the gradient to become less strong, resulting in a gradually decreasing growth, shown in phase 3. Then, a tipping point is reached and a maximum diameter is attained for that day at the end of this phase. Phase 4 is the phase after the tipping point in which the stem storage cells are no longer able to maintain all the water inside their cells. This is caused by an increasing water demand of the atmosphere, with a consequently increasing transpiration, and by the decreased amount of osmotic substances because of the conversion of these substances to osmotically inactive substances. A strong diameter decrease is observed in phase 5 caused by the large water demand from the canopy and the osmotic potential that is becoming less negative. Eventually, some hours after sunset the nightly phase is observed again.

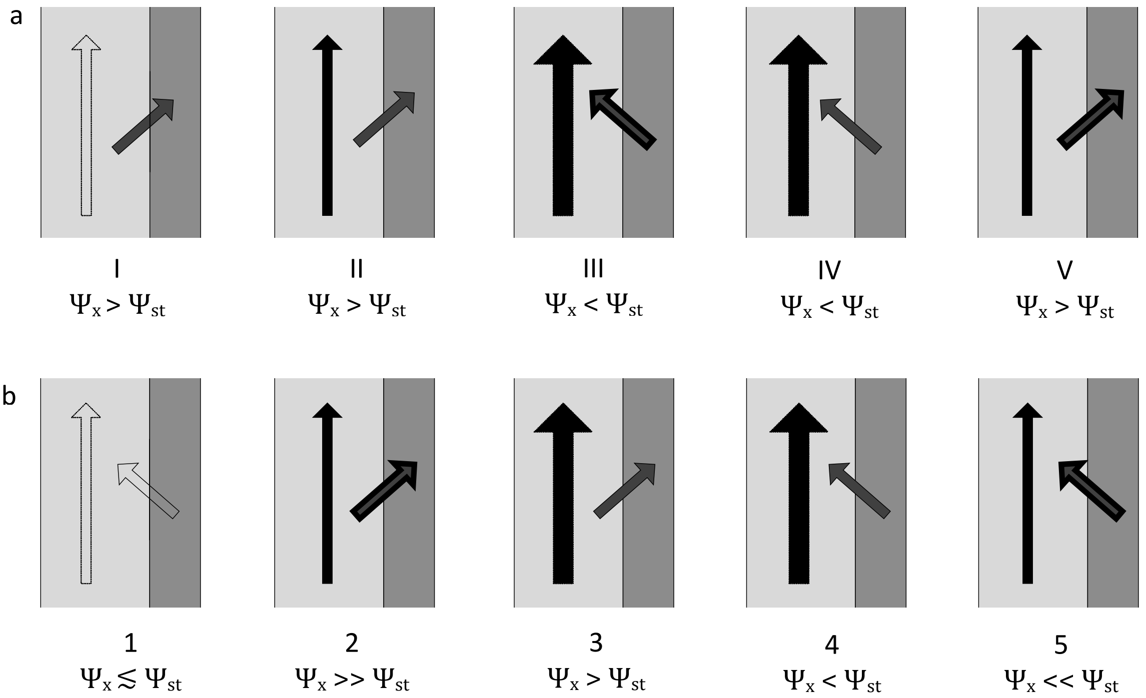

Figure 4.1 A comparison of the water exchanges between the xylem vessels (light) and the stem storage tissue (dark) for the pattern that is generally encountered (a) and for *R. stylosa* (b). The large arrow in the xylem vessel represents the sap flow. The small arrows represent the water exchange between the xylem vessels and the stem storage cell. The extent of the flow is represented by the thickness of the arrow. The exchange of the water is according to the difference in water potential of the xylem (Ψ_x) and the storage cells (Ψ_{st}). The figure is based on the representation of Herzog et al. (1995).

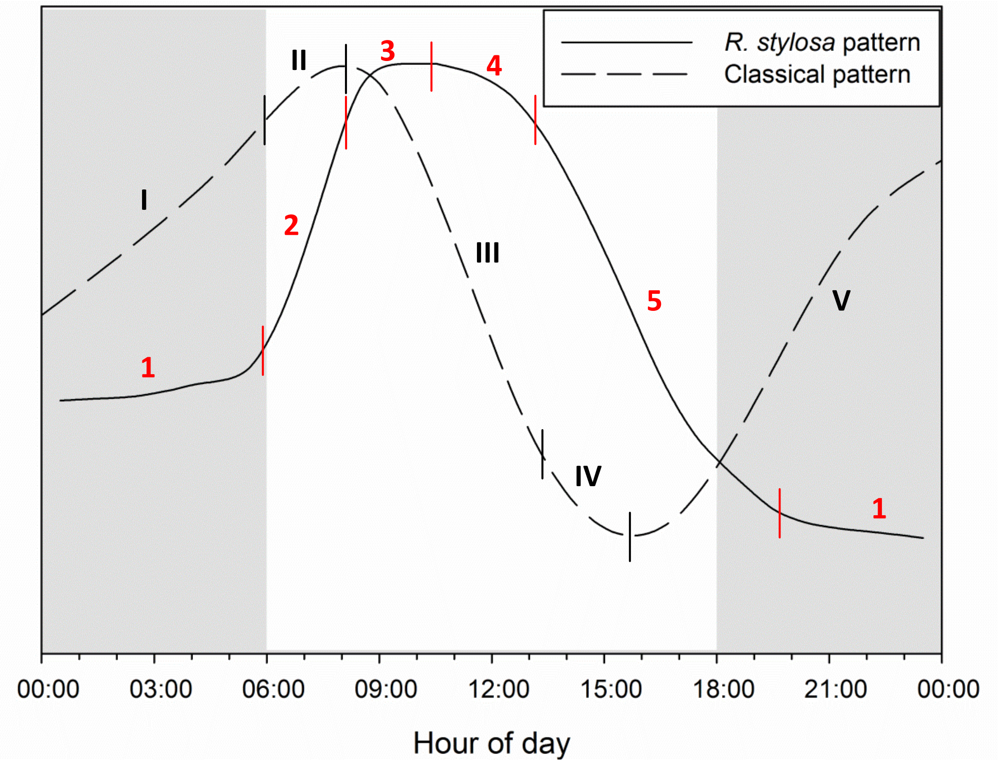

Figure 4.2 The phases described in Figure 4.1 are indicated on the stem diameter growth curves in red for the pattern of *R. stylosa* and in black for the classical pattern. Shaded areas represent nighttime and unshaded area represents daytime.

4.6.4 Benefits of osmotic regulation

The osmotic regulation proposed in this dissertation could provide significant benefits to *R. stylosa*. Due to the water uptake in the morning, the cells will swell and will be able to operate under full turgor which performs the high functionality of the cells (Figure 1.2). As already mentioned, the unraveling of the processes responsible for an increase in osmotic substances should be an important research objective in future experiments. The osmotic substances could be osmotically active assimilates, formed by photosynthesis, or salt and organics, related with salt uptake in the cell. Both mechanisms are probably triggered by the presence of photosynthetic energy and both mechanisms need an active conversion of osmotically inactive or less active substances to more active substances. If these substances are photosynthetic assimilates that are further used in the process of photosynthesis and in the production of required building stones for the tree, then the metabolic cost can be low, because these substances are further used in the photosynthetic pathway. If the process is rather a conversion to osmotically active substances which are reconverted to inactive substances during the course of the day, the metabolic cost could be significant for the tree. Due to the swell in the morning, the tree will be operating at high turgor during most part of the morning and around noon. In this time period the concentration of sugars in the leaves will be lowest (Mitchell et al. 1992) and because of the high turgor, the photosynthetic process can operate in favorable conditions and can produce a high amount of assimilates. When the photosynthetic conditions turn worse again due to a lowered turgor pressure in the afternoon, the need for assimilates will be lower and the disadvantage of the lowered turgor for the photosynthetic performance can be modest. If the formation of such osmotic substances is truly part of the photosynthetic pathway, the possibility arises that *R. stylosa* makes use of a new or hybrid form of the photosynthetic metabolism. For decisive answers, the photosynthetic metabolism of this species should be thoroughly investigated in the future.

Chapter 5: Conclusion

In this master dissertation the plant-water relations of the mangrove species *Rizophora stylosa* were explored by combining several types of sensors to obtain data on different physiological variables. Although mangroves have been intriguing scientist since a very longtime, a lot of the mechanisms enabling mangroves to be capable of surviving in the intertidal zone still need to be discovered. In this preliminary research, several observations were made that *R. stylosa* exhibited some very particular features which have never been observed before on tree species. A first finding is the measured diurnal diameter variation of *R. stylosa* that differs from almost every other tree species in the past. A second finding is the resemblance of the growth pattern of *R. stylosa* with CAM-plants. Furthermore, most CAM-plants possess succulent leaves and also *R. stylosa* has succulent leaves. However, the general conclusion was that *R. stylosa* is not a CAM-plant, because on the one hand stomata are opened during daylight and on the other hand, previous studies already found that *R. stylosa* photosynthesizes via the C3-mechanism.

Although the growth pattern differed, the sap flux density and the water potential at the branches (Ψ_b) was similar for *R. stylosa* as for most other tree species. The measurements of the water potential at the leaves (Ψ_l) gave an indication that the force exerted by the atmosphere on the water column remained low until 9 h and the decrease of Ψ_l was insignificantly during the morning. At the same time, the stem diameter increased at the highest rate of the day. Later, the growth became gradually less and became negative around noon. The most severe shrinkage occurred at approximately 16 h, when the water potentials were minimum and growth figures became roughly 0 at about 20 h until the next morning, indicating a state of equilibrium during the night.

A decisive theory could not be formulated based on the data collected during the field work. Nevertheless, an effort was made to formulate a plausible hypothesis that could explain the diurnal observations. The hypothesis was based on the rapid formation of osmotic substances after dawn. These substances would result in a sudden drop of the osmotic potential creating a large influx of water into the cells enabling the tree to operate with well-watered cells and with high turgor pressure during the first hours of the day. Around noon, water uptake reached a maximum and the amount of osmotic substances was declining while the atmospheric water demand was still increasing. As a result, the tree diameter decreased in the afternoon. The benefits of this mechanism are that most of the water lost in the afternoon was gained in the morning. The final result is a much smaller net decrease of the total water content inside the tree. In case the osmotic substance is an intermediate of the photosynthetic mechanism, the metabolic cost of the water retention strategy could even be modest.

This study focused on the water relations of *R. stylosa*, but the data collection and information delivery during the field measurements should be combined with information on the photosynthetic metabolism of the tree. It might not be unlikely to discover new features in the investigated tree that explain the observations of this study and helps understanding how this tree and other trees with similar characteristics cope with the challenging environment. In case these osmotic substances are involved in the photosynthetic pathway and metabolism, it could be possible that this tree species uses a hybrid form or even a new form of photosynthesis, however the results of this master thesis first need to be further confirmed and more and further research on these osmotic substances is necessary.

In this study evidence was found that *R. stylosa* makes use of rain in order to maintain a positive water budget. The data was collected during a dry period when all three monitored trees exhibited negative growth until a growth spurt as a response to rain was measured. At the end of the experiment only one out of three trees had a larger stem radius compared to the initial state. If growth figures during days with rain were excluded, the average shrinkage per day would have been almost threefold than what it was now, with rain. Therefore, rain is an important factor for this species. Furthermore, indications were found that water uptake of fresh rain water could occur at the leaves, most likely through the cuticle, and through the bark.

The preliminary research in this dissertation can be used as a starting point for new experiments that use this unique dataset as a basis to gather new insights. In order to obtain a confirmation of the hypotheses, a lot of new research will be needed. This knowledge will not only enrich the ecophysiological theories but can also be important for conservation strategies to preserve mangroves around the world. The alarming rate at which mangroves are disappearing, emphasizes the urgency to protect and manage these unique ecosystems. A solid base of knowledge about the functionality and how these systems react to changes in their environment need to be developed to achieve this goal. Especially in the scope of climate change, this knowledge will be very valuable.

Chapter 6: Future research

This master dissertation aimed to explore the water relations of the salt excluder *R. stylosa*. The assessment of the usage of water on a daily base was based on the information gathered from measurements of the diameter variation, sap flux density, water potential and stomatal resistance. The trial period only ran for 63 days, which is rather a short time interval and included only part of the winter and the spring. Experiments that run over an entire year or even several years and several growth periods would enable the assessment of the intra-annual and inter-annual differences in the growth pattern. The outcome of the average growth pattern would be further elaborated because the diurnal cycle should yield a positive value at the end of the day for viable mangroves. Furthermore, it would be interesting to see whether this deviating growth pattern remains the same during the other seasons of the year.

Beforehand, the outcome of these measurements was unknown because this study was one of the first experiments on this mangrove species. This exploratory study presented some surprising results, such as the pattern of the stem diameter variation. Because the result was not anticipated, a lot of data and measurements, required to obtain the full picture, were not yet obtained. Nevertheless, a hypothesis that could explain the measurements was proposed.

Further research needs to be conducted in order to refine, confirm or alter this hypothesis. During this experiment physiological variables were related to meteorological variables. By placing different types of sensors as close as possible to each other, the data obtained would be easier to interpret because less spatial variability and lag times are encountered. Sap flux density and stem diameter were measured at breast height and water potentials were measured in the canopy which complicated the interpretation of the data. Because the experiment was performed under natural conditions, it was impossible to assess the separate influence of each meteorological variable on the tree. In a controlled environment, where different treatments can be applied on the tree, it would be possible to assess the influence of drought, more favorable or less favorable atmospheric conditions, different levels of radiation and the influence of different amounts of rainfall and of different time periods in between two consecutive rain events. For instance, a difference could arise in the response to rain events between well-watered trees and water stressed trees. The influence of inundation could also be evaluated under atmospheric conditions that are kept stable. In controlled conditions, new measurements of the water potential should be obtained with both a pressure bomb and a psychrometer. By keeping the conditions constant and making several full day measurements a general pattern should be obtained which can provide information on the gradients present in the tree throughout the day.

Indication for rain uptake through the leaves and the bark were present but only indirect observations of this phenomenon were registered. A gradient for such a water uptake seems to be present, because of the large difference between the water potential of fresh rain water and the water potential inside the tree. The usage of seawater or rain water by the tree could be distinguished by measuring the isotope composition of water inside the tree, because seawater is enriched in the heavier isotopes of O and H (Ehleringer and Dawson 1992). Another possibility would be to spray parts of the tree with dyed water and to investigate whether this dye is also found inside the tree or in parts of the tree that were not sprayed. A final possibility proposed, is the usage of labeled water that could be sprayed on the tree. Finding labeled water inside the tree indicates that water was taken up by the tree and transported. Another manner to investigate this is to apply rain conditions in a controlled environment during high tide, when the soil is prevented to take up this fresh water or by simply covering the roots and the soil in order to avoid fresh water uptake through the roots. These experiments should be carried out during both daily and nocturnal conditions. This makes it possible to assess the difference between open and closed stomata and the possible uptake through the cuticle and/or bark. In order to quantify water uptake through the bark it is important to make a distinction between hygroscopic water uptake by the bark and uptake through the bark inside stem cells. An experiment that could be performed is spraying the bark with water droplets and monitoring the swell at the same level. To make the distinction the value of the diameter should be registered only when the water content of the bark is the same again as before the spraying was applied. It might be necessary to create conditions similar to conditions of a rainy day. Measurements taken after the spraying experiment should be compared to measurements taken with the same rainy conditions, but without the spraying to prevent other mechanisms having any effect. If predawn Ψ_l would remain higher than Ψ_b, This could be additional evidence for foliar uptake as has been registered in other species by for instance Yates and Hutley (1995), Gouvra and Grammatikopoulos (2003), Burgess and Dawson (2004) and Limm et al. (2009). If this species does exhibit foliar uptake, the Ψ_l could become lower than in the stem and a negative sap flow at least in the canopy is expected. This could be measured by HRM sensors in the canopy, near the leaves.

One of the major assumption made in this dissertation is the formation of osmotically active substances in response to daylight. These substances could be the main driver for the variations in the stem diameter. A chemical analysis could provide a lot of information on which chemicals are present in *R. stylosa* and how their concentrations alter throughout the day. Besides this, it could be interesting to know how the chemical composition differs in several plant parts, because now stem diameter was measured while the production of osmotic substances is rather expected to occur inside the leaves. The growth pattern exhibited by *R. stylosa* resembles the growth pattern of CAM-plants. Other factors, such as stomatal behavior, are more similar to the patterns that C3-plants exhibit. Therefore it would be interesting to evaluate the photosynthetic characteristics of *R. stylosa* with instrumentation such as a LI-COR device. The combination of the photosynthetic behavior and the course of the concentrations of osmotic substances can provide proves of the increase of these osmotic substances under influence of photosynthesis. Furthermore, a decisive answer should be found on which photosynthetic metabolism is present in *R. stylosa*. The characteristics that these species exhibited in its water household showed resemblances with both C3 and C4-plants and with CAM-plants. Therefore, it could be possible to discover a hybrid form or even a new form of photosynthetic metabolism in *R. stylosa*.

A final proposal for future research is a comparative research between different mangrove species. Is *R. stylosa* the only species that exhibits this particular growth pattern or is it more widely spread? For *Avicennia marina*, a salt secretor, the general diurnal growth pattern is comparable to non-mangrove species (unpublished work). It would be interesting to discover which species show these special adaptations to the saline environment and how widespread this adaptations are. Furthermore, it would be interesting to get an overview of the water relations of different mangrove species. This could greatly contribute to the knowledge and understanding of the physiological processes, not only in mangroves, but also for the general ecophysiological theories present today.

References

Acevedo, E., I. Badilla, and P. S. Nobel. 1983. Water Relations, Diurnal Acidity Changes, and Productivity of a Cultivated Cactus, Opuntia ficus-indica. Plant Physiology 72:775-780.

Acevedo, E., E. Fereres, T. C. Hsiao, and D. W. Henderson. 1979. Diurnal Growth Trends, Water Potential, and Osmotic Adjustment of Maize and Sorghum Leaves in the Field. Plant Physiology 64:476-480.

Adam, P. 1994. Saltmarsh and mangrove. Pages 395-435 *in* R. H. Groves, editor. Australian vegetation. Cambridge University Press.

Ainsworth, E. A. and A. Rogers. 2007. The response of photosynthesis and stomatal conductance to rising [CO2]: mechanisms and environmental interactions. Plant, Cell & Environment 30:258-270.

Allen, J. A., J. L. Chambers, and M. Stine. 1994. Prospects for increasing the salt tolerance of forest trees: a review. Tree Physiology 14:843-853.

Allen, R. G., L. S. Pereira, D. Raes, and M. Smith. 1998. Crop evapotranspiration-Guidelines for computing crop water requirements-FAO Irrigation and drainage paper 56. FAO, Rome 300:6541.

Alongi, D. M. 2008. Mangrove forests: Resilience, protection from tsunamis, and responses to global climate change. Estuarine, Coastal and Shelf Science 76:1-13.

Andrews, T. J., B. F. Clough, and G. J. Muller. 1984. Photosynthetic gas exchange properties and carbon isotope ratios of some mangroves in North Queensland. Pages 15-23 *in* H. J. Teas, editor. Physiology and management of mangroves. Springer Netherlands.

Aziz, I. and M. A. Khan. 2001. Effect of Seawater on the Growth, Ion Content and Water Potential of Rhizophora mucronata Lam. Journal of Plant Research 114:369-373.

Ball, M. C. 1988. Ecophysiology of mangroves. Trees 2:129-142.

Ball, M. C., M. J. Cochrane, and H. M. Rawson. 1997. Growth and water use of the mangroves Rhizophora apiculata and R. stylosa in response to salinity and humidity under ambient and elevated concentrations of atmospheric CO2. Plant, Cell & Environment 20:1158-1166.

Becker, P. 1996. Sap flow in Bornean heath and dipterocarp forest trees during wet and dry periods. Tree Physiology 16:295-299.

Begg, J. E. and N. C. Turner. 1970. Water Potential Gradients in Field Tobacco. Plant Physiology 46:343-346.

Blasco, F., P. Saenger, and E. Janodet. 1996. Mangroves as indicators of coastal change. CATENA 27:167-178.

Bleby, T. M., A. J. McElrone, and S. S. O. Burgess. 2008. Limitations of the HRM: great at low flow rates, but not yet up to speed?*in* Book of abstract of the 7th sap flow workshop, Seville.

Bohnert, H. J., D. E. Nelson, and R. G. Jensen. 1995. Adaptations to environmental stresses. The plant cell 7:1099.

Bohnert, H. J. and E. Sheveleva. 1998. Plant stress adaptations — making metabolism move. Current Opinion in Plant Biology 1:267-274.

Bond, B. J. and K. L. Kavanagh. 1999. Stomatal behavior of four woody species in relation to leaf-specific hydraulic conductance and threshold water potential. Tree Physiology 19:503-510.

Bouriaud, O., J. M. Leban, D. Bert, and C. Deleuze. 2005. Intra-annual variations in climate influence growth and wood density of Norway spruce. Tree Physiology 25:651-660.

Boyer, J. S. 1968. Relationship of Water Potential to Growth of Leaves. Plant Physiology 43:1056-1062.

Brodribb, T. J., N. M. Holbrook, E. J. Edwards, and M. V. Gutiérrez. 2003. Relations between stomatal closure, leaf turgor and xylem vulnerability in eight tropical dry forest trees. Plant, Cell & Environment 26:443-450.

Brough, D. W., H. G. Jones, and J. Grace. 1986. Diurnal changes in water content of the stems of apple trees, as influenced by irrigation. Plant, Cell & Environment 9:1-7.

Buck, A. L. 1981. New equations for computing vapor pressure and enhancement factor. Journal of Applied Meteorology 20:1527-1532.

Bureau of Meteorology. 2012. Daily rainfall Dunwich Australian Government.

Burgess, S. S. O., M. A. Adams, N. C. Turner, C. R. Beverly, C. K. Ong, A. A. H. Khan, and T. M. Bleby. 2001. An improved heat pulse method to measure low and reverse rates of sap flow in woody plants. Tree Physiology 21:589-598.

Burgess, S. S. O. and T. E. Dawson. 2004. The contribution of fog to the water relations of Sequoia sempervirens (D. Don): foliar uptake and prevention of dehydration. Plant, Cell & Environment 27:1023-1034.

Burghardt, M. and M. Riederer. 2003. Ecophysiological relevance of cuticular transpiration of deciduous and evergreen plants in relation to stomatal closure and leaf water potential*. Journal of Experimental Botany 54:1941-1949.

Čermák, J., J. Kučera, W. L. Bauerle, N. Phillips, and T. M. Hinckley. 2007. Tree water storage and its diurnal dynamics related to sap flow and changes in stem volume in old-growth Douglas-fir trees. Tree Physiology 27:181-198.

Chen, S.-S. and C. C. Black. 1983. Diurnal Changes in Volume and Specific Tissue Weight of Crassulacean Acid Metabolism Plants. Plant Physiology 71:373-378.

Coder, K. D. 1999. Water movement in trees. Daniel B. Warnell School of Forest Resources, University of Georgia. Extension publication FOR99-007. 4pp.

Comstock, J. P. 2000. Correction of Thermocouple Psychrometer Readings for the Interaction of Temperature and Actual Water Potential. Crop Sci. 40:709-712.

Cuevas, E., P. Baeza, and J. R. Lissarrague. 2006. Variation in stomatal behaviour and gas exchange between mid-morning and mid-afternoon of north–south oriented grapevines (Vitis vinifera L. cv. Tempranillo) at different levels of soil water availability. Scientia Horticulturae 108:173-180.

Dahdouh-Guebas, F., L. P. Jayatissa, D. Di Nitto, J. O. Bosire, D. Lo Seen, and N. Koedam. 2005. How effective were mangroves as a defence against the recent tsunami? Current Biology 15:R443-R447.

Daudet, F.-A., T. Améglio, H. Cochard, O. Archilla, and A. Lacointe. 2005. Experimental analysis of the role of water and carbon in tree stem diameter variations. Journal of Experimental Botany 56:135-144.

Dawson, T. E., S. S. O. Burgess, K. P. Tu, R. S. Oliveira, L. S. Santiago, J. B. Fisher, K. A. Simonin, and A. R. Ambrose. 2007. Nighttime transpiration in woody plants from contrasting ecosystems. Tree Physiology 27:561-575.

Day, J. W., R. H. Day, F. Ley-Lou, and C. J. Madden. 1982. Primary production in the Laguna de Terminos, a tropical estuary in the Southern Gulf of Mexico. Oceanologica Acta.

De Swaef, T. and K. Steppe. 2010. Linking stem diameter variations to sap flow, turgor and water potential in tomato. Functional Plant Biology 37:429-438.

Deslauriers, A., T. Anfodillo, S. Rossi, and V. Carraro. 2007a. Using simple causal modeling to understand how water and temperature affect daily stem radial variation in trees Tree Physiology 27:1125-1136.

Deslauriers, A., H. Morin, C. Urbinati, and M. Carrer. 2003. Daily weather response of balsam fir (Abies balsamea (L.) Mill.) stem radius increment from dendrometer analysis in the boreal forests of Québec (Canada). Trees 17:477-484.

Deslauriers, A., S. Rossi, and T. Anfodillo. 2007b. Dendrometer and intra-annual tree growth: What kind of information can be inferred? Dendrochronologia 25:113-124.

Dixon, M. A. and M. T. Tyree. 1984. A new stem hygrometer, corrected for temperature gradients and calibrated against the pressure bomb. Plant, Cell & Environment 7:693-697.

Dolman, A. J. and G. J. Van Den Burg. 1988. Stomatal behaviour in an oak canopy. Agricultural and Forest Meteorology 43:99-108.

Donovan, L., M. Linton, and J. Richards. 2001. Predawn plant water potential does not necessarily equilibrate with soil water potential under well-watered conditions. Oecologia 129:328-335.

Downes, G., C. Beadle, and D. Worledge. 1999. Daily stem growth patterns in irrigated Eucalyptus globulus and E. nitens in relation to climate. Trees 14:102-111.

Drew, D. M. and G. M. Downes. 2009. The use of precision dendrometers in research on daily stem size and wood property variation: A review. Dendrochronologia 27:159-172.

Drew, D. M., A. P. O'Grady, G. M. Downes, J. Read, and D. Worledge. 2008. Daily patterns of stem size variation in irrigated and unirrigated Eucalyptus globulus. Tree Physiology 28:1573-1581.

Duke, N. C., E. Lo, and M. Sun. 2002. Global distribution and genetic discontinuities of mangroves – emerging patterns in the evolution of Rhizophora. Trees 16:65-79.

Duke, N. C., J. O. Meynecke, S. Dittmann, A. M. Ellison, K. Anger, U. Berger, S. Cannicci, K. Diele, K. C. Ewel, C. D. Field, N. Koedam, S. Y. Lee, C. Marchand, I. Nordhaus, and F. Dahdouh-Guebas. 2007. A World Without Mangroves? Science 317:41-42.

Ehleringer, J. R. and T. E. Dawson. 1992. Water uptake by plants: perspectives from stable isotope composition. Plant, Cell & Environment 15:1073-1082.

Elfving, D. C., M. R. Kaufmann, and A. E. Hall. 1972. Interpreting Leaf Water Potential Measurements with a Model of the Soil-Plant-Atmosphere Continuum. Physiologia Plantarum 27:161-168.

Fereres, E. and D. A. Goldhamer. 2003. Suitability of stem diameter variations and water potential as indicators for irrigation scheduling of almond trees. Journal of Horticultural Science and Biotechnology 78:139-144.

Fernández, J. E., F. Moreno, M. J. Martín-Palomo, M. V. Cuevas, J. M. Torres-Ruiz, and A. Moriana. 2011. Combining sap flow and trunk diameter measurements to assess water needs in mature olive orchards. Environmental and Experimental Botany 72:330-338.

Fernández, J. E., M. J. Palomo, A. Díaz-Espejo, B. E. Clothier, S. R. Green, I. F. Girón, and F. Moreno. 2001. Heat-pulse measurements of sap flow in olives for automating irrigation: tests, root flow and diagnostics of water stress. Agricultural Water Management 51:99-123.

Field, C. D. 1995. Impact of expected climate change on mangroves. Hydrobiologia 295:75-81.

Genard, M., S. Fishman, G. Vercambre, J. G. Huguet, C. Bussi, J. Besset, and R. Habib. 2001. A biophysical analysis of stem and root diameter variations in woody plants. Plant Physiology 126:188-202.

Giri, C., E. Ochieng, L. L. Tieszen, Z. Zhu, A. Singh, T. Loveland, J. Masek, and N. Duke. 2011. Status and distribution of mangrove forests of the world using earth observation satellite data. Global Ecology and Biogeography 20:154-159.

Goldstein, G., J. L. Andrade, F. C. Meinzer, N. M. Holbrook, J. Cavelier, P. Jackson, and A. Celis. 1998. Stem water storage and diurnal patterns of water use in tropical forest canopy trees. Plant, Cell & Environment 21:397-406.

Gouvra, E. and G. Grammatikopoulos. 2003. Beneficial effects of direct foliar water uptake on shoot water potential of five chasmophytes. Canadian Journal of Botany 81:1278-1284.

Hall, R. C. 1944. A vernier tree-growth band. Journal of forestry 42:742-743.

Hao, G.-Y., T. J. Jones, C. Luton, Y.-J. Zhang, E. Manzane, F. G. Scholz, S. J. Bucci, K.-F. Cao, and G. Goldstein. 2009. Hydraulic redistribution in dwarf Rhizophora mangle trees driven by interstitial soil water salinity gradients: impacts on hydraulic architecture and gas exchange. Tree Physiology 29:697-705.

Herzog, K., R. Häsler, and R. Thum. 1995. Diurnal changes in the radius of a subalpine Norway spruce stem: their relation to the sap flow and their use to estimate transpiration. Trees 10:94-101.

Hetherington, A. M. and F. I. Woodward. 2003. The role of stomata in sensing and driving environmental change. Nature 424:901-908.

Hoegh-Guldberg, O. 1999. Climate change, coral bleaching and the future of the world's coral reefs. Marine and Freshwater Research 50:839-866.

Hoste, P. 2011. Ecophysiology of mangrove in Australia: hydraulic functioning. University of Gent, Gent.

Hosy, E., A. Vavasseur, K. Mouline, I. Dreyer, F. Gaymard, F. Porée, J. Boucherez, A. Lebaudy, D. Bouchez, A.-A. Véry, T. Simonneau, J.-B. Thibaud, and H. Sentenac. 2003. The Arabidopsis outward K+ channel GORK is involved in regulation of stomatal movements and plant transpiration. Proceedings of the National Academy of Sciences 100:5549-5554.

Hsiao, T. C. and E. Acevedo. 1974. Plant responses to water deficits, water-use efficiency, and drought resistance. Agricultural Meteorology 14:59-84.

Hughes, L. 2003. Climate change and Australia: Trends, projections and impacts. Austral Ecology 28:423-443.

Ibrahim, D. G., M. E. Gilbert, B. S. Ripley, and C. P. Osborne. 2008. Seasonal differences in photosynthesis between the C3 and C4 subspecies of Alloteropsis semialata are offset by frost and drought. Plant, Cell & Environment 31:1038-1050.

Irvine, J. and J. Grace. 1997. Continuous measurements of water tensions in the xylem of trees based on the elastic properties of wood. Planta 202:455-461.

Jintana, V., A. Komiyama, H. Moriya, and K. Ogino. 1985. Forest ecological studies of mangrove ecosystem in Ranong, Southern Thailand - 4. Diameter growth measurement by dendrometry. Pages 227-233 Studies on the mangrove ecosystem. Nodai Research Institute, Tokyo University of Agriculture, Japan.

Kanemasu, E. T., G. W. Thurtell, and C. B. Tanner. 1969. Design calibration and field use of a stomatal diffusion porometer. Plant Physiology 44:881-885.

Kathiresan, K. and B. L. Bingham. 2001. Biology of mangroves and mangrove Ecosystems. Pages 81-251 Advances in Marine Biology. Academic Press.

Katul, G., S. Manzoni, S. Palmroth, and R. Oren. 2010. A stomatal optimization theory to describe the effects of atmospheric CO2 on leaf photosynthesis and transpiration Annals of Botany 105:431-442.

Katz, C., R. Oren, E. D. Schulze, and J. A. Milburn. 1989. Uptake of water and solutes through twigs of Picea abies (L.) Karst. Trees 3:33-37.

Kelly, P. M. and W. N. Adger. 2000. Theory and Practice in Assessing Vulnerability to Climate Change and Facilitating Adaptation. Climatic Change 47:325-352.

Klepper, B. 1968. Diurnal Pattern of Water Potential in Woody Plants. Plant Physiology 43:1931-1934.

Klepper, B., V. D. Browning, and H. M. Taylor. 1971. Stem diameter in relation to plant water status. Plant Physiology 48:683-685.

Knapp, A. K. 1993. Gas Exchange Dynamics in C3 and C4 Grasses: Consequence of Differences in Stomatal Conductance. Ecology 74:113-123.

Kozlowski, T. T. and C. H. Winget. 1964. Diurnal and Seasonal Variation in Radii of Tree Stems. Ecology 45:149-155.

Kramer, P. J. and J. S. Boyer. 1995a. The Absorption of Water and Root and Stem Pressures. Pages 167-200 Water relations of plants and soils. Academic Press, Inc.

Kramer, P. J. and J. S. Boyer. 1995b. Functions and Properties of Water. Pages 14-41 Water relations of plants and soils. Academic Press, Inc.

Kramer, P. J. and J. S. Boyer. 1995c. Transpiration and the Ascent of Sap. Pages 201-256 Water relations of plants and soils. Academic Press, Inc.

Krauss, K. W., B. D. Keeland, J. A. Allen, K. C. Ewel, and D. J. Johnson. 2007. Effects of Season, Rainfall, and Hydrogeomorphic Setting on Mangrove Tree Growth in Micronesia. Biotropica 39:161-170.

Kume, T., H. Takizawa, N. Yoshifuji, K. Tanaka, C. Tantasirin, N. Tanaka, and M. Suzuki. 2007. Impact of soil drought on sap flow and water status of evergreen trees in a tropical monsoon forest in northern Thailand. Forest Ecology and Management 238:220-230.

Lal, P. 2003. Economic valuation of mangroves and decision-making in the Pacific. Ocean & Coastal Management 46:823-844.

Lawton, J. R., A. N. N. Todd, and D. K. Naidoo. 1981. Preliminary investigations into the structure of the roots of the mangroves, Avicennia marina and Bruguiera gymnorrhiza, in relation to ion uptake. New Phytologist 88:713-722.

Lee, R. 1967. The hydrologic importance of transpiration control by stomata. Water Resources Research 3:737-752.

Leuning, R., A. Tuzet, and A. Perrier. 2004. Stomata as Part of the Soil-Plant-Atmosphere Continuum. Pages 9-28 *in* M. Mencuccini, J. Grace, J. Moncrieff, and K. G. McNaughton, editors. Forests at the Land-Atmosphere Interface. CABI.

Limm, E., K. Simonin, A. Bothman, and T. Dawson. 2009. Foliar water uptake: a common water acquisition strategy for plants of the redwood forest. Oecologia 161:449-459.

Lo Gullo, M. A., S. Salleo, E. C. Piaceri, and R. Rosso. 1995. Relations between vulnerability to xylem embolism and xylem conduit dimensions in young trees of Quercus corris. Plant, Cell & Environment 18:661-669.

Lugo, A. E. and S. C. Snedaker. 1974. The Ecology of Mangroves. Annual Review of Ecology and Systematics 5:39-64.

Lüttge, U. 2004. Ecophysiology of Crassulacean Acid Metabolism (CAM). Annals of Botany 93:629-652.

MacDougal, D. T. 1936. Studies in Tree-growth by the Dendrographic Method. Carnegie Institution of Washington.

Mäkinen, H., P. Nöjd, and P. Saranpää. 2003. Seasonal changes in stem radius and production of new tracheids in Norway spruce. Tree Physiology 23:959-968.

Mansfield, T. A. 2004. Stomatal Control of Transpiration: a Major Dilemma 100 years Ago. Pages 1-8 *in* M. Mencuccini, J. Grace, J. Moncrieff, and K. G. McNaughton, editors. Forests at the Land-Atmosphere Interface.

Martin, C. E. and V. S. Loeschen. 1993. Photosynthesis in the mangrove species Rhizophora mangle L.: No evidence for CAM-cycling. Photosynthetica 28:391-400.

Matimati, I., C. F. Musil, L. Raitt, and E. C. February. 2012. Diurnal stem diameter variations show CAM and C3 photosynthetic modes and CAM–C3 switches in arid South African succulent shrubs. Agricultural and Forest Meteorology 161:72-79.

McCully, M. E. 1999. Root Xylem Embolisms and Refilling. Relation to Water Potentials of Soil, Roots, and Leaves, and Osmotic Potentials of Root Xylem Sap. Plant Physiology 119:1001-1008.

McCutchan, H. and K. A. Shackel. 1992. Stem-water Potential as a Sensitive Indicator of Water Stress in Prune Trees (Prunus domestica L. cv. French). Journal of the American Society for Horticultural Science 117:607-611.

McIntyre, D. S. 1980. Basic relationships for salinity evaluation from measurements on soil solution. Soil Research 18:199-206.

McKee, K. L. 1993. Soil Physicochemical Patterns and Mangrove Species Distribution--Reciprocal Effects? Journal of Ecology 81:477-487.

McLaughlin, S. B., S. D. Wullschleger, and M. Nosal. 2003. Diurnal and seasonal changes in stem increment and water use by yellow poplar trees in response to environmental stress. Tree Physiology 23:1125-1136.

McLeod, E. and R. V. Salm. 2006. Managing mangroves for resilience to climate change. World Conservation Union (IUCN).

Medina, E. 1999. Mangrove physiology: the challenge of salt, heat, and light stress under recurrent flooding. Ecosystemas de manglar em América tropical. Yánez-Arancibia A. & Lara-Domínguez AL (eds), Instituto de Ecología AC Xalapa, México. UICN/ORMA Costa Rica, NOAA/NMFS, Silver Spring, Md. USA:109-126.

Meinzer, F. C., S. A. James, and G. Goldstein. 2004. Dynamics of transpiration, sap flow and use of stored water in tropical forest canopy trees. Tree Physiology 24:901-909.

Mitchell, D. E., M. V. Gadus, and M. A. Madore. 1992. Patterns of Assimilate Production and Translocation in Muskmelon (Cucumis melo L.) : I. Diurnal Patterns. Plant Physiology 99:959-965.

Motzer, T., N. Munz, M. Küppers, D. Schmitt, and D. Anhuf. 2005. Stomatal conductance, transpiration and sap flow of tropical montane rain forest trees in the southern Ecuadorian Andes. Tree Physiology 25:1283-1293.

O'Brien, J. J., S. F. Oberbauer, and D. B. Clark. 2004. Whole tree xylem sap flow responses to multiple environmental variables in a wet tropical forest. Plant, Cell & Environment 27:551-567.

Offenthaler, I., P. Hietz, and H. Richter. 2001. Wood diameter indicates diurnal and long-term patterns of xylem water potential in Norway spruce. Trees 15:215-221.

Oguntunde, P. G. and A. M. Oguntuase. 2007. Influence of environmental factors on the sap flux density of mango trees under rain-fed cropping systems in West Africa. International Journal of Plant Production 1:179-188.

Oparka, K. J. 1994. Plasmolysis: new insights into an old process. New Phytologist 126:571-591.

Oren, R. and D. E. Pataki. 2001. Transpiration in response to variation in microclimate and soil moisture in southeastern deciduous forests. Oecologia 127:549-559.

Ortuño, M. F., Y. García-Orellana, W. Conejero, M. C. Ruiz-Sánchez, J. J. Alarcón, and A. Torrecillas. 2006a. Stem and leaf water potentials, gas exchange, sap flow, and trunk diameter fluctuations for detecting water stress in lemon trees. Trees 20:1-8.

Ortuño, M. F., Y. García-Orellana, W. Conejero, M. C. Ruiz-Sánchez, O. Mounzer, J. J. Alarcón, and A. Torrecillas. 2006b. Relationships Between Climatic Variables and Sap Flow, Stem Water Potential and Maximum Daily Trunk Shrinkage in Lemon Trees. Plant and Soil 279:229-242.

Parida, A. and B. Jha. 2010. Salt tolerance mechanisms in mangroves: a review. Trees 24:199-217.

Perämäki, M., E. Nikinmaa, S. Sevanto, H. Ilvesniemi, E. Siivola, P. Hari, and T. Vesala. 2001. Tree stem diameter variations and transpiration in Scots pine: an analysis using a dynamic sap flow model. Tree Physiology 21:889-897.

Phillips, N., A. Nagchaudhuri, R. Oren, and G. Katul. 1997. Time constant for water transport in loblolly pine trees estimated from time series of evaporative demand and stem sapflow. Trees 11:412-419.

Polidoro, B. A., K. E. Carpenter, L. Collins, N. C. Duke, A. M. Ellison, J. C. Ellison, E. J. Farnsworth, E. S. Fernando, K. Kathiresan, N. E. Koedam, S. R. Livingstone, T. Miyagi, G. E. Moore, V. Ngoc Nam, J. E. Ong, J. H. Primavera, S. G. Salmo, III, J. C. Sanciangco, S. Sukardjo, Y. Wang, and J. W. H. Yong. 2010. The Loss of Species: Mangrove Extinction Risk and Geographic Areas of Global Concern. PLoS ONE 5:e10095.

Poole, D. K. and P. C. Miller. 1975. Water Relations of Selected Species of Chaparral and Coastal Sage Communities. Ecology 56:1118-1128.

Popp, M. 1984. Chemical Composition of Australian Mangroves I. Inorganic Ions and Organic Acids. Zeitschrift für Pflanzenphysiologie 113:395-409.

Porporato, A., F. Laio, L. Ridolfi, and I. Rodriguez-Iturbe. 2001. Plants in water-controlled ecosystems: active role in hydrologic processes and response to water stress: III. Vegetation water stress. Advances in Water Resources 24:725-744.

Robert, E. M. R., N. Koedam, H. Beeckman, and N. Schmitz. 2009. A safe hydraulic architecture as wood anatomical explanation for the difference in distribution of the mangroves Avicennia and Rhizophora. Functional Ecology 23:649-657.

Romero, P. and P. Botía. 2006. Daily and seasonal patterns of leaf water relations and gas exchange of regulated deficit-irrigated almond trees under semiarid conditions. Environmental and Experimental Botany 56:158-173.

Scarth, G. W. 1927. Stomatal movement: Its regulation and regulatory rôle a review. Protoplasma 2:498-511.

Scholander, P. F. 1968. How mangroves desalinate water. Physiologia Plantarum 21:251-261.

Scholander, P. F., E. D. Bradstreet, E. A. Hemmingsen, and H. T. Hammel. 1965. Sap Pressure in Vascular Plants: Negative hydrostatic pressure can be measured in plants. Science (New York, N.Y.) 148:339-346.

Scholander, P. F., H. T. Hammel, E. Hemmingsen, and W. Garey. 1962. Salt Balance in mangroves. Plant Physiology 37:722-729.

Scholander, P. F., H. T. Hammel, E. A. Hemmingsen, and E. D. Bradstreet. 1964. Hydrostatic pressure and osmotic potential in leaves of mangroves and some other plants. Proceedings of the National Academy of Sciences of the United States of America 52:119.

Scholander, P. F., L. Van Dam, and S. I. Scholander. 1955. Gas exchange in the roots of mangroves. American Journal of Botany:92-98.

Scholz, F. C., S. J. Bucci, G. Goldstein, F. C. Meinzer, A. C. Franco, and F. Miralles-Wilhelm. 2008. Temporal dynamics of stem expansion and contraction in savanna trees: withdrawal and recharge of stored water. Tree Physiology 28:469-480.

Schöngart, J., M. T. F. Piedade, S. Ludwigshausen, V. Horna, and M. Worbes. 2002. Phenology and stem-growth periodicity of tree species in Amazonian floodplain forests. Journal of Tropical Ecology 18:581-597.

Schulze, E. D., J. Čermák, M. Matyssek, M. Penka, R. Zimmermann, F. Vasícek, W. Gries, and J. Kučera. 1985. Canopy transpiration and water fluxes in the xylem of the trunk of Larix and Picea trees — a comparison of xylem flow, porometer and cuvette measurements. Oecologia 66:475-483.

Sevanto, S., T. Vesala, M. Perämäki, J. Pumpanen, H. Ilvesniemi, and E. Nikinmaa. 2001. Xylem diameter changes as an indicator of stand-level evapo-transpiration. Boreal environment research 6:45-52.

Simonin, K. A., L. S. Santiago, and T. E. Dawson. 2009. Fog interception by Sequoia sempervirens (D. Don) crowns decouples physiology from soil water deficit. Plant, Cell & Environment 32:882-892.

Slatyer, R. O. 1969. Physiological significance of internal water relations to crop yield. Agronomy--Faculty Publications:186.

Smith, D. M. and S. J. Allen. 1996. Measurement of sap flow in plant stems. Journal of Experimental Botany 47:1833-1844.

Steppe, K., D. J. W. De Pauw, T. M. Doody, and R. O. Teskey. 2010. A comparison of sap flux density using thermal dissipation, heat pulse velocity and heat field deformation methods. Agricultural and Forest Meteorology 150:1046-1056.

Steppe, K., D. J. W. De Pauw, R. Lemeur, and P. A. Vanrolleghem. 2006. A mathematical model linking tree sap flow dynamics to daily stem diameter fluctuations and radial stem growth. Tree Physiology 26:257-273.

Steppe, K. and R. Lemeur. 2004. An experimental system for analysis of the dynamic sap-flow characteristics in young trees: results of a beech tree. Functional Plant Biology 31:83-92.

Stiles, W., J. L. Monteith, and T. A. Bull. 1970. A diffusive resistance porometer for field use. Journal of Applied Ecology:617-638.

Tardieu, F. and T. Simonneau. 1998. Variability among species of stomatal control under fluctuating soil water status and evaporative demand: modelling isohydric and anisohydric behaviours. Journal of Experimental Botany 49:419-432.

Tardif, J., M. Flannigan, and Y. Bergeron. 2001. An Analysis of the Daily Radial Activity of 7 Boreal Tree Species, Northwestern Quebec. Environmental Monitoring and Assessment 67:141-160.

Taub, D. 2010. Effects of rising atmospheric concentrations of carbon dioxide on plants. Nature Education Knowledge 1:21.

Ting, I. P., L. Bates, L. O. R. Sternberg, and M. J. Deniro. 1985. Physiological and Isotopic Aspects of Photosynthesis in Peperomia. Plant Physiology 78:246-249.

Tomlinson, P. B. 1995. The botany of mangroves. Cambridge University Press.

Tyree, M. T. and F. W. Ewers. 1991. The hydraulic architecture of trees and other woody plants. New Phytologist 119:345-360.

Upmeyer, D. J. and H. R. Koller. 1973. Diurnal Trends in Net Photosynthetic Rate and Carbohydrate Levels of Soybean Leaves. Plant Physiology 51:871-874.

Van Bavel, C. H. M., F. S. Nakayama, and W. L. Ehrler. 1965. Measuring transpiration resistance of leaves. Plant Physiology 40:535.

Vandegehuchte, M. W. and K. Steppe. 2012. Sapflow+: a four-needle heat-pulse sap flow sensor enabling nonempirical sap flux density and water content measurements. New Phytologist 196:306-317.

Vandegehuchte, M. W. and K. Steppe. 2013. Sap-flux density measurement methods: working principles and applicability. Functional Plant Biology 40:213-223.

Walters, B. B., P. Rönnbäck, J. M. Kovacs, B. Crona, S. A. Hussain, R. Badola, J. H. Primavera, E. Barbier, and F. Dahdouh-Guebas. 2008. Ethnobiology, socio-economics and management of mangrove forests: A review. Aquatic Botany 89:220-236.

Wells, S., C. Ravilious, and E. Corcoran. 2006. In the front line: Shoreline protection and other ecosystem services from mangroves and coral reefs. United Nations Publications.

White, D. A., N. C. Turner, and J. H. Galbraith. 2000. Leaf water relations and stomatal behavior of four allopatric Eucalyptus species planted in Mediterranean southwestern Australia. Tree Physiology 20:1157-1165.

Whitehead, D. 1998. Regulation of stomatal conductance and transpiration in forest canopies. Tree Physiology 18:633-644.

Williams, L. E. and F. J. Araujo. 2002. Correlations among Predawn Leaf, Midday Leaf, and Midday Stem Water Potential and their Correlations with other Measures of Soil and Plant Water Status in Vitis vinifera. Journal of the American Society for Horticultural Science 127:448-454.

Wullschleger, S. D. and A. W. King. 2000. Radial variation in sap velocity as a function of stem diameter and sapwood thickness in yellow-poplar trees. Tree Physiology 20:511-518.

Wullschleger, S. D., F. C. Meinzer, and R. A. Vertessy. 1998. A review of whole-plant water use studies in tree. Tree Physiology 18:499-512.

Xiong, W., Y. Wang, P. Yu, H. Liu, Z. Shi, and W. Guan. 2007. Growth in stem diameter of Larix principis-rupprechtii and its response to meteorological factors in the south of Liupan Mountain, China. Acta Ecologica Sinica 27:432-440.

Yates, D. J. and L. B. Hutley. 1995. Foliar Uptake of Water by Wet Leaves of *Sloanea woollsii*, an Australian Subtropical Rainforest Tree. Australian Journal of Botany 43:157-167.

Zeppel, M., C. O. Macinnis-Ng, C. Ford, and D. Eamus. 2008. The response of sap flow to pulses of rain in a temperate Australian woodland. Plant and Soil 305:121-130.

Zufferey, V., H. Cochard, T. Ameglio, J. L. Spring, and O. Viret. 2011. Diurnal cycles of embolism formation and repair in petioles of grapevine (Vitis vinifera cv. Chasselas). Journal of Experimental Botany 62:3885-3894.

Zweifel, R., J. P. Böhm, and R. Häsler. 2002. Midday stomatal closure in Norway spruce—reactions in the upper and lower crown. Tree Physiology 22:1125-1136.

Zweifel, R. and R. Häsler. 2001. Dynamics of water storage in mature subalpine Picea abies: temporal and spatial patterns of change in stem radius. Tree Physiology 21:561-569.

Zweifel, R., H. Item, and R. Häsler. 2000. Stem radius changes and their relation to stored water in stems of young Norway spruce trees. Trees 15:50-57.

Zweifel, R., L. Zimmermann, F. Zeugin, and D. M. Newbery. 2006. Intra-annual radial growth and water relations of trees: implications towards a growth mechanism. Journal of Experimental Botany 57:1445-1459.